REPORT NO.
UCB/EERC-88/05
MAY 1988

EARTHQUAKE ENGINEERING RESEARCH CENTER

EXPERIMENTAL EVALUATION OF SEISMIC ISOLATION OF A 9-STORY BRACED STEEL FRAME SUBJECT TO UPLIFT

by

M. C. GRIFFITH
I. D. AIKEN
J. M. KELLY

Report to the National Science Foundation

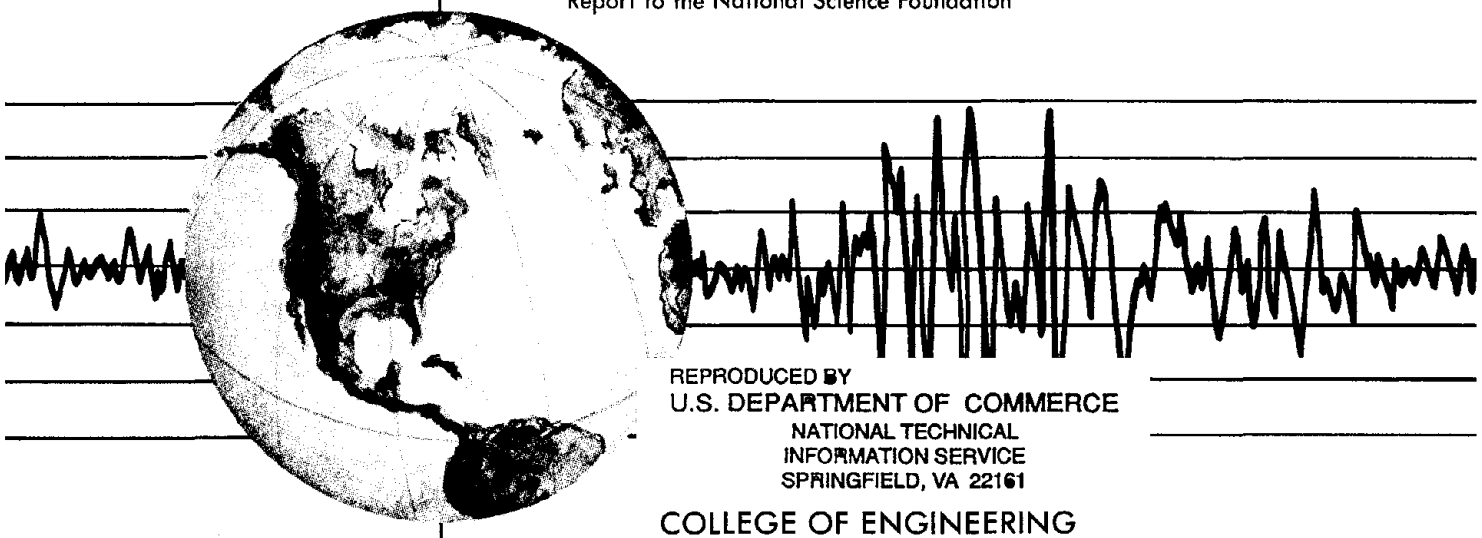

COLLEGE OF ENGINEERING

UNIVERSITY OF CALIFORNIA AT BERKELEY

For sale by the National Technical Information Service, U.S. Department of Commerce, Springfield, Virginia 22161

See back of report for up to date listing of EERC reports.

50272-101

REPORT DOCUMENTATION PAGE	1. REPORT NO. NSF/ENG-88042	2.	3. PB91-217968

4. Title and Subtitle
Experimental Evaluation of Seismic Isolation of a 9-story Braced Steel Frame Subject to Uplift

5. Report Date
May 1988

6.

7. Author(s)
M.C. Griffith, I.D. Aiken, and J.M. Kelly

8. Performing Organization Rept. No.
UCB/EERC-88/05

9. Performing Organization Name and Address
Earthquake Engineering Research Center
University of California, Berkeley
1301 S 46th St.
Richmond, CA 94804

10. Project/Task/Work Unit No.

11. Contract(C) or Grant(G) No.
(C)
(G) ECE-8414036

12. Sponsoring Organization Name and Address
National Science Foundation
1800 G. St. NW
Washington, DC 20550

13. Type of Report & Period Covered

14.

15. Supplementary Notes

16. Abstract (Limit: 200 words)

In the second phase of an experimental study of base isolation of medium-rise buildings subject to column uplift, earthquake simulator tests were performed on a 1/4-scale 9-story braced steel frame structure with height to width ratio of 1.59, for two types of base isolation bearings, neoprene and natural rubber with lead plug, against a wide range of earthquake ground motions.

The study found that base isolation of medium-rise structures provides significant reductions in base shear and story accelerations. Both the neoprene and lead-plug bearings proved to be effective isolators. The neoprene bearings did not provide as much damping as the lead-plug bearings, but did not experience any significant change in stiffness while the lead-plug bearing shear stiffness decreased by 50% after many cycles of displacement. The lead-plug bearings also tended to excite more higher mode response in the structure than the neoprene bearing isolators.

Comparison of the test results with response spectrum analysis showed that the latter is an effective technique for determining the maximum responses of a base-isolated structure. The accuracy of the technique is limited by the accuracy of the computer model of the structure and, more important, it is limited by the accuracy of the response (or design) spectrum.

The SEAONC design formula for calculating bearing displacements in base-isolated structures was shown to be, in general, conservative when using the velocity related coefficients A_v.

17. Document Analysis a. Descriptors
isolation bearings
neoprene
natural rubber

b. Identifiers/Open-Ended Terms
response spectrum
stiffness
shear stiffness

c. COSATI Field/Group

18. Availability Statement:	19. Security Class (This Report)	21. No. of Pages
Release Unlimited	unclassified	145
	20. Security Class (This Page) unclassified	22. Price

(See ANSI-Z39.18) See Instructions on Reverse

OPTIONAL FORM 272 (4-77)
(Formerly NTIS-35)
Department of Commerce

EXPERIMENTAL EVALUATION OF SEISMIC ISOLATION OF A 9-STORY BRACED STEEL FRAME SUBJECT TO UPLIFT

by

M. C. Griffith

I. D. Aiken

J. M. Kelly

Report No. UCB/EERC-88/05

Earthquake Engineering Research Center

College of Engineering

University of California, Berkeley

May 1988

ABSTRACT

This report presents the results of the second phase of an experimental study of base isolation of medium-rise buildings subject to column uplift. This phase of the research consisted of earthquake simulator tests on a 1/4-scale 9-story braced steel frame structure with height to width ratio of 1.59. The main objectives of this study were to:

(1) evaluate the feasibility of base isolation for medium-rise structures subject to column uplift during severe seismic loads;

(2) evaluate the relative effectiveness of two types of base isolation bearings, neoprene and natural rubber with lead plug, against a wide range of earthquake ground motions; and

(3) evaluate the effectiveness of the response spectrum method for predicting maximum bearing displacement and base shear.

The test results were compared with values given by the tentative base isolation design provisions proposed by the seismology committee of SEAONC.

The study found that base isolation of medium-rise structures provides significant reductions in base shear and story accelerations. Both the neoprene and lead-plug bearings proved to be effective isolators, however, the neoprene bearings did not provide as much damping as the lead-plug bearings. On the other hand, the neoprene bearings did not experience any significant change in stiffness while the lead-plug bearing shear stiffness decreased by 50% after many cycles of displacement. The lead-plug bearings also tended to excite more higher mode response in the structure than the neoprene bearing isolators.

Comparison of the test results with the response spectrum analysis showed that the response spectrum method is an effective technique for determining the maximum

responses of a base-isolated structure. However, the accuracy of the technique is limited by the accuracy of the computer model of the structure and, more important, it is limited by the accuracy of the response (or design) spectrum.

Finally, the SEAONC design formula for calculating bearing displacements in base-isolated structures was shown to be, in general, conservative when using the velocity related coefficient A_v. The acceleration related coefficients are less conservative, nonconservative in fact for low frequency ground motions, because they are poor indicators of ground motion magnitude for structures with periods in the constant velocity region of the ground motion spectra.

ACKNOWLEDGMENTS

The research reported herein was supported by the National Science Foundation under Grant No. ECE-8414036 and was conducted at the Earthquake Simulator Laboratory of the University of California at Berkeley. The views and conclusions expressed in this report are those of the authors and not necessarily those of the National Science Foundation. Professor James Kelly was the principal investigator for this project.

The authors would like to thank the National Science Foundation for its support, especially Dr. Eggenberger, and Oil States Industries in Texas for providing the base isolation bearings.

The staff of the Earthquake Engineering Research Center, especially Messrs. D. Clyde, I. Van Asten and Drs. J. Dimsdale, C. Uang, and B. Bolt provided invaluable assistance and advice over the course of the experimental work.

Table of Contents

List of Tables

List of Figures

1. INTRODUCTION

Base isolation is a strategy for reducing the effects of earthquake ground motions on a building by uncoupling the building from the two horizontal components of earthquake ground motion while simultaneously supporting the vertical weight of the structure. This technique is becoming widely accepted for providing additional structural strength against earthquake ground motions for short, stiff buildings up to about 5 stories in height [1]. However, the feasibility of base isolation for taller, less stiff buildings has only recently begun to be investigated [2]. It has generally been accepted that the longest feasible period for a base-isolated structure is about 2 to 3 seconds and that the increase in period due to base isolation should be at least 1 second. Thus, taller structures are, in general, less practical to base isolate.

Two factors which must be considered when studying the feasibility of base isolation for taller structures are: (1) the fixed-base period of the structure and (2) the possibility of column uplift due to the overturning moment caused by horizontal ground motion. Column uplift is not accommodated by the usual base-isolation device [3].

The main purpose of this research was to investigate the feasibility of base isolation for structures which tend to experience column uplift and to study the behavior of elastomeric bearing pads used to base isolate a medium-rise structure during such loadings. In order to do this earthquake simulator tests were performed on a 1/4-scale model of a nine-story braced steel frame structure. The base-isolated model was found to uplift off the outer bearings under extreme earthquake loadings even though the isolation scheme significantly reduced the peak values of base shear and acceleration from those seen in fixed-base tests. The response of the base-isolated structure was nearly that of a rigid body supported on a horizontally flexible system of bearings, thereby providing a fairly simple problem to model analytically.

2. EXPERIMENTAL MODEL

2.1 Model Details

The earthquake simulator experiments were carried out on a nine-story three bay welded steel frame model (Figure 2.1). The lowest story of the model was 4 feet high and the others were 3 feet high. The top of the model was approximately 29 feet above the top of the isolation bearings and the width of the model was 18 feet. The aspect ratio (height-to-width) was sufficiently large (1.59) that the model experienced uplift in the corner columns with moderate accelerations in the structure.

The model was not specifically designed for this test series but was adapted from that of a previous series of uplift tests [4]. The model represented a section in the weak direction of a typical steel-frame building at approximately 1/4-scale. The additional mass necessary for similitude requirements (Table 2.1) was provided by concrete blocks at each floor level. The total weight of the structure and the concrete blocks was 122 kips, but the loading was rearranged after the structure was tested on the neoprene bearings (Figure 2.2). This was done to raise the center of gravity to encourage column uplift with the subsequent tests since no uplift had occurred with the neoprene bearings. The two rows of columns were bolted to stiff wide flange sections (W8x31) which ran the length of the base of the model, and with cross beams these represented the base mat of a prototype structure. The base isolators were placed between these W8x31 beams and the shaking table.

The test structure was instrumented with a combination of accelerometers, linear potentiometers (LPs), direct current linear voltage differential transformers (DCDTs), and force transducers to record the response of the structure to all input loads. The force transducers were used to record axial force, shear force and moment immediately below the rubber bearings. Thus, the support reactions were measured by the force transducers.

A total of 83 channels of data were recorded for each test; 12 channels recorded shaking table response and 71 channels recorded model response. Figure 2.3 shows the instrumentation and Table 2.2 lists the instruments and the corresponding model or table response. One accelerometer was placed on each floor to measure the horizontal acceleration of that floor. An accelerometer was also placed on top of each end of the steel frame to measure vertical acceleration and an accelerometer was placed at the top of each of column NO1 and SO1 to measure horizontal accelerations of the roof perpendicular to the direction of table shaking. In addition, an accelerometer was placed at each corner of the model above the bearings to measure the vertical acceleration of the model at its base. These accelerometers helped determine when the model uplifted from its bearing supports. Two DCDTs were located at each corner of the model (NO1, NO2, SO1 & SO2); one between the shaking table and the top of the model, the other between the W8X31 wide flange section and the top of the model. These also helped to detect column uplift. Thirteen LPs were used to measure displacement of the model. Two LPs were used to record the relative displacement of the rubber bearings under columns SO1 and SO2. One LP on each floor recorded the total horizontal displacement at those levels and two LPs were used to record the relative displacement of the model perpendicular to the direction of input motion of the shaking table.

Each bearing was supported by a force transducer [5], from which time series records of the forces acting on the bearing were collected. The shear force at the base of the model structure was calculated for all excitations using the data acquired from these force transducers.

3. BASE ISOLATION BEARINGS

The isolation system consisted of eight elastomeric bearings of multilaminate construction with a bearing located under each column of the steel frame. Two types of elastomers were used for the bearings in this study: neoprene and natural rubber. Damping in the isolation system was enhanced by additives to the neoprene rubber compound while the natural rubber bearings provided for the addition of a lead core.

3.1 Neoprene Bearings

The neoprene bearings were 6-inches square in plan with 6 layers of 3/8-inch thick neoprene, 5 steel reinforcing shims of 1/8-inch thickness, and 1-inch thick top and bottom end plates (Figure 3.1). The bearings were designed with 4 dowel holes on the top and bottom end plates to provide shear connections between the isolation system and the structure. The dowel holes were fitted by 3/4-inch long tapered pins to accommodate column uplift while still providing a transfer of shear force.

The high nonlinearity of the neoprene bearing shear stiffness is illustrated by Figure 3.2. The neoprene bearings had a shear stiffness of about 2.1 kips/inch at 50% rubber shear strain. The shear stiffness at 2% shear strain was approximately twice as large as the 50% shear strain stiffness. Large stiffness at small shear strain is desired in isolation systems so that isolated structures will perform similarly to conventional structures under wind or small earthquake loads.

3.2 Lead-Plug Bearings

The lead-plug bearings were geometrically similar to the neoprene bearings except that each lead-plug bearing had a 1.25-inch diameter hole through its center (Figure 3.3). This hole was filled by pressing a cylinder of lead into it. The natural rubber compound used in these bearings is designated EDS 39 [6] by the Malaysian Rubber Producers Research Association (MRPRA). It is a high-strength lightly-filled rubber which has a shear modulus of approximately 100 psi at 50% shear strain. The damping of the rubber is relatively low; the equivalent viscous damping ratio at 50% shear

strain is in the range of 5—7%. However, with the addition of a lead plug the equivalent viscous damping ratio for a bearing at 50% shear strain is in the range of 20—25%.

The lead-plug bearings had the shear stiffness properties shown in Figure 3.4. Note the increased stiffness due to the presence of the lead plug. In the absence of the lead plug these bearings had a stiffness of about 1.6 kips/inch at 50% shear strain which provided an isolation frequency for the model of about 1 Hz. This frequency was too low to generate uplift forces at the corner columns for this model since the isolation system did not transmit enough acceleration to the model to generate tension in the corner columns. In order to increase the likelihood of uplift, lead plugs were inserted in the central holes of the four bearings under the center columns. Lead yields at a stress of approximately 1500 ksi which corresponds to 1.8 kips shear load in the lead plug, and at 50% shear strain the effective contribution of each lead plug to the stiffness was 1.6 kips/inch. With four bearings filled with lead the isolation frequency at 50% shear strain rose to 1.24 Hz. Another step taken to encourage column uplift was the shifting of some of the concrete blocks upward in the structure (Figure 2.2 — Loading Condition No.2). This raised the center of gravity and increased the overturning moments for similar levels of shaking table input.

4. TEST PROGRAM FOR BASE-ISOLATED MODEL

4.1 Dynamic Test Program

The test program for the structure on each set of isolation bearings consisted of free vibration tests, harmonic base input tests, white noise input tests, and earthquake input tests. The first three types of tests were performed to determine the dynamic characteristics of the model and to evaluate the effectiveness of existing analytical methods for predicting these quantities.

The free vibration test was performed to determine the fundamental frequency and the approximate equivalent viscous damping ratio of the model. This test was performed by enforcing an initial lateral displacement in the bearings and releasing the structure from this position. A shear force of approximately 5 kips was applied to the model just above the top of the bearings by pulling the structure there. This load was applied with a cable and a turnbuckle connected by shackles to the cable. In line with the cable was a short length of 5/8-inch diameter threaded rod which, after the lateral load was applied, was cut using bolt cutters. This instantly released the structure from its displaced position. Story accelerations and displacements, bearing displacements and column forces of axial, shear, and moment were monitored as the structure went through its transient response ending in static equilibrium.

An approximate value for the equivalent viscous damping ratio was estimated from the column shear force measurements taken just above the rubber bearings. The natural frequency of the model was estimated directly from the shear force time history by counting the number of zero crossings and it was also estimated by taking the fast Fourier transform (FFT) of the shear force time history and noting the frequencies associated with the peaks in the Fourier spectra.

The harmonic vibration test determined the fundamental frequency and the approximate viscous damping ratio of the structure. The model was loaded dynamically with sinusoidal base input of a fixed frequency. The model was subjected to this

input and once the model reached a steady-state harmonic motion, data from the table and the model were monitored for three seconds. This test procedure was repeated for a range of frequencies around the expected natural frequency of the structure. The peak story acceleration normalized to peak table acceleration was plotted against frequency, and from these plots the fundamental frequencies were estimated. These quantities were also estimated by taking FFTs of the story acceleration and bearing displacement time histories.

The white noise vibration test determined the modal frequencies of the structure. The test consisted of subjecting the isolated model to white noise base displacement in the frequency range of 0—20 Hz. This motion was applied for 30 seconds during which the response quantities of floor accelerations and displacements, relative bearing displacements and column forces of axial, shear, and moment were monitored.

The FFT of ideal white noise input over the range of frequency of 0—20 Hz should have a constant Fourier amplitude for that range of frequency. Note that in Figure 4.1, which shows the actual table displacement time history and the FFT of the table displacement time series, the frequency content is reasonably constant only for the frequency range of 0—10 Hz. Although the input base displacement was not true white noise input, for the purposes of these tests it was sufficient to enable estimation of the modal frequencies below 10 Hz by taking FFTs of the model roof acceleration and relative bearing displacement time histories.

The test program for each set of bearings concluded with extensive testing of the model for eight different earthquake inputs (described in Section 4.2) in order to evaluate the effectiveness of the different bearings in isolating the structure from earthquake ground motions. The earthquake inputs were varied in amplitude (with respect to peak horizontal base acceleration) to study the effect of bearing displacement and column uplift on the effectiveness of the base isolation system. The test programs for each set of bearings are given in Tables 4.1 to 4.4. The table span refers to the

amplitude of shaking table displacement. A span setting of 1000 corresponds to ±5 inches of table displacement (the maximum possible). Fractions of span 1000 setting vary approximately linearly so that a span setting of 500 corresponds to a peak input table displacement of approximately 2.5 inches.

4.2 Earthquakes Used in Dynamic Test Program

The isolated models were tested for response to eight different earthquake input motions. The types of earthquakes varied from those with predominantly low frequency content, like the 1985 Mexico City Earthquake, to earthquakes with predominantly high frequency content, like the 1957 San Francisco Earthquake. The following earthquake ground motions were used for input [7,8,9,10]:

(1) Imperial Valley Earthquake (El Centro) of May 18, 1940 - S00E component

(2) Kern County Earthquake (Taft Lincoln School Tunnel) of July 21, 1952 - S69E component

(3) San Francisco Earthquake (Golden Gate Park) of March 22, 1957 - S80E component

(4) Parkfield Earthquake (Cholame, Shandon, Calif. Array No.2) of June 27, 1966 - N65E component

(5) San Fernando Earthquake (Pacoima Dam) of February 9, 1971 - S14W component

(6) Bucharest Earthquake (Building Research Institute) of March 7, 1977 - EW component

(7) Miyagi-Ken-Oki Earthquake (Tohoku University) of June 12, 1978 - S00E component

(8) Mexico City Earthquake (Mexico City Station SCT) of September 19, 1985 - S60E component

The records were time scaled by a factor of the square root of four to satisfy similitude requirements for the 1/4-scale model. For example, an earthquake record which lasted 60 seconds in real time would have lasted 30 seconds during the earthquake simulator tests on the 1/4-scale model. A list of the earthquakes used in the testing program and the symbols subsequently used to refer to each earthquake in the rest of this report are given in Table 4.5.

Plots of the real-time earthquake ground motions normalized to 1g peak acceleration and their FFTs are given in Figure 4.2. As can be seen in the FFT plots for each earthquake, there is a wide range of earthquake characteristics represented by this group. The real-time Mexico City has a frequency content concentrated almost entirely in the region of 0.5 Hz. The real-time Bucharest signal has a significant amount of low frequency content which gradually decreases to near zero at a frequency of about 5 Hz. The real-time El Centro record has most of its frequency content between 1 Hz and 3 Hz and the Miyagi-Ken-Oki record has most of its frequency content around 1 Hz. Parkfield has a frequency content ranging between 0.5 Hz and 3 Hz while the frequency content of the Pacoima Dam record ranges between 1 Hz and 4 Hz. The frequency of the San Francisco record has a peak near 4 Hz and another at about 7 Hz. The Taft earthquake record has a broad range of frequency (0.5 Hz to 5 Hz).

5. TEST RESULTS FOR MODEL ON NEOPRENE BEARINGS

5.1 Free Vibration Test Results

Free vibration tests were conducted on the steel model isolated with the neoprene bearings. An initial displacement of 0.25 inch was a result of the force applied to the stiffeners directly above the bearings. Recognizing the strong nonlinearity of the bearings, it is important to note the shear strain in the bearings when comparing frequency results with those obtained from other tests. Thus, the 1.5 Hz natural frequency indicated by this test was at an initial shear strain level of 11%. The approximate equivalent viscous damping obtained from the log decrement curve (Figure 5.1) was 11% of critical and the second lateral mode frequency, obtained from the Fourier amplitude plot of the roof acceleration time history, was 5.7 Hz (Figure 5.2).

5.2 Harmonic Vibration Test Results

The model was then subjected to harmonic base motions at a variety of frequencies ranging from 1.0 Hz to 6.0 Hz. The input frequencies are given in Table 4.1. Peak lateral floor acceleration for each level of the model was normalized to peak lateral table acceleration at each frequency of input and was plotted against frequency (Figure 5.3). From these plots the fundamental lateral frequencies were estimated. These frequencies were confirmed by taking FFTs of the story acceleration and bearing displacement time histories. The fundamental lateral frequency was estimated to be 1.05 Hz at a peak shear strain of 65%. The same test conducted at a shear strain level of 8% gave a fundamental frequency of 1.4 Hz and a second mode lateral frequency of 5.2 Hz.

The approximate equivalent viscous damping ratio was determined by plotting hysteresis loops (Figure 5.4) for bearing shear force versus relative horizontal bearing displacement from which the loss angle (δ) of the rubber bearing was obtained and from which the approximate equivalent viscous damping ratio (ξ) was calculated using the equations:

$$\delta = \sin^{-1} \frac{4A_c}{\pi A_r} \quad \text{and} \quad \xi = 0.5 \tan \delta ,$$

where A_c is the area of one cycle of the hysteresis loop and A_r is the area of the circumscribing rectangle. From these equations, the equivalent viscous damping was estimated to be 9.9% at 8% maximum shear strain and 7.6% at 65% maximum shear strain.

5.3 White Noise Vibration Test Results

The base-isolated structure was then subjected to the white noise base input motion described in Section 4.1. By taking FFTs of the 9th story horizontal acceleration and the bearing shear force time histories (Figures 5.5 and 5.6), the modal frequencies were estimated. The peak magnitude of bearing displacement during this test corresponded to a peak shear strain in the rubber of 6%. From this test, the fundamental lateral frequency was estimated to be 1.53 Hz and the 2nd mode frequency to be 5.26 Hz.

5.4 Discussion of Preliminary Tests

The preliminary test results are summarized in Table 5.1, but the decrease in stiffness with increasing shear strain that the rubber experienced made direct comparisons between the free vibration, harmonic vibration and white noise vibration tests difficult. However, as a first step, the relation

$$f_{res} = C_p \sqrt{k_h(\epsilon_{max})} \tag{5.1}$$

was assumed between the resonant frequency (f_{res}) and the shear stiffness of the rubber (k_h). The term C_p is a proportionality constant which depends on the mass of the system. The shear stiffness was taken as that given by Figure 3.2 at the maximum shear strain (ϵ_{max}) during the test.

Following this simple approach, the free vibration test which gave a fundamental frequency of 1.5 Hz at 11% shear strain implied a frequency of 1.18 Hz at 100% shear

strain. The harmonic test gave a fundamental frequency of 1.05 Hz for a 65% shear strain and a fundamental frequency of 1.4 Hz at 8% shear strain which implied fundamental frequencies of 1.02 Hz and 1.06 Hz, respectively, at 100% shear strain. The white noise test gave a fundamental frequency of 1.53 Hz at 6% shear strain and this implied a frequency of 1.13 Hz at 100% shear strain. Thus, the three tests gave results which were reasonably consistent - assuming Equation 5.1 and the test data for the bearings given in Figure 3.2. This result is unlike that found during previous tests on the reinforced concrete structure [2], however, this was probably due to the higher level of shear strain achieved in these free vibration tests.

As a first order estimation of the natural frequency of the model on the neoprene bearings the single degree-of-freedom equation:

$$f = \frac{1}{2\pi}\sqrt{\frac{k_h}{m}} \tag{5.2}$$

was used; where m = the mass of the structure = 122 kips and the value for k_h at 100% shear strain is given by Figure 3.2. The results are presented in Table 5.2.

The results indicate that the natural frequency of the isolated structure determined by the free-vibration test was about 6% higher than that given by the simple rigid body theory, the harmonic test frequency was about 6% lower, and the white noise test result was about 2% higher than the rigid body result.

5.5 Earthquake Motion Test Results

The model supported on the neoprene bearings was designed primarily to be a 1/4-scale model of a building isolated against strong ground motion in firm soil conditions. The isolated natural frequency of the model was approximately 1 Hz for large bearing displacements - corresponding to approximately 0.5 Hz (T = 2 sec) for the full-scale building represented.

The isolated model was subjected to the time-scaled earthquakes listed in Table 4.2. Each earthquake was input at a level of peak table acceleration sufficient to cause maximum bearing shear strains greater than 50%. It was particularly hoped that the response of the structure be observed during column uplift, especially since the design of the bearing connections used in these tests differed from the design used in the previous study [2]. The connections used in these tests were designed to accommodate up to 0.75 inch of uplift before the base of the column would disengage from the top of the bearing.

The key points of interest which are discussed in the next section include:

(1) the effectiveness of the neoprene bearings at reducing the levels of acceleration from those of the table acceleration;

(2) the degree to which the isolated structure responded in its first mode;

(3) the performance of the bearing connections near or during column uplift; and

(4) the effect of vertical ground motions on the response of the structure.

By studying the acceleration profiles presented in Figure 5.7 for each of the different earthquakes, the effectiveness of the isolation system for the different ground motions was seen. The profiles are plots of maximum horizontal story acceleration for each level divided by the maximum horizontal table acceleration versus the story height. The peak story acceleration values used for these plots did not necessarily all occur at the same time. However, subsequent analysis showed that the peak values occurred at times very close to each other. The values used were the maximum accelerations for each floor over the duration of the earthquake motion. Thus, the profiles are really envelopes defining the maximum value of the acceleration at each story for the earthquake signal.

The effectiveness of the isolation system depended greatly on the frequency content of the earthquake signal. That is, for an earthquake signal rich in frequencies

near the resonant frequency of the isolated structure, the isolation system's effectiveness was limited and, in fact, if sufficient damping had not been provided in the isolation system then a significant increase in structure acceleration over ground acceleration would have resulted. It was also clear that for earthquake signals with the dominant portion of their frequency content well away from the isolated frequency, the isolation system provided significant reductions in structure accelerations over ground accelerations, on the order of 1/4 in some cases (San Francisco, for example).

Figure 5.8 shows the acceleration time histories of all nine stories superimposed for each earthquake signal used in this set of tests. For all but the San Francisco signal, generally, all the stories were moving in phase. This is important since the use of simple design formulae based on site design response spectra for design of base-isolated structures implies an assumption of single degree-of-freedom behavior, which in-phase floor accelerations would help justify.

The performance of the neoprene bearings at all levels of shear strain tested (up to 114%) was studied and felt to be excellent. The bearings displayed no tendency to roll out [11], even at shear strains exceeding 100%, and the shear force versus shear displacement plots (Figure 5.9) for the combined system of bearings at large shear strains do not indicate any significant changes in the stiffness properties of the bearings even though the bearings were subjected to a large number of displacement cycles which exceeded 50% shear strain. It should be noted that the hysteresis loops in Figure 5.9 are for the entire system of bearings, not an individual bearing. The presence of the relatively thick top and bottom plates of these bearings was felt to be primarily responsible for the favorable performance.

In order to ascertain whether the horizontal response of the model structure was affected by vertical ground motions, the El Centro ground motion was used to excite the model twice at the same levels of input. For both runs the horizontal table

control was set at a span of 300. In the first case (860627.04) only horizontal motion was supplied to the shaking table. The peak horizontal acceleration for the table was 0.645g and the peak horizontal acceleration in the model was 0.407g.

In the second case (860627.13) both horizontal and vertical motions were input to the table. The peak horizontal accelerations in the table and model were 0.650g and 0.434g, respectively. It appears from these tests that the addition of vertical motion had little influence on the horizontal response of the model.

6. TEST RESULTS FOR MODEL ON LEAD-PLUG BEARINGS

After testing was completed on the steel structure isolated with neoprene bearings, the structure was base isolated with eight natural rubber bearings. The four bearings located under the interior columns each contained a solid lead core while the central cores of the four bearings located under the corner columns were hollow. As was done for the structure on the neoprene bearings, the model was subjected to a set of preliminary dynamic tests before being tested with earthquake ground motions. The results of these tests are presented in the following sections.

6.1 Free Vibration Test Results

The free vibration tests indicated that the fundamental frequency of the isolated model was 2.85 Hz and the second mode lateral frequency was 9.1 Hz (Figure 6.1). The high shear stiffness of this isolation system meant that the approximate equivalent viscous damping ratio could not be found from the free vibration tests. The maximum pull-back force that could be generated resulted in less that 1% initial shear strain, and this strain was insufficient to allow an analysis of the log-decrement curve for the damping ratio.

6.2 Harmonic Vibration Test Results

The model was then subjected to harmonic base motion at a variety of frequencies ranging from 1.0 Hz to 1.7 Hz (Table 4.3 lists the input frequencies). The model responses of peak lateral floor acceleration normalized to peak table acceleration at each input frequency were plotted against frequency (Figure 6.2). The fundamental frequency was determined from this plot and also by taking FFTs of the 9th story acceleration time history and the relative bearing displacement time history.

The fundamental lateral frequency indicated by this test was 1.15 Hz at a peak shear strain of approximately 26% in the rubber, and the second mode frequency was 5.85 Hz. Hysteresis loops for bearing shear force versus relative bearing displacement are shown in Figure 6.3. The equivalent viscous damping for the bearings was calculated directly from the area of the hysteresis loops and was found to be 6.7% of critical for the bearings

without a lead core and 24% of critical for the bearings with a lead core.

6.3 White Noise Vibration Test Results

The isolated model was then subjected to white noise base motion. By taking FFTs of the 9th story acceleration time history and the relative bearing displacement time history and observing the frequencies associated with the peaks in the Fourier spectra plots the modal frequencies were estimated (Figures 6.4 and 6.5). The first mode frequency was 2.42 Hz and the second mode frequency was 7.5 Hz. The level of peak shear strain in the rubber for this test was very low, 0.4%.

6.4 Discussion of Preliminary Tests

As was found for the preliminary tests performed with the neoprene bearings, the non-linearity of the bearing shear stiffness with respect to horizontal bearing displacement made comparisons of preliminary test results difficult. However, for these tests, the results were not adjusted for comparison at 100% shear strain since insufficient shear stiffness data existed for the lead-plug bearings below strain levels of 5%. This problem, however, illustrates one of the advantages of a lead-plug isolation system; extremely stiff behavior of the bearings at small shear strains. This would cause a structure isolated with lead-plug bearings to perform similarly to a fixed-base structure. Unfortunately, the magnitudes of load which could be applied in the free vibration and white noise tests were insufficient to cause significant deformation in the lead core so that minimal amounts of information could be obtained from these two tests.

The bearings were, however, displaced sufficiently during the harmonic vibration test and those results were adjusted to give an estimate of the isolated frequency at 100% shear strain. This value was 0.97 Hz and compared favorably with the value of 1.06 Hz given by Equation 5.2 using the known mass and the stiffness at 100% shear strain.

6.5 Earthquake Motion Test Results

The 1/4-scale steel frame and the lead-plug bearings were subjected to the earthquake tests listed in Table 4.4. The following discussion is limited to the sequence of tests which caused maximum rubber shear strains in excess of 50% but did not cause any significant column uplift (860707.09-860707.16). Structural and bearing behavior during column uplift will be discussed separately in Section 6.6.

The key points of interest here are:

(1) the effectiveness of the lead-plug isolation system for the variety of earthquake motions used in these tests;

(2) the degree to which the isolated building responded in the 1st mode; and

(3) the performance of the bearings at large shear strains.

The effectiveness of the isolation system at reducing the accelerations transmitted to the structure can be seen by studying the story acceleration profiles (Figure 6.6) for each of the earthquake signals. In general, the isolation system performed best against the highest frequency ground motions. This is consistent with previous shaking table test results [2]. The acceleration profiles also indicated that the structure responded predominantly in the first mode, and the plots of the story acceleration time histories were superimposed to help verify this (Figure 6.7). As was seen previously, all the stories were, in general, moving in phase with each other and the story acceleration amplitudes were similar for all levels. The San Francisco signal was the only earthquake motion for which this was not the case. The San Francisco signal had a significantly higher frequency content than the other signals so it was most able to excite some higher mode response in the structure.

The performance of the isolation bearings is illustrated by the plot of the shear force hysteresis loops for the combined system of bearings (Figure 6.8) for each earthquake signal. Note that the shear force plotted in these loops is the sum of the shear forces in all the bearings, and this was the structure base shear. It was apparent that, as with the

neoprene bearings, the lead-plug bearings performed extremely well at large shear strains but in this case, deterioration of the stiffness properties of the bearings containing lead plugs became evident as testing continued. This is most clearly shown in Figure 6.9 where the effective stiffness for a lead-plug bearing is plotted versus the number of earthquake tests which caused at least one cycle of shear strain in excess of 25%. The lead-plug bearing shear stiffness after 36 earthquake tests decreased to approximately 33% of its initial stiffness. This is not considered to be a problem, however, since in practice an isolation bearing would not be expected to undergo such a large number of significant displacement cycles.

6.6 Performance During Column Uplift

In order to study the effect of column uplift on the structure and the isolation system the Bucharest, El Centro, and the Mexico City earthquake motions were selected and each was input at increasing magnitudes until significant column uplift was induced. These ground motions were selected because column uplift could be generated at modest levels of table input using them.

6.6.1 Bucharest Tests

The sequence of tests using the Bucharest earthquake ground motions had peak table accelerations of 0.241g, 0.296g, 0.343g, and 0.348g. Two observations can be made from the story acceleration profiles (Figure 6.10) for these tests. First, the amplitude of the profile increased modestly as the input magnitude increased and secondly, the shape of the profile became more curved with increased input. Significant amounts of column uplift occurred during the tests with input accelerations of 0.343g and 0.348g and a small amount of uplift occurred during the 0.296g test (Figure 6.11).

The principal effect of column uplift on the structure appeared to be to increase the higher mode responses in the structure. This was due to impact of the column base on top of the bearings when the column came back down after uplifting. Figure 6.12 illustrates this point. The high frequency responses of the structure were greatest for the earthquake

tests during which column uplift occurred (Bucharest 0.348g). This would appear to have some serious implications for buildings with contents sensitive to high frequencies.

The effect of column uplift on the bearings was evaluated from individual bearing hysteresis loops (Figure 6.13) and the combined isolation system hysteresis loops (Figure 6.14). The hysteresis loops for the individual bearings subject to column uplift show that column uplift affected shear hysteresis loops in two ways. When the column lifted, the axial force on the bearing was reduced to zero from the static dead load compressive force. This resulted in a slight change in the shear stiffness of the bearing and shows up in the extreme left side of the hysteresis loop for bearing NO1. The right hand side of the hysteresis loop shows what happened when the axial load on the bearing increased dramatically during the extreme lateral bearing displacement associated with column uplift. The hysteresis loop for bearing NO1 appears temporarily to become unstable and start to roll over. However, because there was a bearing at the other end of the structure which was in an axially unloaded state while bearing NO1 was experiencing its peak compressive load, the effect of column uplift was barely felt on the isolation system as a whole. This is shown by the stability of the hysteresis loop plot for the complete isolation system (Figure 6.14). Clearly, the action of the bearings in parallel prevented a localized instability from causing a failure of the isolation system.

6.6.2 El Centro Tests

Unlike the story acceleration profiles for the Bucharest test sequence, the story acceleration profiles for the El Centro test sequence did not change significantly in magnitude or shape (Figure 6.15). This was probably due to the fact that the effect of the frequencies associated with column uplift was masked by the effect of the higher frequencies of the El Centro ground motion. The magnitude of column uplift during this test sequence varied from no uplift for the 0.313g test to 0.75 inch for the 0.842g test (Figure 6.16). The effect of column uplift on the bearings is best shown by hysteresis loops for the individual bearings (Figure 6.17). The El Centro earthquake motion caused uplift only at one end of

the structure so the hysteresis loops do not have the symmetric shape of those for the Bucharest tests (Figure 6.13), although at their extreme left end the same shape occurs. The shape of the hysteresis loop for the total isolation system again illustrates the stable nature of the bearings when acting in unison (Figure 6.18).

6.6.3 Mexico City Tests

The story acceleration profiles for the Mexico City sequence of tests are shown in Figure 6.19. The profiles are similar to those for the Bucharest test sequence, although the change in profile magnitude is more dramatic for the Mexico City test sequence. It is worth noting that both the Mexico City and Bucharest ground motions are predominantly low frequency motions and that only with column uplift would any higher frequency input be introduced to the base of the structure. The amount of column uplift generated by the Mexico City 0.219g test was 0.42 inch (Figure 6.20); no significant uplift occurred during the other tests in this sequence. The effect of column uplift on the structure and isolation system was identical to that for the Bucharest and El Centro test sequences, and is shown by the hysteresis loop for a bearing subject to uplift (Figure 6.21) and by the hysteresis loop for the entire isolation system (Figure 6.22).

7. RESPONSE SPECTRUM ANALYSIS

7.1 Experimental and Theoretical Frequencies and Mode Shapes

The 1/4-scale braced steel frame structure was analyzed using the commercial finite element program IMAGES-3D [12]. The structure was modeled as a two dimensional frame. Beam-column elements were used to model the columns and beams while truss elements were used to model the bracing. Spring elements were used to model the bearing shear stiffness and axial stiffness. No rotation was assumed to occur at the base of the model. The computer model is shown in Figure 7.1 and Table 7.1 lists the element cross-section properties which were used in the analysis. The first loading condition (Figure 2.2) was applied to the neoprene bearing base-isolated structure and the second loading condition was used for the model of the lead-plug base-isolated structure.

The spring stiffness used to model the bearings corresponded to the axial and shear stiffness of the bearing system. For this analysis, an axial stiffness of 600 kips/inch was used. Since the shear stiffness of the bearings was sensitive to the amount of shear strain in the rubber, the effective shear stiffness of the entire isolation system was divided by four and used for each of the spring stiffnesses in the horizontal direction. The effective stiffness of the neoprene bearing system varied between 14.9 kips/inch and 16.4 kips/inch. The effective shear stiffness of the lead-plug system varied more; between 9.7 kips/inch and 14.0 kips/inch. The larger variation of stiffness for the lead-plug system was due in part to degradation of the lead core.

The first three natural frequencies and mode shapes for the horizontal modes were calculated; the results are presented in Table 7.2. Only the first two modes were determined experimentally. The analytically determined first and second mode frequencies compare quite closely with the experimental frequencies: the theoretical frequencies slightly overestimate the experimental values. Comparison of the experimental and analytical mode shapes (Figure 7.2) reveals that the theory gave results which

compare well with the experimental results, however, the first mode shape determined experimentally indicates that the superstructure was more flexible than the theory predicted — a result not consistent with the result of analytical frequencies lower than experimental frequencies.

The modal participation factor for each mode 'i' is defined by

$$PF_i = \frac{\phi_i^T \mathbf{M}\, \mathbf{r}}{M_i} ,$$

where

ϕ_i = the mode shape vector for mode 'i' ;

$\mathbf{M}$ = the mass matrix ;

$\mathbf{r}$ = the load influence vector ; and

M_i = the modal mass = $\phi_i^T \mathbf{M}\, \phi_i$.

The load influence vector is a vector of 1's and 0's, with the rows corresponding to horizontal displacement degrees-of-freedom being 1's, all other rows being 0's.

From these equations the modal participation factors for the first three modes were determined to be 1.08, -0.09, and 0.01, respectively. These values indicate that the first mode was the predominant mode of response for the base-isolated structure. This was confirmed by calculating the effective modal weight for each mode 'i'. The effective modal weight is defined as

$$EMW_i = (PF_i)^2\, g \,/\, M_i ,$$

where g is the acceleration of gravity. The effective modal weights were determined to be 199 kips, 0.310 kips, and 0.008 kips, respectively, for the first 3 modes. Thus, the effective modal weight for the first mode was approximately 99% of the total weight of the structure. This again suggests that the predominant response of the structure was in the first mode, and agrees with the experimental results presented in Chapters

5 and 6. On the basis of these results it was concluded that only the first mode needed to be considered in a linear elastic response spectrum analysis for this structure.

7.2 Response Spectrum Analysis

A linear elastic analysis using the response spectrum method was performed to estimate the maximum bearing displacements and maximum base shear for each of the earthquake tests conducted on both of the isolation systems tested. The spectra used for input were the 10% damped linear elastic spectra of the actual shaking table acceleration time history recorded from each test. Only the first mode was included in each analysis. The analytical results for the model isolated on both sets of bearings were found to compare reasonably well with the test results (Table 7.2). Only for the Mexico City test did the experimental results differ significantly from the analytical values. The difference between the analytical and experimental results for the Mexico City test signal shows that the response spectrum technique can underestimate the maximum bearing displacements significantly for ground motion spectrums which vary greatly in amplitude near the fundamental frequency of the structure. It should be remembered that the unsmoothed spectra from the actual shaking table motions were used for this analysis. Unless a smoothed spectrum is used for analysis, it is possible to use a value from the spectrum which may be in either a trough or peak and this could cause a large difference between the experimental and analytical results.

On the basis of these results, it was concluded that structures which remain elastic can be reliably analyzed using the response spectrum method to give estimates for maximum base shear and bearing displacement. This assumes, of course, that the spectrum used for the analysis is a reasonable representation of ground motion that could be expected for the particular site.

8. SEAONC BASE ISOLATION DESIGN FORMULA

The Structural Engineers Association of California (SEAOC) has recognized the "need to supplement existing codes with design requirements developed specifically for seismically isolated buildings. This need is shared by the public which requires assurance that seismically isolated buildings are *safe* and by the engineering profession which requires a minimum standard upon which design and construction can be based." [13] Out of this need the "Tentative Seismic Isolation Design Requirements, September, 1986" were developed by the Base Isolation Subcommittee of the Seismology Committee of the Structural Engineers Association of Northern California (SEAONC). These requirements were intended to supplement the SEAOC "Tentative Lateral Force Requirements, October, 1985" document [14]. The seismic isolation design requirements are tentative and at the time of writing have not been adopted by the SEAOC Seismology Committee. The basic design philosophy and design formulae recommended by this document are discussed here and experimental results from the tests discussed in Chapters 5 and 6 are compared with values given by the proposed design formulae.

8.1 Summary of SEAONC Design Procedure

The general design philosophy requires that: (1) the base-isolated structure remain stable for required design displacements; (2) the isolation system should provide resistance which increases with increases in displacement; (3) the system should be capable of repeated cyclic loads without any significant degradation; (4) the isolation system should have quantifiable engineering parameters.

Either of two design procedures are permitted under the proposed design guidelines. The first uses a set of simple equations to prescribe design values of displacement and base shear. These formulae are similar to the seismic lateral force formula now in use for conventional building design. The second procedure requires a dynamic analysis to determine the peak responses of the base-isolated structure pertinent to

design. This procedure would be required of any structure with geometric irregularities or of any especially flexible structures.

The tentative design provisions are based on a level of earthquake ground motion that corresponds to a 500-year return-period earthquake as described by the ATC 3-06 recommended ground motion spectra [15]. The provisions require the base-isolation system and all structural components at or below this level to withstand the full force and effects of this ground motion without damage. Structural elements above the isolation level are not, however, required to be designed for the full force of this motion. A small amount of inelastic damage is allowed above the isolation level if sufficient ductility is provided. The overall philosophy is that base-isolated structures should be at least as safe as conventional buildings during extreme earthquake loadings. The inelastic factor of 2.76 for the 500-year return-period earthquake is meant to ensure elastic response of the structure for ground motions less severe than those of the 50- to 100-year earthquake.

The purpose of the following comparisons between the test results and the values for bearing displacement given by the simple design equations is to evaluate the reliability of the design formulae for this particular structural system. Further work is being conducted in this area for a wide range of isolation systems.

8.2 Comparison of Experimental and Design Displacements

The shaking table test displacements for the 1/4-scale test structure were compared with the displacements predicted by the SEAONC Tentative Seismic Isolation Design Requirements. The SEAONC base-isolation code formula for displacement, D, is given by equation (1) from section B.2:

$$D = \frac{10\,Z\,N\,S\,T}{B}, \tag{8.1}$$

where the terms are defined as follows:

D = minimum displacement for which the isolation system must be designed ;

Z = earthquake zone factor (0.3 or 0.4 for California) ;

N = coefficient to modify displacement due to distance from fault ;

S = soil factor, ranging between 1.0 and 2.7 ;

T = period of the isolated structure ;

W = weight of isolated structure above and including the isolation surface ;

g = acceleration of gravity ;

k_{min} = minimum effective stiffness of the isolation system ; and

B = damping coefficient, ranging between 0.8 and 2.0 .

The period for the prototype isolated structure is calculated from the single degree-of-freedom equation

$$T = 2\pi \sqrt{\frac{W}{k_{min}\, g}} \quad . \tag{8.2}$$

In order to compare the experimental displacements and values given by the proposed code equation (Equation 8.1) the experimental displacements had to be converted to full-scale values. This required that the experimental displacements be multiplied by the scale factor of 4 (Table 2.1).

The values for S and B used in the calculations are explained below. A value for S of 2.7 was used for the Mexico City earthquake since the soil condition at the data collection site for that signal fell into the S_4 category. A value of 2.0 was used for S for the Bucharest earthquake signal since that signal also consisted mostly of low frequency motion although not as low as the Mexico signal. A value of 1.0 was used for the San Francisco signal comparisons since that motion was comprised of high frequency content. A value of 1.5 was used for all the other earthquake signals. The isolated period for the scale model was calculated from Equation 8.2 using values from Figure 3.2 and Figure 3.4 for the stiffness term k_{min} based on the shear strain which

corresponded to the maximum experimental displacement, D_{exp}, for the particular test. For use in Equation 8.1, the scale-model period was multiplied by the square root of the scale factor (Table 2.1). A value of 1.2 was used for B since each isolation system had a damping ratio of about 10%. Three different types of values were used for Z N in Equation 8.1. They were:

(1) the peak shake table acceleration, PGA;

(2) the coefficient A_a based on the effective peak acceleration (as defined by ATC 3-06) for each of the table signals; and

(3) the coefficient A_v based on the effective peak velocity (as defined by ATC 3-06) for each of the table signals.

Displacement values were calculated for the different tests using Equations 8.1 and 8.2 and the ratios D_{code}/D_{exp} were computed for the series of tests and are given in Table 8.1.

The use of the design formula with Z N = PGA gave conservative results for all the earthquake test signals except Bucharest, Mexico City, and Miyagi-Ken-Oki. These signals contained significant low frequency motion and therefore the model responses were more velocity dependent than acceleration dependent. The use of the effective peak acceleration coefficient A_a was less conservative than the use of the PGA coefficient for all the signals except San Francisco. San Francisco contained very little low frequency motion so the difference between the results using the PGA and A_a coefficients was negligible. Results using the effective peak velocity coefficient A_v were generally more conservative than when using either the PGA or A_a coefficients for the test signals containing significant low frequency content. A less conservative result was obtained for the high frequency San Francisco motion using the coefficient A_v than when using either the PGA or A_a coefficients, however this result was still conservative relative to the experimental results.

The comparison of test results with the design formula was extended to include two modified earthquake signals. These signals are referred to here as ATC-S1 El Centro, ATC-S2 El Centro, ATC-S1 Taft, and ATC-S2 Taft. The S1 and S2 terms refer to the soil conditions, S1 being firm and S2 soft. These signals have been modified to represent ground motions which would have response spectra similar in shape to the ATC design spectra for S1 and S2 soil types. The response spectrum for the normalized ATC-S1 El Centro shaking table motion is shown in Figure 8.1. The structure isolated with the lead-plug bearings was tested with these signals and the results were compared to the SEAONC design formula values as described above. Only the procedure using the velocity based coefficient A_v gave results consistently more conservative than the experimental results. The ATC modified signals were clearly more severe to low frequency structures than the unmodified Taft and El Centro signals.

On the basis of the test results using both the modified and unmodified shaking table motions, it was concluded that the velocity based coefficient A_v is the most reliable coefficient for use in the design formula and that with use of a reliable velocity based design coefficient the simple design formula can be expected to yield reliable estimates for the maximum bearing displacements.

9. IMPLICATIONS OF THE TEST RESULTS

On the basis of the earthquake simulator tests of the scale model, conclusions were drawn in several areas. The test results show that base isolation can be effective for medium-rise structures if an adequate shift in the fundamental period of the structure is provided by the isolators. For the 1/4-scale model tested, the fundamental fixed-base frequency was 2.82 Hz (with the 2nd loading distribution) and the isolated first mode frequency was about 1 Hz. The two isolation systems tested provided reductions of acceleration levels of up to 1/4 (for the San Francisco signal).

Column uplift was shown to have a significant effect on both the performance of the bearings and the response of the structure. The large variations in axial load, which were present when column uplift occurred, had an effect on the shear stiffness of the bearings. While the bearings at one end of the model became unloaded axially they were still displaced in shear, and the stability of bearings has been shown [11] to be highly dependent upon axial load. Simultaneously, the bearings at the opposite end of the structure experienced axial loads approximately double their static dead loads while being displaced laterally, and thus they also experienced a momentary change in horizontal stiffness. However, if the amount of column uplift exceeds the height of the bearing shear connection the bearing will become detached from the base of the structure. This is, of course, unacceptable. A further complication of column uplift is that the pounding which occurs when the building comes back into contact with the foundation excites higher mode responses in the structure. This would be a problem for any structure or internal components sensitive to high frequency motions, especially vertical motions.

The effect of uplift was especially evident in the story acceleration profiles for the Bucharest and Mexico City test sequences. The tests conducted on the steel frame with the two kinds of isolation system were quite extensive and consisted of a large number of earthquake tests which caused several cycles of shear displacement in excess

of 25% shear strain. The cumulative effect of the large strain displacement cycles on the shear stiffness was quite dramatic for the lead-plug bearings. This was in contrast to the effect on the neoprene bearings or the natural rubber bearings without a lead core. Only the bearings which contained a lead core showed any signs of decreased stiffness. The shear stiffness of the lead-plug bearings was seen to decrease from 7.9 kips/inch to 2.6 kips/inch after 36 earthquake tests each of which caused at least one displacement cycle exceeding 25% shear strain.

The shaking table tests also showed that the lead-plug isolation system tended to excite more high mode responses in the structure than did the neoprene isolation system. There was not, however, as dramatic a difference between the responses for the two isolation systems as there was when column uplift occurred.

The response spectrum method of analysis was shown to be effective for calculating values of the maximum model responses of bearing displacement and base shear. The analysis used the unsmoothed response spectra of the actual table acceleration as input for each of the earthquake signals. Comparisons between the test results and the response spectrum analysis showed that the results agreed best for the higher frequency earthquake signals. This was felt to be due to the unsmoothed nature of the response spectra and the sensitivity of the method to change in the spectral values for the range of period around the period of the isolated model. The lower frequency earthquake signals (such as Bucharest and Mexico City) had greater variations in the spectral acceleration ordinates in the region of the fundamental period of the isolated model than the higher frequency motions. Thus, a slight difference between the analytical and experimental periods could result in a large difference in the spectral accelerations used for the analyses. While the response spectrum method was found to give results comparable with the experimental results, it should be noted that the accuracy of the method is highly dependent on the accuracy, or reliability, of the spectra.

Finally, the proposed SEAONC code design formula for bearing displacement was found to be most accurate, and in general conservative, if the velocity based coefficient A_v was used to represent the earthquake ground motion magnitude. The proposed formula was not conservative for the low frequency motions when the coefficients based on peak acceleration or effective peak acceleration were used. The design values compared most closely to the experimental values when the term A_v, which is based on the effective peak velocity, was used to represent the product Z N in the design formula. This is because the period of a base-isolated structure is in the constant velocity region of the response spectra for most earthquake motions.

REFERENCES

[1] J. M. Kelly, "Aseismic Base Isolation: Review and Bibliography," *Soil Dynamics and Earthquake Engineering*, Vol. 5, No. 3, (1986).

[2] M. C. Griffith, J. M. Kelly, V. A. Coveney and C. G. Koh, "Experimental Evaluation of Seismic Isolation of Medium Rise Structures Subject to Uplift," Report No. UCB/EERC-88/02, Earthquake Engineering Research Center, University of California, Berkeley, (1988).

[3] J. M. Kelly, M. C. Griffith and I. D. Aiken, "A Displacement Control and Uplift Restraint Device for Base Isolated Structures," Report No. UCB/EERC-87/03, Earthquake Engineering Research Center, University of California, Berkeley, (1987).

[4] Arthur A. Huckelbridge, "Earthquake Simulation Tests of a Nine Story Steel Frame with Columns Allowed to Uplift," Report No. UCB/EERC-77/23, Earthquake Engineering Research Center, University of California, Berkeley, (1977).

[5] R. Sause and V. V. Bertero, "A Transducer for Measuring the Internal Forces in the Columns of a Frame-Wall Reinforced Concrete Structure," Report No. UCB/EERC-83/05, Earthquake Engineering Research Center, University of California, Berkeley, (1983).

[6] C. J. Derham and H. G. Thomas, "The Stability of Rubber/Steel Laminated Building Bearings," *Natural Rubber Technology*, Vol. 14, No. 3, (1983).

[7] "Earthquake Catalog of California, January 1, 1900 to December 31, 1974," Charles R. Read et. al., California Division of Mines and Geology, Special Publication No. 52, 1st Edition and Cal. Tech. Report No., EERL 80-01, D.M. Lee, P.C. Jennings, G.W. Housner, (January 1980).

[8] N. Ambraseys, "The Romanian Earthquake of March 4, 1977," Preliminary Report of UNESCO Earthquake Reconnaissance Mission, (1977).

[9] Bruce Ellingwood (Ed.), "An Investigation of the Miyagi-Ken-Oki, Japan, Earthquake of June 12, 1978," National Bureau of Standard Center for Building Technology, Washington, D. C., (1980).

[10] S. Suzuki and A. S. Kiremidjian, "The Mexico Earthquake of September 19, 1985, A Preliminary Report," The John A. Blume Earthquake Engineering Center, Dept. of Civil Engineering, Stanford University, Report No. 77, (1986).

[11] J. M Kelly, I. G. Buckle and H. C. Tsai, "Earthquake Simulator Testing of a Base-Isolated Bridge Deck," Report No. UCB/EERC-85/09, Earthquake Engineering Research Center, University of California, Berkeley, (1985).

[12] "IMAGES-3D User Manual," Celestial Software, Berkeley, California (1983).

[13] "Tentative Seismic Isolation Design Requirements," Report prepared by the Base Isolation Subcommittee of the Seismology Committee of the Structural Engineers Association of Northern California, (1986).

[14] "Tentative Lateral Force Requirements: October 1985," Report prepared by the Seismology Committee of the Structural Engineers Association of California, (1985).

[15] "Tentative Provisions for the Development of Seismic Regulations for Buildings," ATC Publication No. ATC 3-06, prepared by the Applied Technology Council, (1978).

TABLES

PARAMETER	1/4-SCALE MODEL/PROTOTYPE	
Length	L	1/4
Time	$\sqrt{L}$	1/2
Mass	L^2	1/16
Displacement	L	1/4
Acceleration	1	1/1
Stress	1	1/1
Strain	1	1/1
Force	L^2	1/16
Area	L^2	1/16

Table 2.1 Similitude Scale Factors for Prototype Responses

Channel	Instr.	Variable	Channel	Instr.	Variable
1	DCDT	hor. table dis.	43	FT	Column NO1 shear
2	DCDT	ver. table dis.	44	FT	Column NO1 mom.
3	ACCL	hor. table acc.	45	DCDT	Column NO1 tvdisp
4	ACCL	ver. table acc.	46	DCDT	Column NO1 rvdisp
5	ACCL	pit. table acc.	47	DCDT	Column NO2 tvdisp
6	ACCL	roll table acc.	48	DCDT	Column NO2 rvdisp
7	ACCL	twi. table acc.	49	DCDT	Column SO2 tvdisp
8	DCDT	v1 table dis.	50	DCDT	Column SO2 rvdisp
9	DCDT	v2 table dis.	51	DCDT	Column SO1 tvdisp
10	DCDT	v3 table dis.	52	DCDT	Column SO1 rvdisp
11	DCDT	v1 table span.	53	LP	Column NO1 pdisp
12	DCVT	hor. table vel.	54	LP	Column SO1 pdisp
13	FT	Column NO1 axial	55	LP	Bearing SO1 rdisp
14	FT	Column NO1 shear	56	LP	Bearing SO2 rdisp
15	FT	Column NO1 mom.	57	LP	1st floor hdisp
16	FT	Column NO1 axial	58	LP	2nd floor hdisp
17	FT	Column NO1 shear	59	LP	3rd floor hdisp
18	FT	Column NO1 mom.	60	LP	4th floor hdisp
19	FT	Column NO2 axial	61	LP	5th floor hdisp
20	FT	Column NO2 shear	62	LP	6th floor hdisp
21	FT	Column NO2 mom.	63	LP	7th floor hdisp
22	FT	Column NO2 axial	64	LP	8th floor hdisp
23	FT	Column NO2 shear	65	LP	9th floor hdisp
24	FT	Column NO2 mom.	66	ACCL	Column NO2 vacc
25	FT	Column SO2 axial	67	ACCL	Column NO1 vacc
26	FT	Column SO2 shear	68	ACCL	Column SO2 vacc
27	FT	Column SO2 mom.	69	ACCL	Column SO1 vacc
28	FT	Column SO2 axial	70	ACCL	base floor hacc
29	FT	Column SO2 shear	71	ACCL	1st floor hacc
30	FT	Column SO2 mom.	72	ACCL	2nd floor hacc
31	FT	Column SO1 axial	73	ACCL	3rd floor hacc
32	FT	Column SO1 shear	74	ACCL	4th floor hacc
33	FT	Column SO1 mom.	75	ACCL	5th floor hacc
34	FT	Column SO1 axial	76	ACCL	6th floor hacc
35	FT	Column SO1 shear	77	ACCL	7th floor hacc
36	FT	Column SO1 mom.	78	ACCL	8th floor hacc
37	FT	Column NI2 shear	79	ACCL	9th floor hacc
38	FT	Column NI2 mom.	80	ACCL	Frame NO vacc9
39	FT	Column SI2 shear	81	ACCL	Frame NO pacc9
40	FT	Column SI2 mom.	82	ACCL	Frame SO vacc9
41	FT	Column SI1 shear	83	ACCL	Frame SO pacc9
42	FT	Column SI1 mom.			

DCDT - Direct Current Displacement Transducer DCVT - Direct Current Velocity Transducer
ACCL - Accelerometer FT - Force Transducer LP - Linear Voltage Displ. Transducer

Table 2.2 - Instrumentation and Model Responses

FILE NO.	RUN	PK. TABLE ACCEL.(g's)	PK. MODEL ACCEL.(g's)	REL. BEARING DISPL.(in.)	UPLIFT (Y/N)
860624.02	1.0hz Sine	.053	.038	.068	N
860624.03	1.2hz Sine	.039	.050	.112	N
860624.04	1.4hz Sine	.029	.066	.181	N
860624.05	1.5hz Sine	.028	.060	.154	N
860624.06	1.6hz Sine	.032	.060	.137	N
860624.07	1.8hz Sine	.032	.058	.101	N
860624.08	2.0hz Sine	.043	.058	.097	N
860624.09	3.0hz Sine	.076	.070	.066	N
860624.10	4.0hz Sine	.120	.091	.045	N
860624.11	5.0hz Sine	.155	.252	.036	N
860624.12	5.2hz Sine	.116	.248	.053	N
860624.13	5.4hz Sine	.162	.224	.097	N
860624.14	5.5hz Sine	.163	.214	.086	N
860624.15	5.6hz Sine	.152	.202	.076	N
860624.16	5.8hz Sine	.180	.149	.076	N
860624.17	6.0hz Sine	.213	.126	.082	N
860624.18	12hz Sine	na	na	na	N
860625.01	1.32hz Sine	.078	.129	.447	N
860625.02	1.32hz Sine	.141	.212	.946	N
860625.03	1.30hz Sine	.142	.208	.942	N
860625.04	1.25hz Sine	.130	.210	.945	N
860625.05	1.20hz Sine	.126	.218	1.083	N
860625.06	1.15hz Sine	.115	.204	1.088	N
860625.07	1.10hz Sine	.114	.220	1.289	N
860625.08	1.05hz Sine	.109	.236	1.454	N
860625.09	1.00hz Sine	.106	.216	1.377	N

Table 4.1 Preliminary Tests of Steel Model with Neoprene Bearings

FILE NO.	RUN	SPAN	PK. TABLE ACCEL.(g's)	PK. MODEL ACCEL.(g's)	REL. BEARING DISPL.(in.)	UPLIFT (Y/N)
860624.19	Random Noise	30	1.101	.466		N
860624.20	Random Noise	30v	NA	NA	NA	N
860625.11	Random Noise	200	.036	.038	.103	N
860627.04	√4 ec2	300	.645	.407	2.249	N
860627.05	√4 mko	400	.300	.423	2.117	N
860627.06	√4 taft2	350	.739	.424	1.938	N
860627.07	√4 pac2	300	.495	.307	1.954	N
860627.08	√4 park2	350	.417	.356	2.082	N
860627.09	√4 sf2	230	1.400	.494	1.223	N
860627.10	√4 sf2	300	1.609	.619	1.571	N
860627.11	√4 buc1	250	.236	.328	2.118	N
860627.12	√4 mex2	150	.168	.306	2.570	N
860627.13	√4 ec2	300 h&v	.650	.434	2.378	N
860630.01	√4 ec2	300*	.578	.392	2.223	N
860701.01	√4 ec2	300**	.592	.753	2.247	N
860701.02	√4 mex2m	100	.162	.152	.824	N
860701.03	√4 mex2m	150	.187	.284	1.913	N

Table 4.2 Earthquake Tests of Steel Model with Neoprene Bearings

FILE NO.	RUN	SPAN	PK. TABLE ACCEL.(g's)	PK. MODEL ACCEL.(g's)	REL. BEARING DISPL.(in.)	UPLIFT (Y/N)
860702.01	pull-back	NA	NA	.330	.022	N
860702.02	pull-back	NA	NA	.418	.020	N
860702.03	Random Noise	100	.016	.044	.022	N
860702.04	Random Noise	500	.083	.122	.128	N
860702.05	Random Noise	750	.115	.167	.204	N
860702.06	Random Noise	1000	.170	.197	.298	N
860703.01	1.40hz Sine	20	.092	.189	.500	N
860703.02	1.35hz Sine	15	.080	.183	.541	N
860703.03	1.30hz Sine	15	.077	.168	.560	N
860703.04	1.25hz Sine	15	.066	.145	.496	N
860703.05	1.20hz Sine	20	.068	.143	.551	N
860703.06	1.10hz Sine	25	.079	.132	.552	N
860703.07	1.15hz Sine	26	.068	.154	.592	N
860703.08	1.05hz Sine	20	.089	.128	.523	N
860703.09	1.00hz Sine	40	.106	.180	.900	N
860703.10	1.50hz Sine	40	.099	.198	.509	N
860703.11	1.70hz Sine	60	.158	.176	.528	N

Table 4.3 Preliminary Tests of Steel Model With Lead-Plug Bearings

FILE NO.	RUN	SPAN	PK. TABLE ACCEL.(g's)	PK. MODEL ACCEL.(g's)	REL. BEARING DISPL.(in.)	UPLIFT (Y/N)
860707.01	√4 ec2	150	.296	.258	.806	N
860707.02	√4 miyagi	200	.174	.220	.930	N
860707.03	√4 taft2	220	.428	.334	1.048	N
860707.04	√4 pac2	220	.338	.290	1.252	N
860707.05	√4 park2	220	.243	.226	1.105	N
860707.06	√4 sf2	230	1.411	.467	1.183	N
860707.07	√4 buc1	300	.199	.242	1.348	N
860707.08	√4 mex2m	150	.173	.231	1.317	N
860707.09	√4 mex2m	200	.191	.325	2.337	N
860707.10	√4 buc1	275	.251	.323	2.207	N
860707.11	√4 sf2	300	1.590	.488	1.519	N
860707.12	√4 park2	350	.425	.337	1.942	N
860707.13	√4 pac2	350	.562	.463	1.985	N
860707.14	√4 taft2	400	.848	.407	2.259	N
860707.15	√4 miyagi	400	.310	.343	2.404	N
860707.16	√4 ec2	300	.633	.463	2.797	Y
860707.17	√4 ec2	150	.338	.202	.991	N
860708.03	√4 ec2	150	.313	.244	.904	N
860708.04	√4 ec2	225	.460	.288	1.712	N
860708.05	√4 ec2	300	.604	.453	2.648	Y
860708.06	√4 ec2	400	.842	.607	3.784	Y
860708.07	√4 ec2	150	.328	.205	1.014	N
860709.01	√4 buc1	275	.241	.293	1.825	N
860709.02	√4 buc1	350	.296	.444	2.729	Y
860709.03	√4 buc1	400	.343	.537	3.259	Y
860709.04	√4 mex2m	175	.146	.254	1.898	N
860709.05	√4 mex2m	250	.194	.425	3.063	N
860709.06	√4 mex2m	275	.219	.586	3.372	Y
860709.07	√4 mex2m	275	.217	.520	3.416	Y
860709.08	√4 buc1	400	.348	.767	3.723	Y
860709.09	√4 ec2	375	.723	.579	3.603	Y
860709.10	√4 ec2	150	.353	.213	1.054	N

Table 4.4 Earthquake Tests of Steel Model With Lead-Plug Bearings

SYMBOL	EARTHQUAKE	DATE	PGA (g)
ec1,ec2	Imperial Valley El Centro Site	May 18,1940 S00E	0.35
taft1,taft2	Kern County, Calf. Taft Lincoln School Tunnel	July 21,1952 S69E	0.18
sf1,sf2	San Francisco Golden Gate Park	March 22,1957 S80E	0.10
park1,park2	Parkfield, Calf. Cholame,Shandon,CA array #2	June 27,1966 N65E	0.49
pac1,pac2	San Fernando Pacoima Dam, Calif.	Feb. 9,1971 S14W	1.08
miyagi	Miyagi-Ken-Oki Tohoku University	June 12th 1978 S00E	0.24
buc1	Bucharest Building Research Inst.	March 7th, 1977 EW	0.21
mex2	Mexico City SCT Site	September 19, 1985 S60E	0.20

Note: In this report, if the symbol for the earthquake has a suffix of "1", then no additional filtering was applied to the signal. A suffix of "2" means that the un-time-scaled signal was high pass filtered at 0.1 Hz. For example, "ec1" is unfiltered, "ec2" was high pass filtered. All are digitized records at the EERC of the University of California at Berkeley.

Table 4.5 Earthquake Signals Used In Tests

Test	Rubber Shear Strain (%)	Damping Ratio (%)	Fund. Horiz. Freq. (Hz.)	2nd Horiz. Freq. (Hz.)
Free Vibration	11	11.5	1.55	5.74
Harmonic Vibration	8	9.9	1.40	5.23
Harmonic Vibration	65	7.6	1.05	n.a.
White Noise	6	n.a.	1.53	5.26

Table 5.1 Preliminary Shaking Tests, Neoprene Bearings.

Test	Fund. Horiz. Frequency (Hz.)	Rigid Body Theory (Hz.)
Free Vibration	1.18	1.11
Harmonic Vibration	1.04	1.11
White Noise	1.13	1.11

Table 5.2 Comparison of Results at 100% Shear Strain

Test	Rubber Shear Strain (%)	Damping Ratio (%)	Fund. Horiz. Freq. (Hz.)	2nd Horiz. Freq. (Hz.)
Free Vibration	1	n.a.	2.85	9.1
Harmonic Vibration	26	15.3	1.15	5.85
White Noise	0.4	n.a.	2.42	7.5

Table 6.1 Preliminary Shaking Tests, Lead-Plug Bearings.

ELEMENT	SECTION	AREA (inches^2)	INERTIA (inches^4)
BOTTOM BEAM	**W8X31**	18.26	220.0
COLUMN	**W4X13**	7.66	22.6
GIRDER	**W6X9**	5.36	32.8
BRACING (1,5-9)	**db L's** $1\frac{1}{2}$ **X** $1\frac{1}{2}$ **X** $\frac{1}{4}$	2.82	n.a.
BRACING (2-4)	**db L's 1 X 1 X** $\frac{1}{4}$	1.88	n.a.

Note- The **AREA** and **INERTIA** are doubled to account for the stiffness of the two frames since the total mass was used in the analysis.

Table 7.1 Cross-Section Properties for Braced Steel Frame

FREQUENCIES

	FREQUENCY		
	f_1	f_2	f_3
Test	1.15 Hz	5.85 Hz	n.a.
Theory	1.03 Hz	5.82 Hz	15.5 Hz

MODE SHAPES

1st Mode Shape			2nd Mode Shape		
Story	**Theory**	**Test**	**Story**	**Theory**	**Test**
9	1.00	1.00	9	1.00	1.00
8	0.99	0.98	8	0.85	0.81
7	0.98	0.98	7	0.66	0.63
6	0.97	0.91	6	0.45	0.44
5	0.95	0.91	5	0.24	0.23
4	0.94	0.84	4	0.01	0.01
3	0.92	0.82	3	-0.21	-0.22
2	0.90	0.79	2	-0.42	-0.44
1	0.88	0.74	1	-0.60	-0.62
G	0.86	0.71	G	-0.75	-0.81
B	0.00	0.00	B	0.00	0.00

Table 7.2 Comparison of Experimental and Analytical Results

Neoprene Bearing Isolation System

EARTHQUAKE SIGNAL	MAXIMUM TABLE ACCEL.	RESPONSE SPECTRUM ANALYSIS		SHAKING TABLE RESULTS	
		Maximum Bearing Displacement (inches)	Maximum Base Shear (kips)	Maximum Bearing Displacement (inches)	Maximum Base Shear (kips)
Bucharest	0.236g	1.71	25.8	2.12	30.8
El Centro	0.650g	2.16	33.3	2.38	35.0
Mexico City	0.168g	1.61	24.0	2.57	27.9
Miyagi-Ken-Oki	0.300g	2.18	33.1	2.12	32.1
Pacoima Dam	0.495g	1.90	29.8	1.95	28.6
Parkfield	0.417g	1.92	29.2	2.08	30.3
San Francisco	1.609g	1.55	25.4	1.57	24.3
Taft	0.739g	2.29	35.2	1.94	29.5

Lead-Plug Bearing Isolation System

EARTHQUAKE SIGNAL	MAXIMUM TABLE ACCEL.	RESPONSE SPECTRUM ANALYSIS		SHAKING TABLE RESULTS	
		Maximum Bearing Displacement (inches)	Maximum Base Shear (kips)	Maximum Bearing Displacement (inches)	Base Shear (kips)
Bucharest	0.348g	3.73	36.2	3.73	35.2
El Centro	0.842g	3.55	41.6	3.78	39.5
Mexico City	0.219g	3.44	34.8	3.38	32.3
Miyagi-Ken-Oki	0.310g	2.25	29.8	2.40	30.0
Pacoima Dam	0.562g	2.16	28.6	1.99	26.0
Parkfield	0.425g	1.89	25.0	1.94	25.3
San Francisco	1.590g	1.40	19.6	1.52	20.1
Taft	0.848g	2.25	29.8	2.26	28.8

Table 7.3 Response Spectrum Analysis and Experimental Results

Neoprene Bearing Isolation System

Earthquake Signal	PGA	A_a	A_v	D_{exp} (in.)	$\frac{D_{PGA}}{D_{exp}}$	$\frac{D_a}{D_{exp}}$	$\frac{D_v}{D_{exp}}$
Bucharest	.236g	.175	.440	2.12	0.82	0.61	1.53
El Centro	.650g	.471	.647	2.38	1.52	1.10	1.51
Mexico	.187g	.160	.251	1.91	0.96	0.82	1.29
Miyagi	.300g	.198	.486	2.12	0.79	0.52	1.27
Pacoima Dam	.495g	.387	.385	1.95	1.39	1.08	1.09
Parkfield	.417g	.263	.418	2.08	1.11	0.70	1.11
San Francisco	1.400g	1.387	.431	1.22	4.03	3.99	1.24
Taft	.739g	.531	.550	1.94	2.09	1.50	1.55

Lead-Plug Bearing Isolation System

Earthquake Signal	PGA	A_a	A_v	D_{exp} (in.)	$\frac{D_{PGA}}{D_{exp}}$	$\frac{D_a}{D_{exp}}$	$\frac{D_v}{D_{exp}}$
Bucharest	.241g	.157	.477	1.83	0.97	0.63	1.92
Bucharest	.296g	.194	.603	2.73	0.86	1.54	1.75
Bucharest	.343g	.217	.684	3.26	0.86	0.54	1.70
El Centro	.460g	.348	.486	1.71	1.48	1.12	1.56
El Centro	.604g	.434	.640	2.65	1.31	0.94	1.38
El Centro	.842g	.553	.849	3.78	1.37	0.90	1.38
Mexico	.146g	.132	.271	1.90	0.77	0.70	1.43
Mexico	.194g	.160	.383	3.06	0.68	0.56	1.35
Mexico	.219g	.165	.418	3.37	0.71	0.54	1.35
Miyagi	.310g	.198	.488	2.40	0.73	0.47	1.16
Pacoima Dam	.562g	.451	.449	1.99	1.58	1.27	1.26
Parkfield	.425g	.261	.416	1.94	1.22	0.75	1.20
San Francisco	1.590g	1.595	.559	1.52	3.70	3.72	1.30
Taft	.848g	.600	.629	2.26	2.12	1.50	1.57
ATC-S1 (ec)	.433g	.327	.590	1.98	0.81	0.61	1.11
ATC-S1 (taft)	.428g	.352	.649	2.76	0.62	0.51	0.93
ATC-S2 (ec)	.331g	.240	.528	2.01	0.92	0.67	1.47
ATC-S2 (taft)	.378g	.287	.658	3.19	0.71	0.54	1.24

Table 8.1 Design Code and Experimental Bearing Displacements

FIGURES

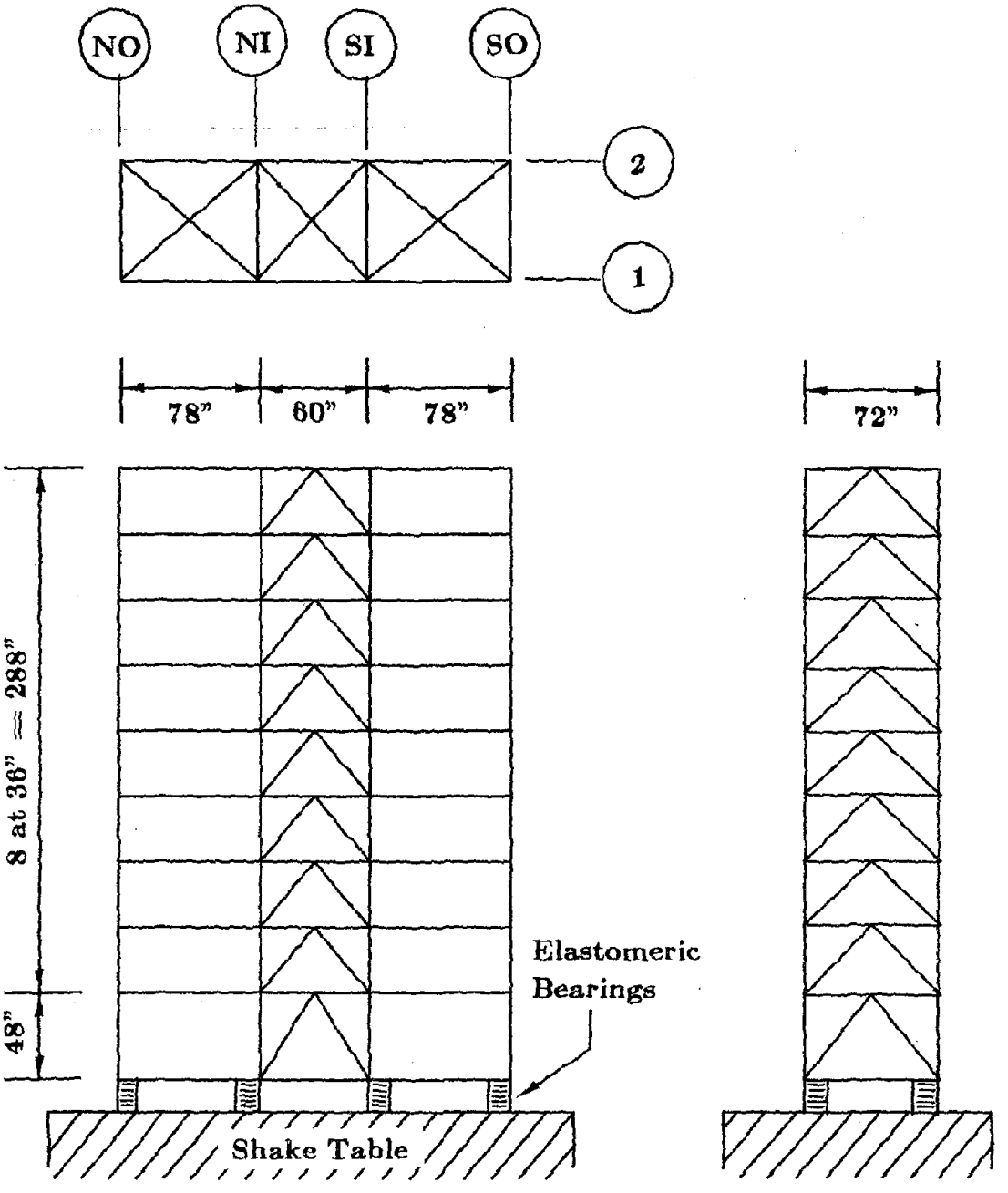

Figure 2.1 Base Isolated 9-Story Steel Frame

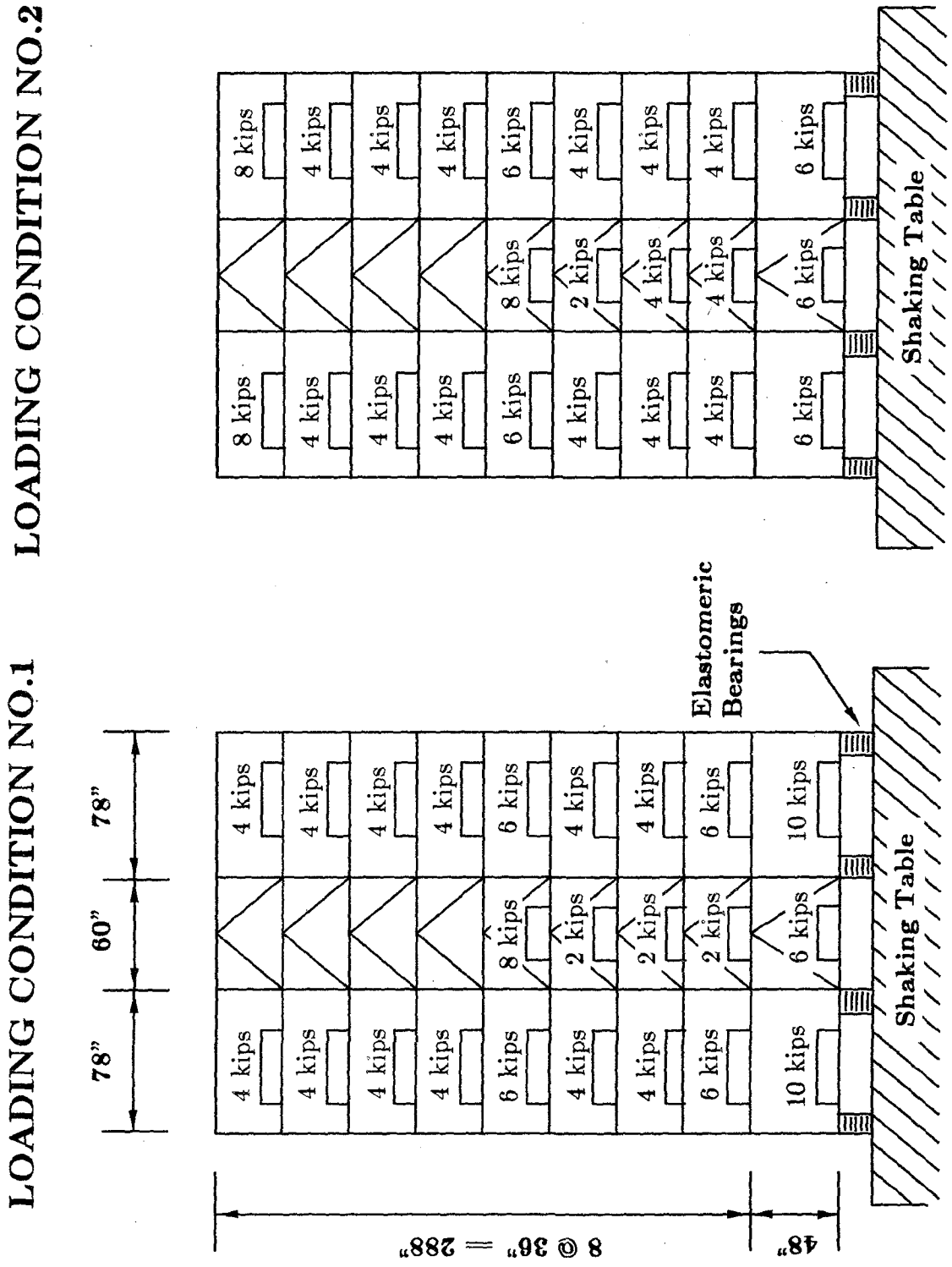

Unloaded Model weighs 10 kips

Figure 2.2 Loading Conditions for Steel Frame

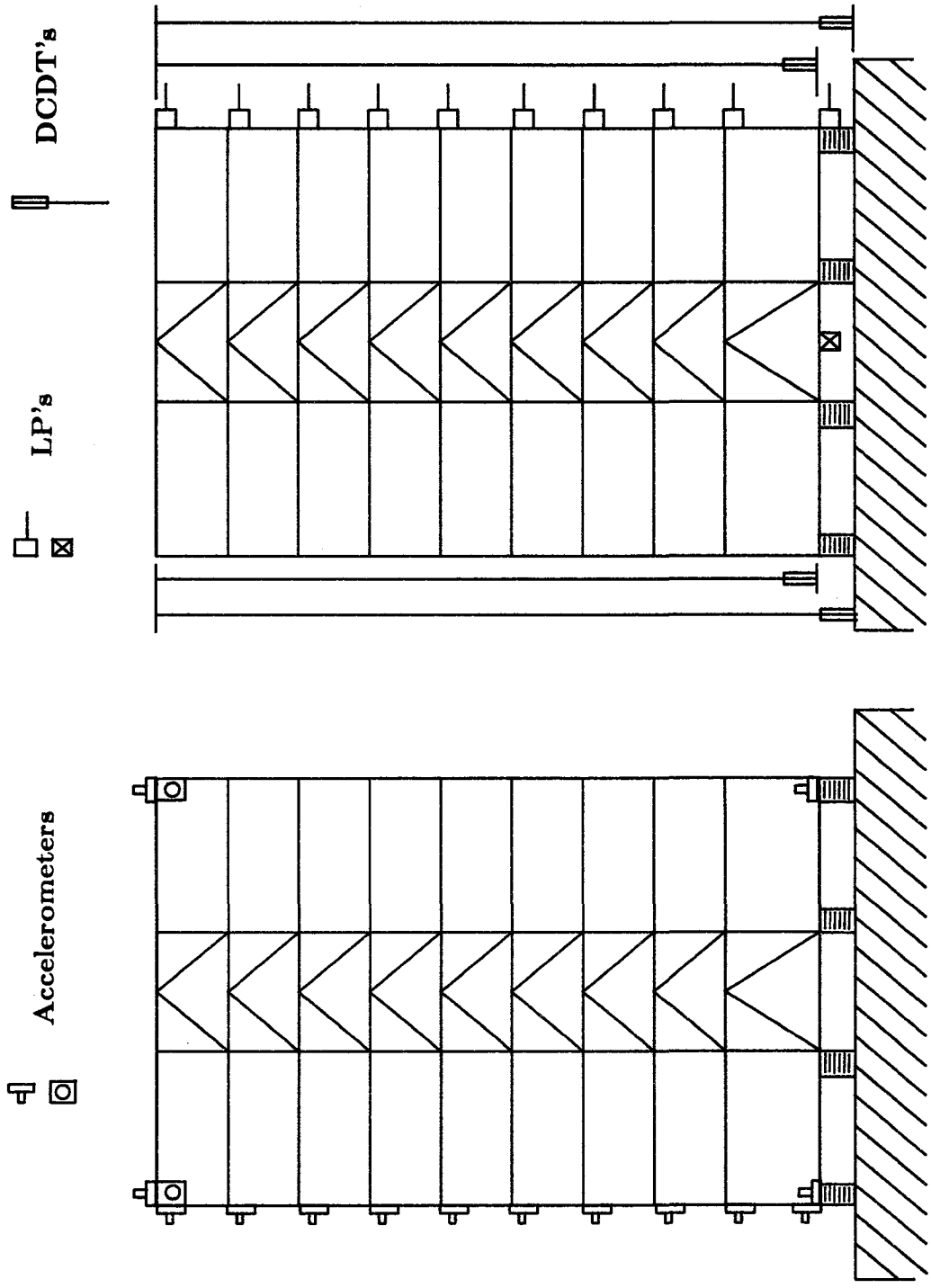

Figure 2.3 Steel Model Instrumentation Diagram

Force Transducer Location Diagram

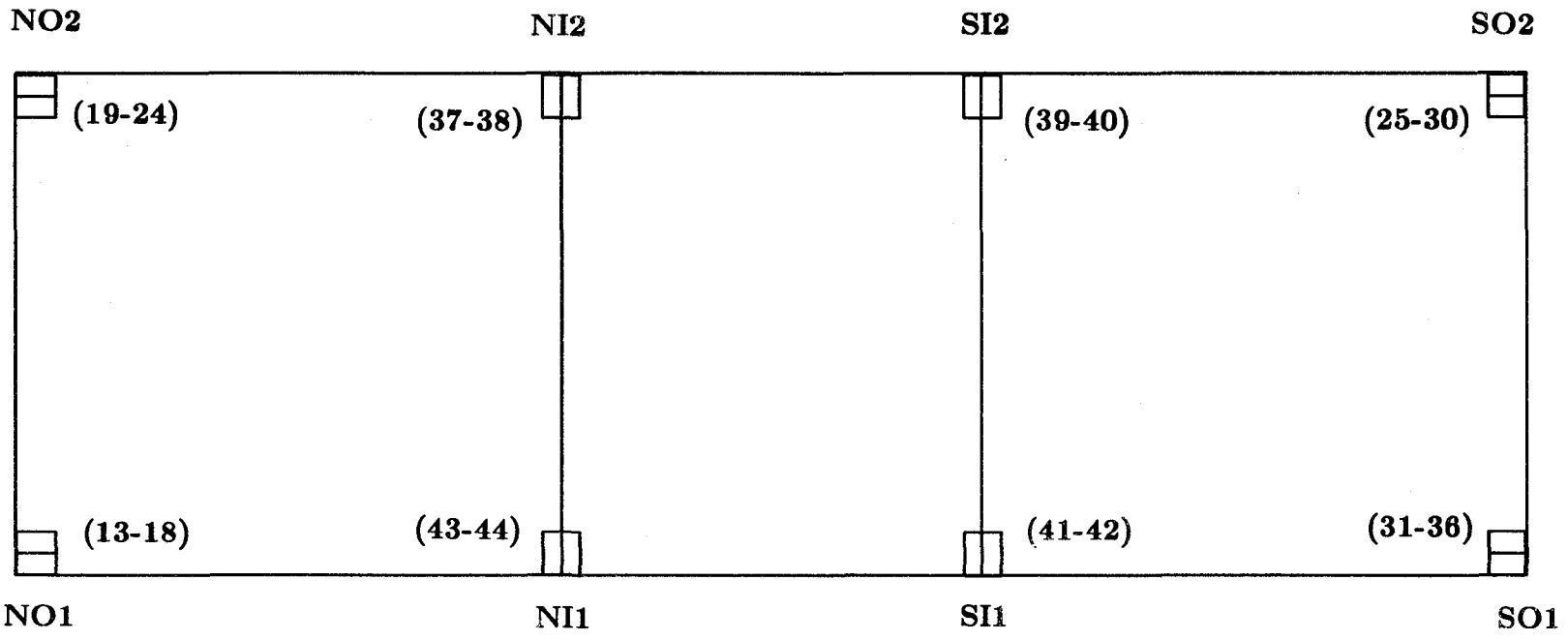

The numbers in brackets refer to the channels used to record axial, shear, and moment data. The Force Transducers under the 4 interior columns recorded only shear and moment data.

Figure 2.3 Continued

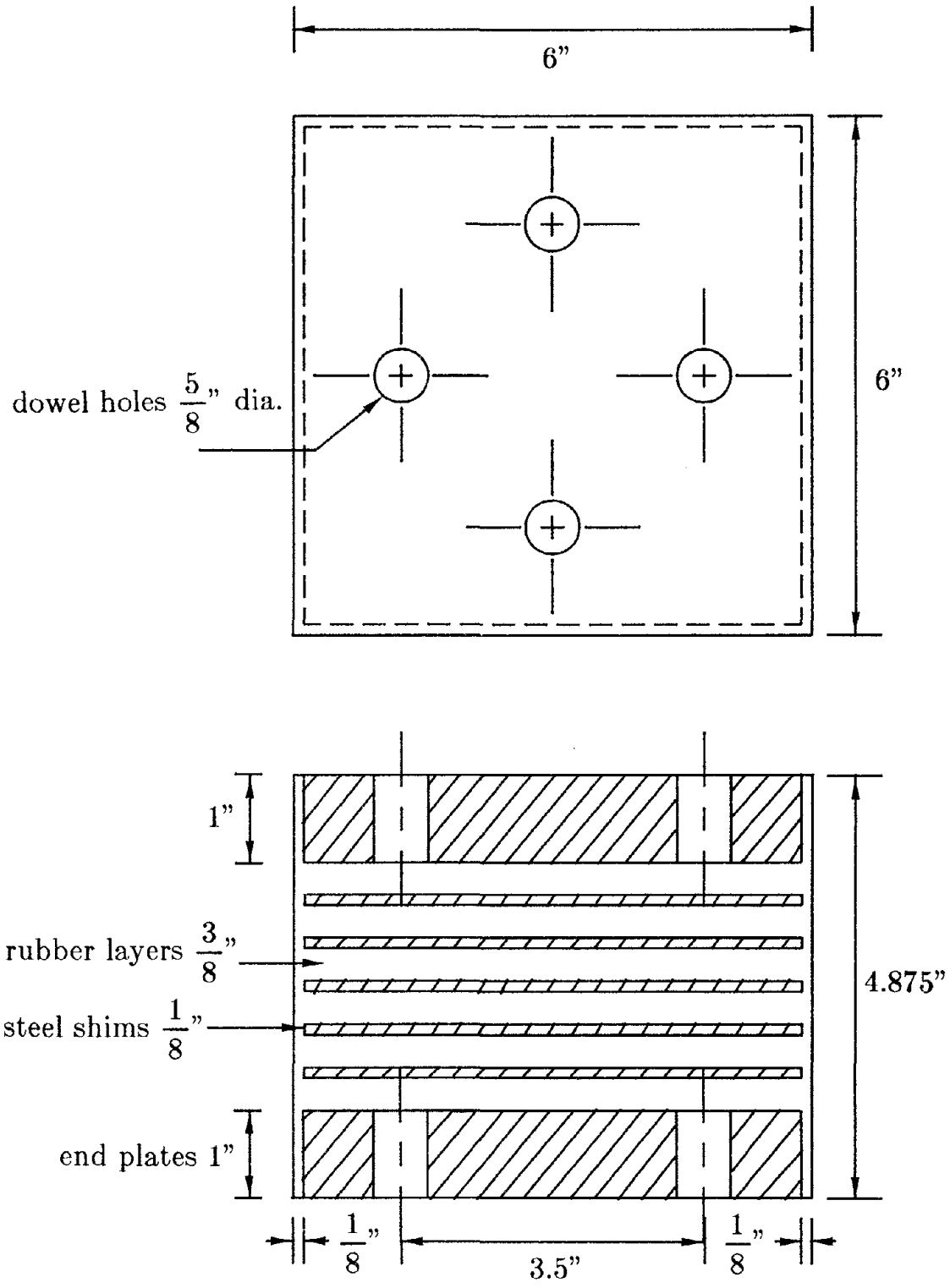

Figure 3.1 Neoprene Bearing Design

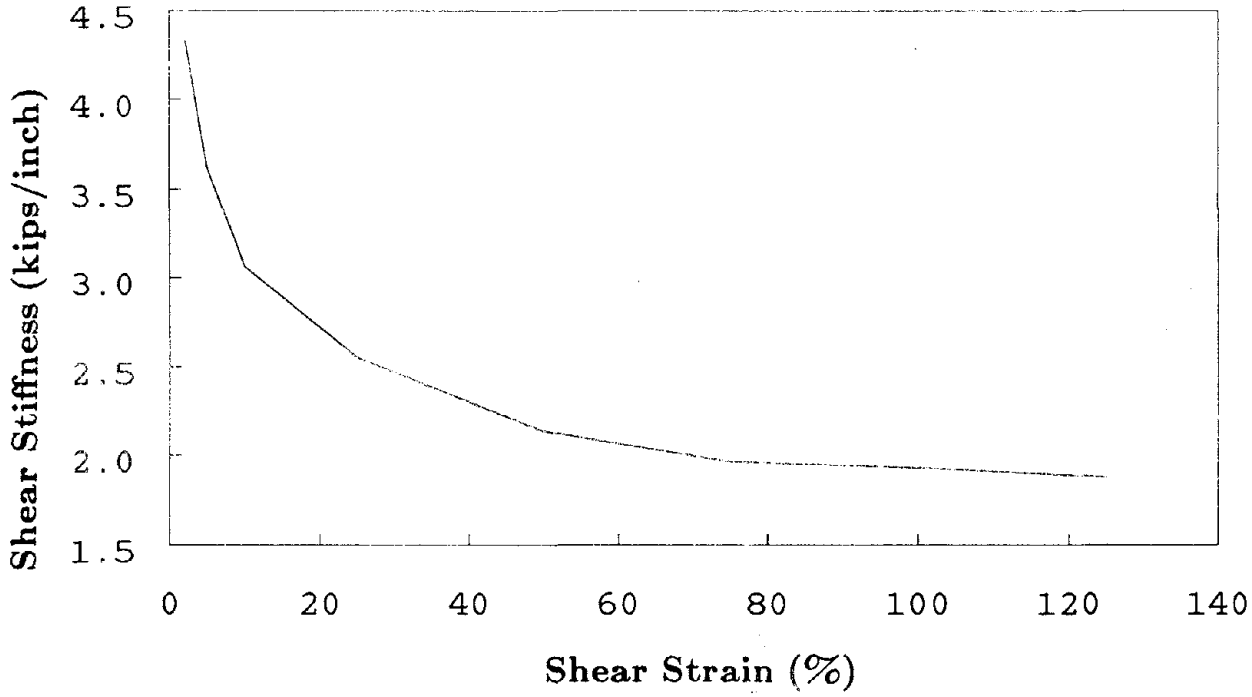

Figure 3.2 Neoprene Bearing Dynamic Shear Stiffness

PLAN VIEW

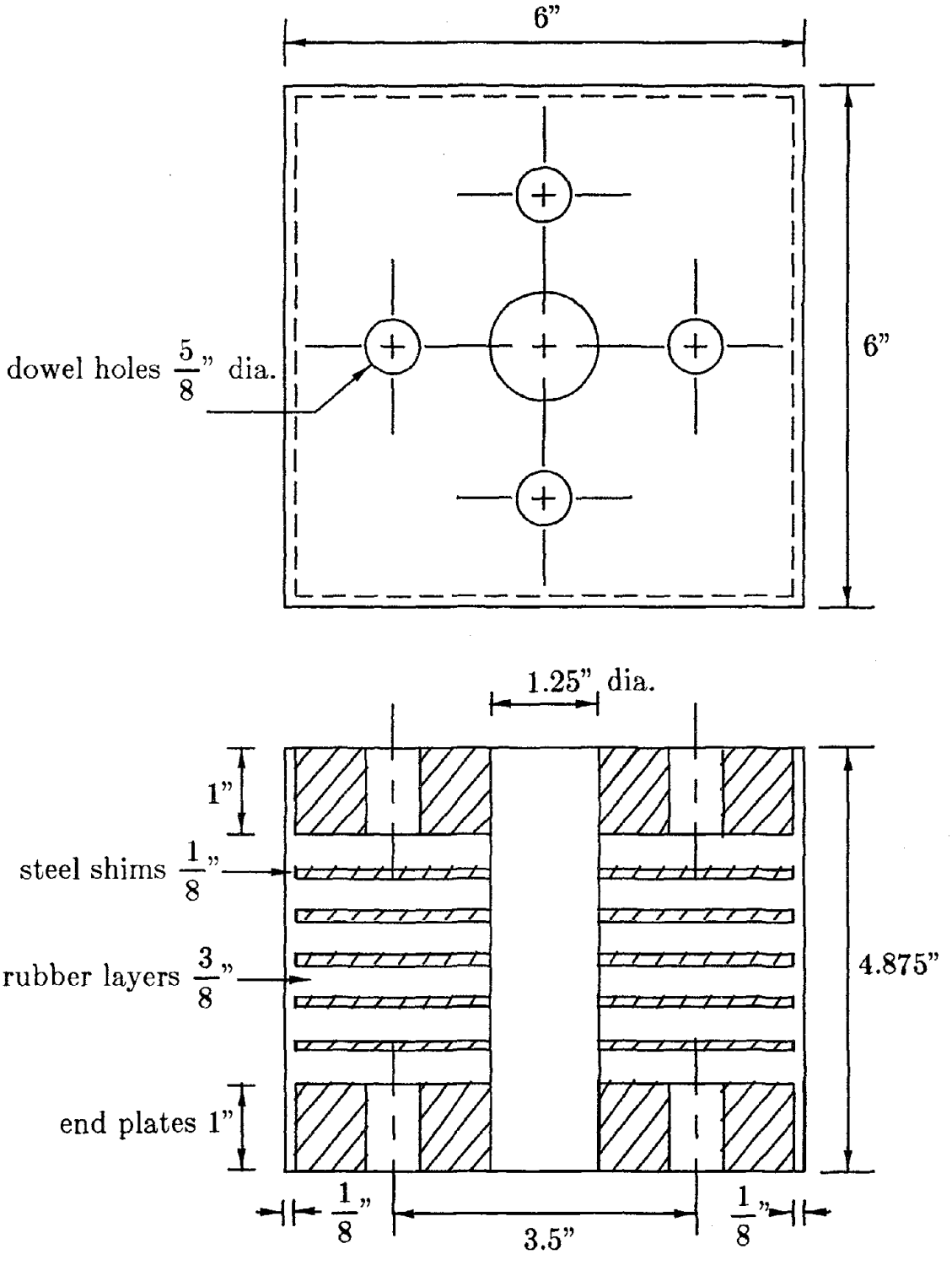

SECTION VIEW

Figure 3.3 Lead-Plug Bearing Design

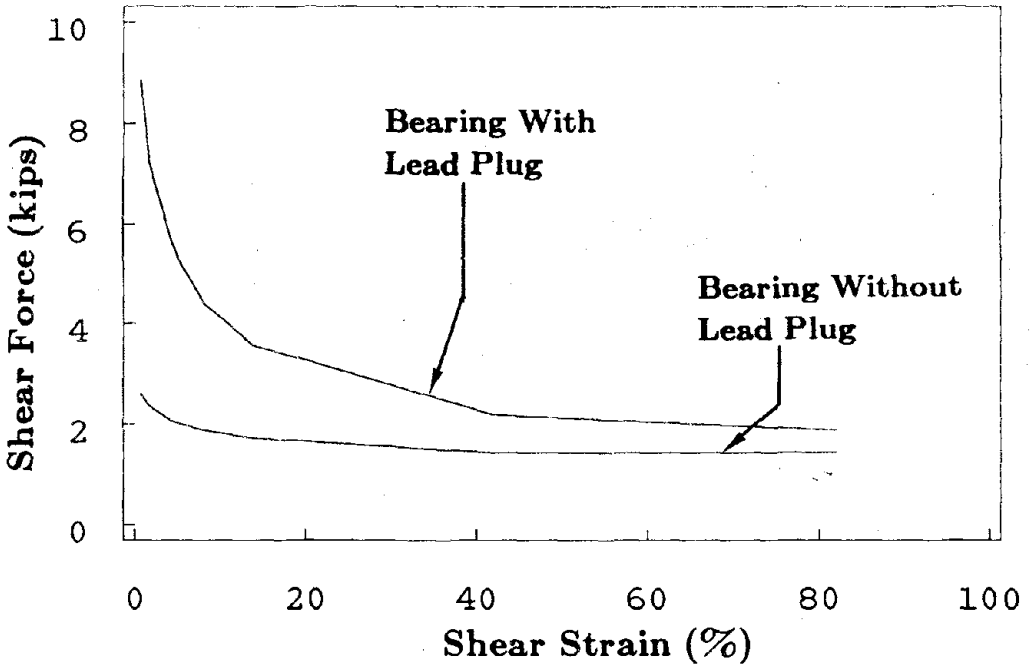

Figure 3.4 Lead-Plug Bearing Dynamic Shear Stiffness

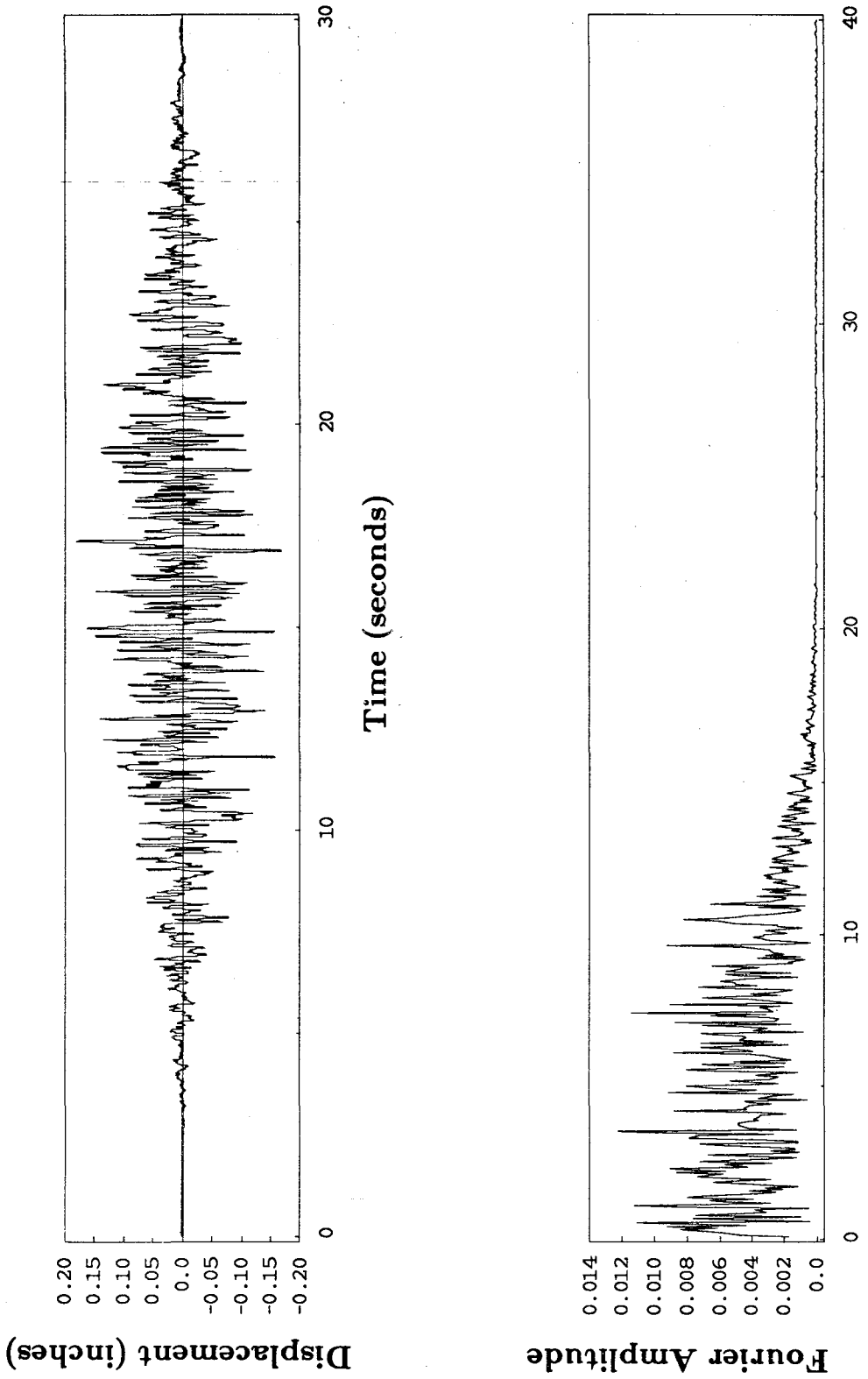

Figure 4.1 White Noise Displacement Time History

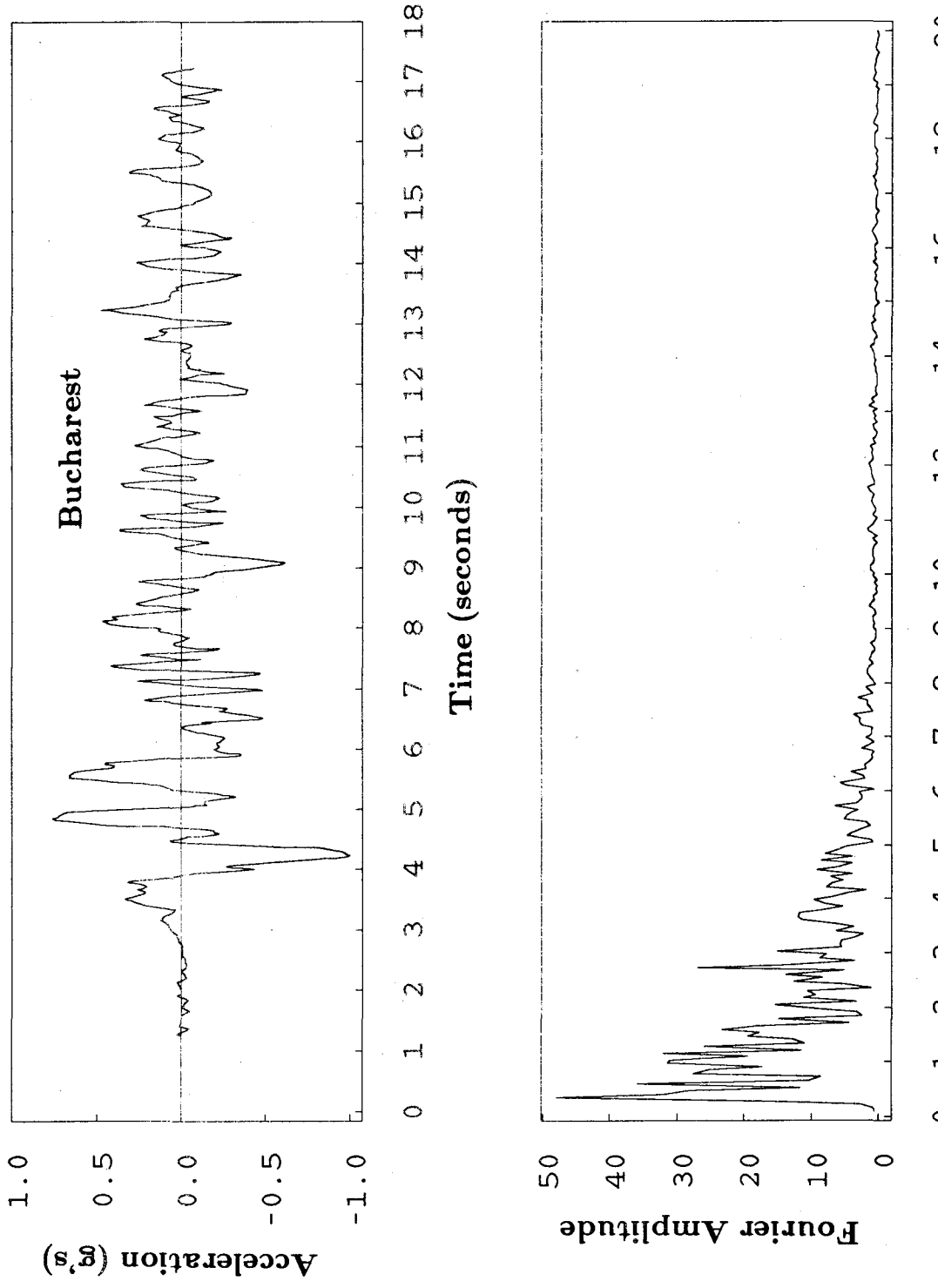

Figure 4.2 Normalized Real-Time Earthquake Record and its Fourier Amplitude

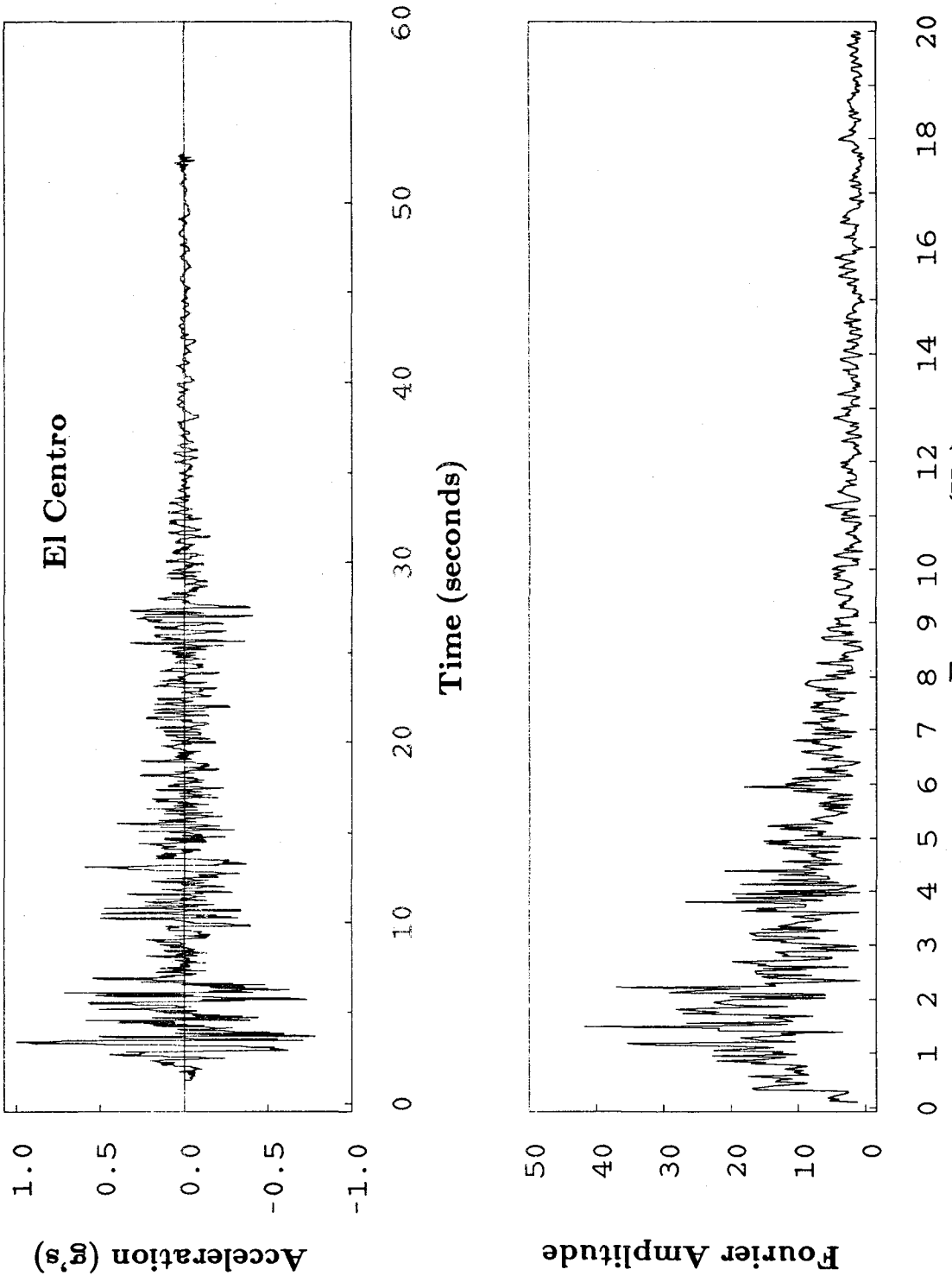

Figure 4.2 Continued

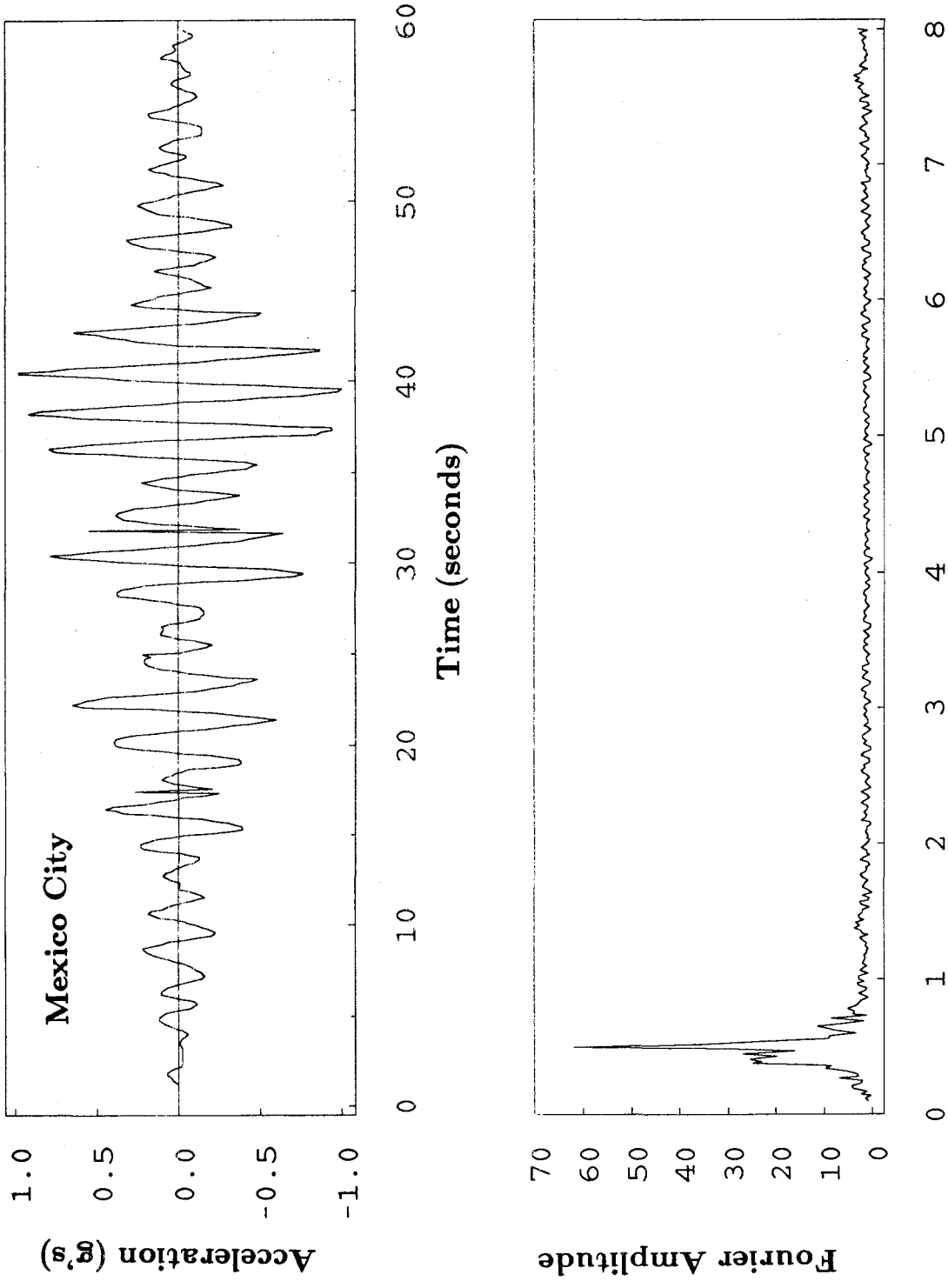

Figure 4.2 Continued

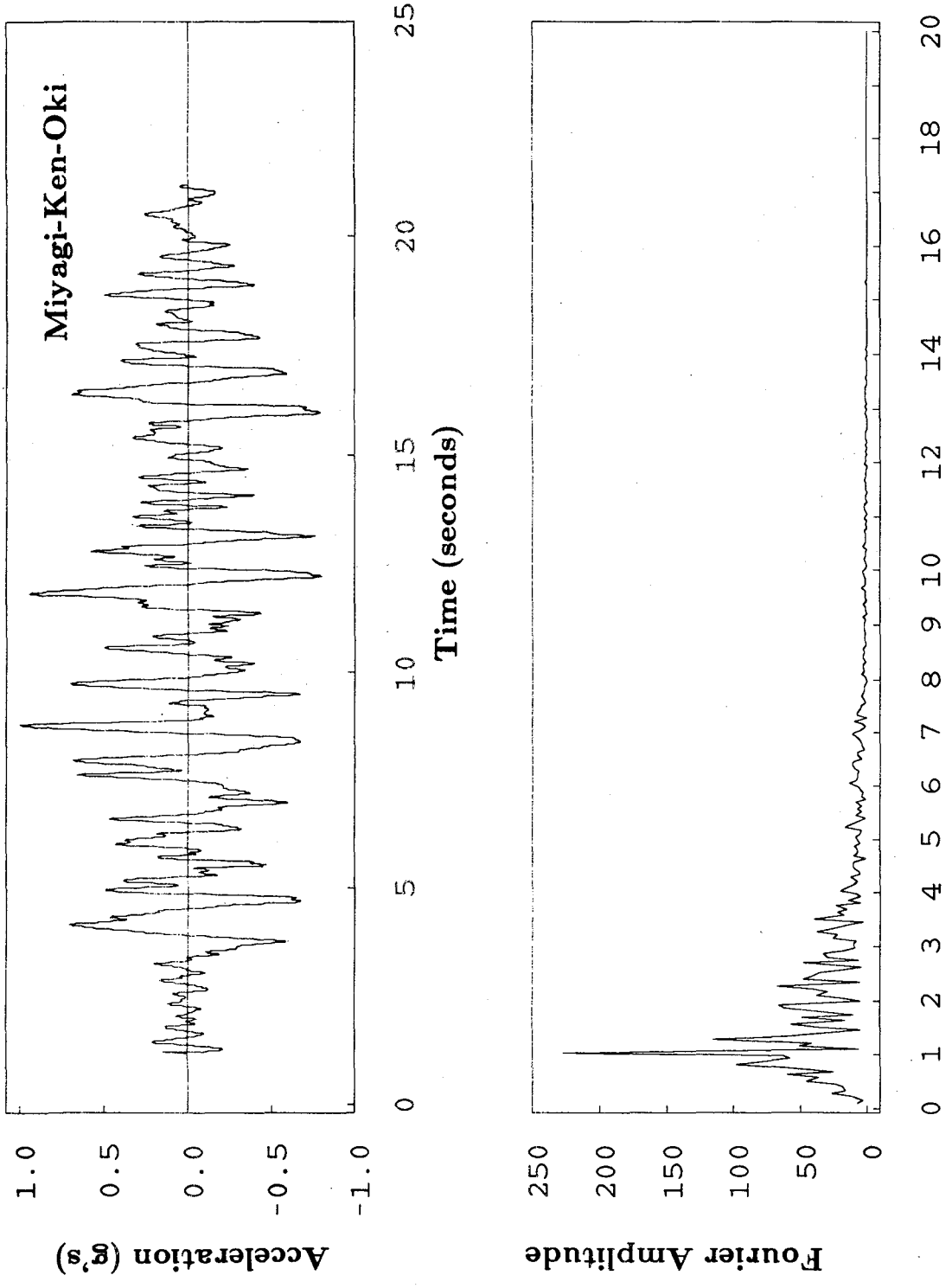

Figure 4.2 Continued

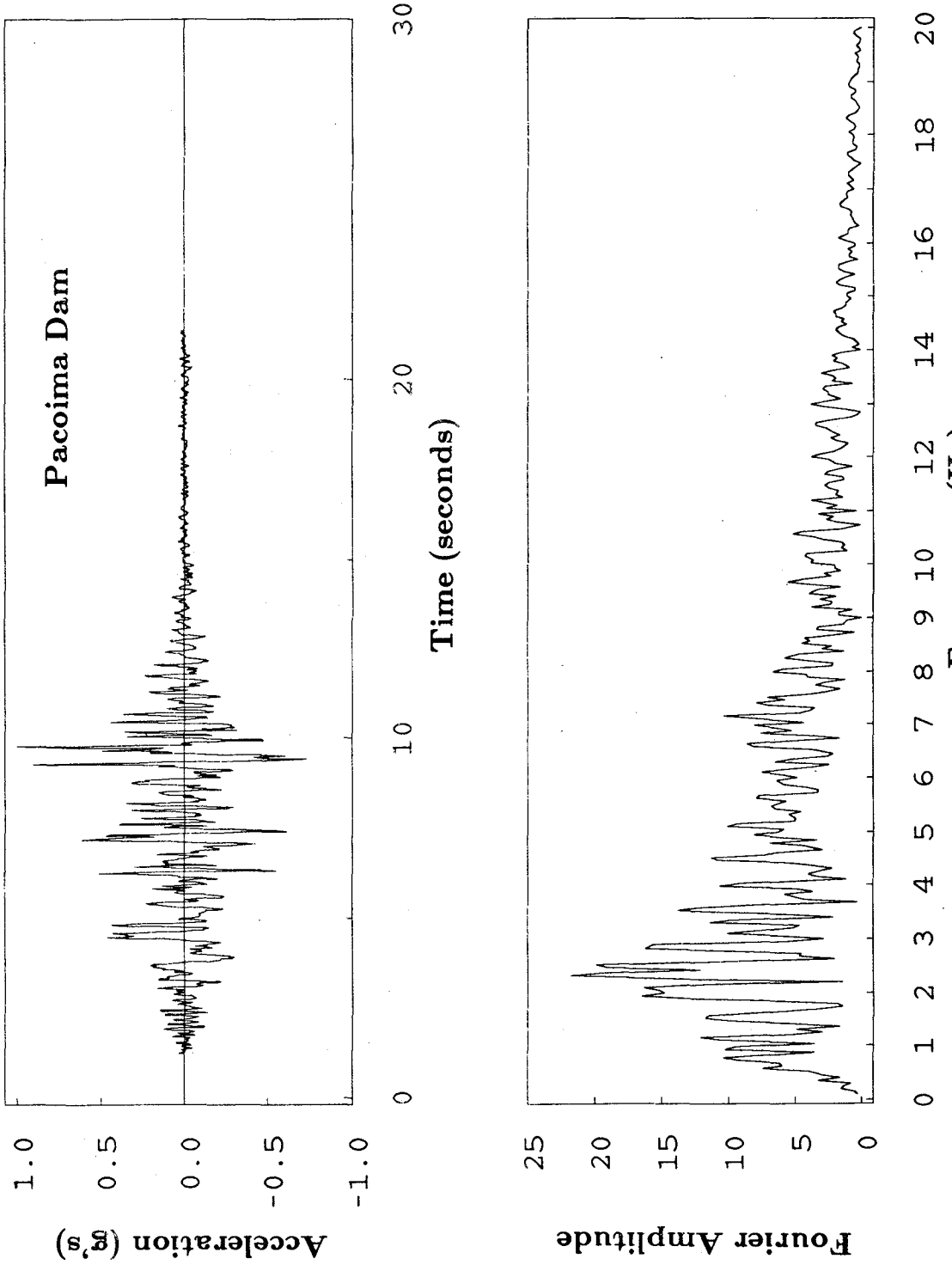

Figure 4.2 Continued

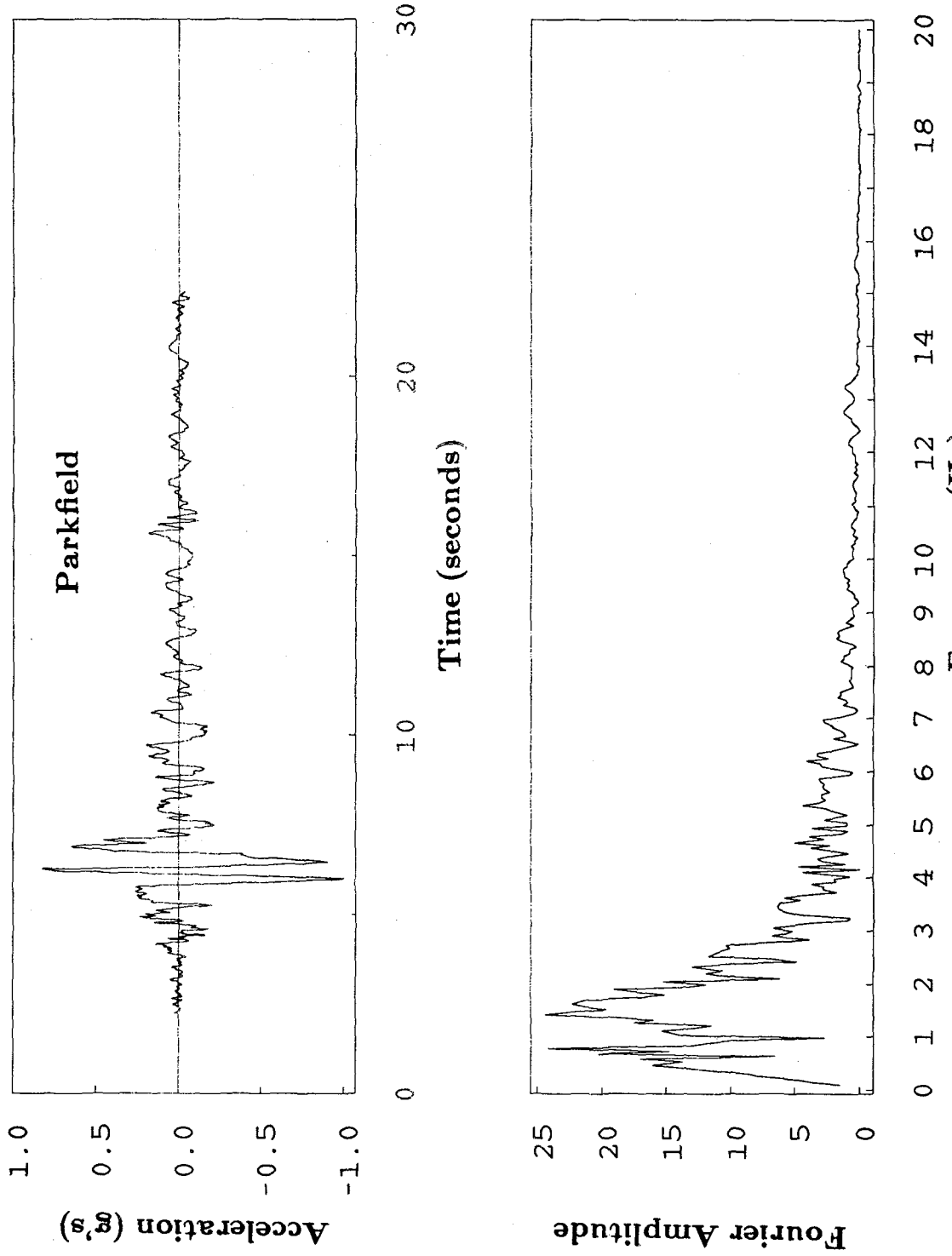

Figure 4.2 Continued

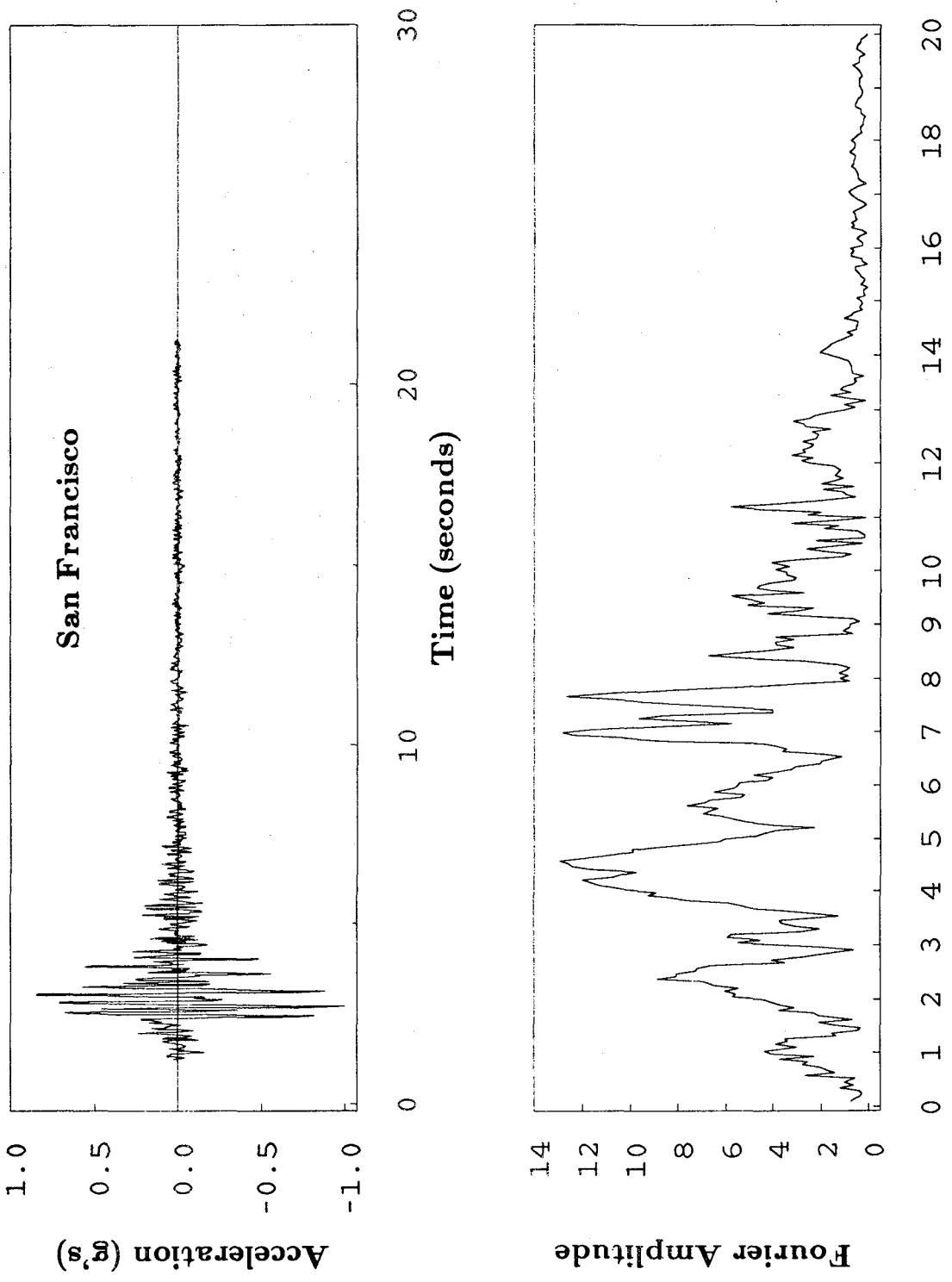

Figure 4.2 Continued

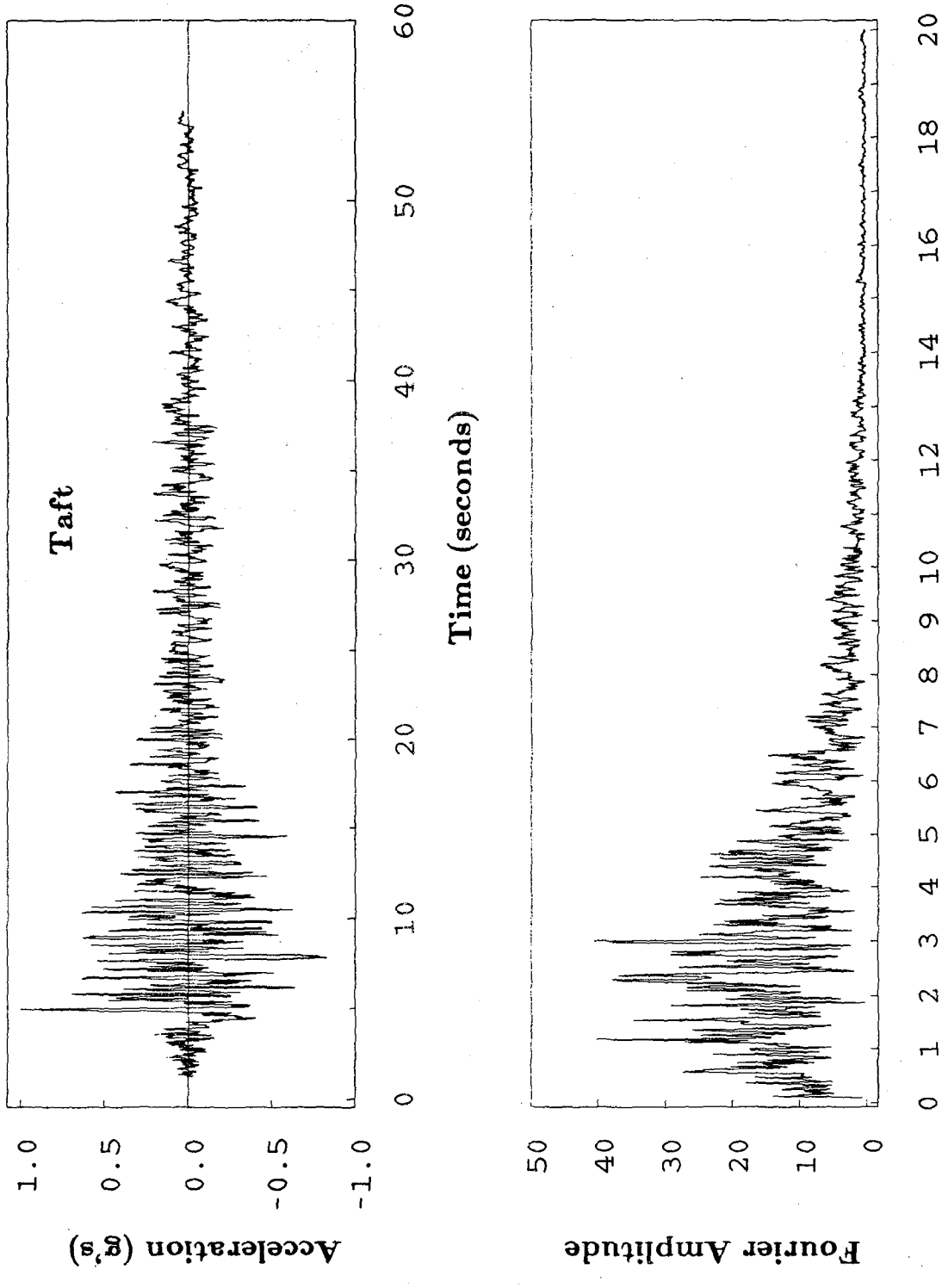

Figure 4.2 *Continued*

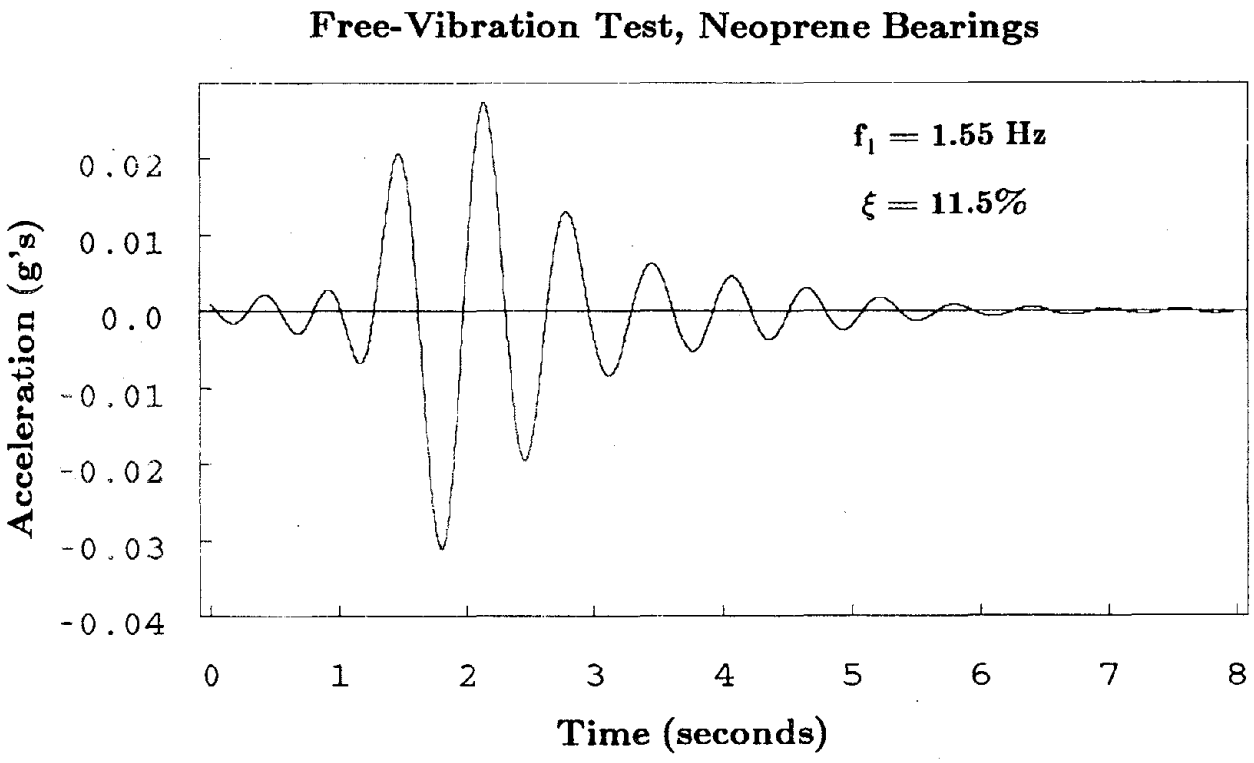

Figure 5.1 Log-Decrement Plot of Roof Acceleration

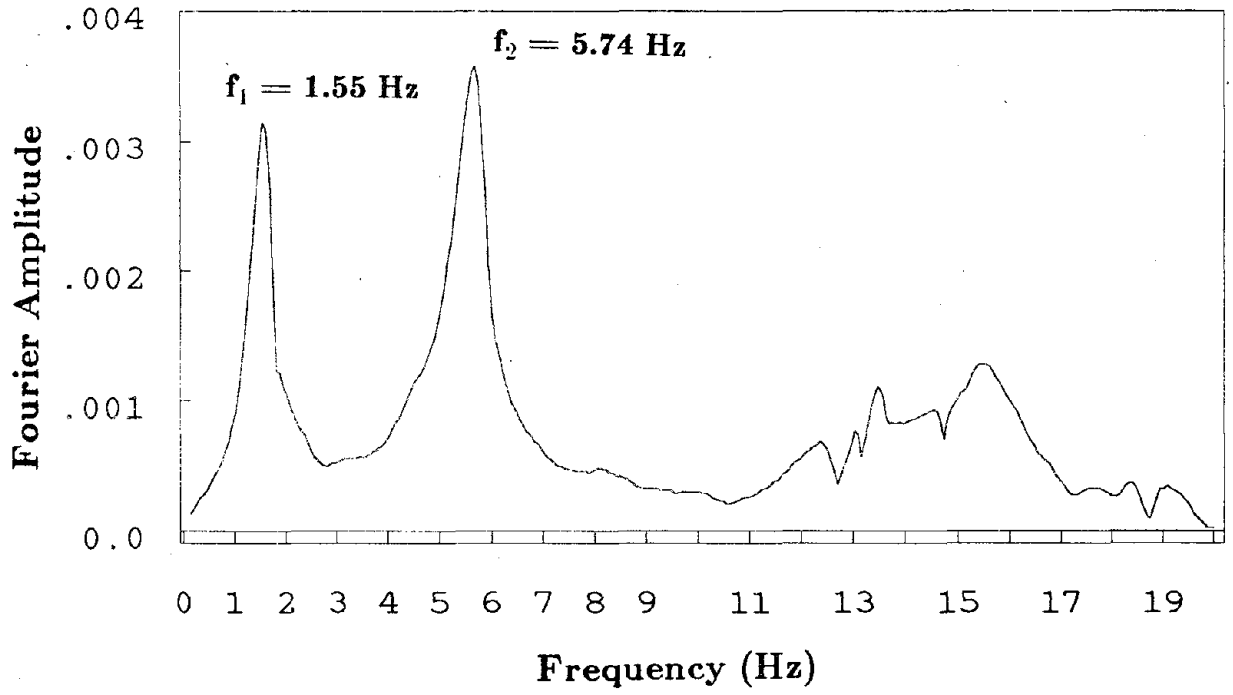

Figure 5.2 Fourier Amplitude Plot of Roof Acceleration

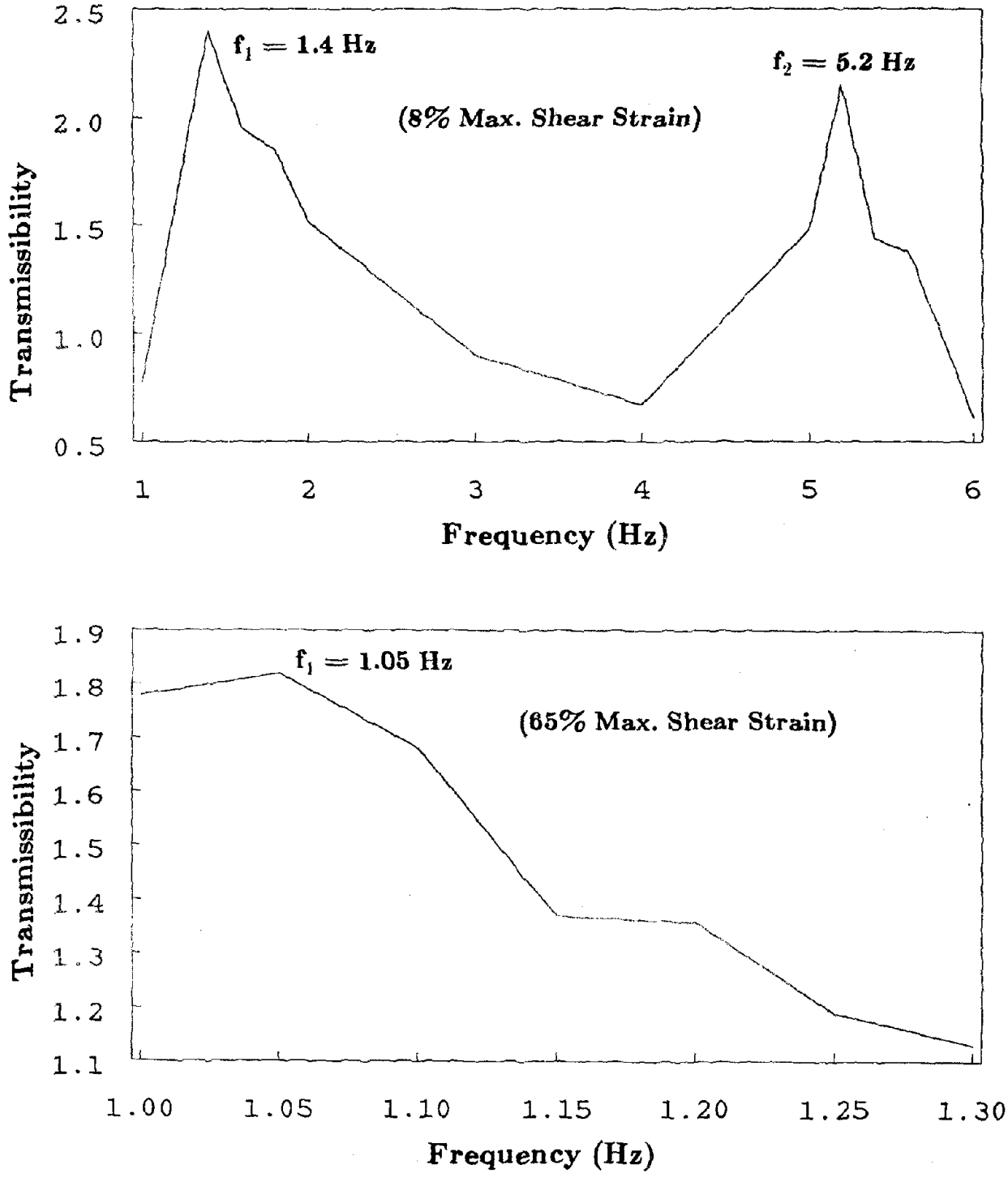

Figure 5.3 Transmissibility Plot for Roof Acceleration Harmonic Vibration Test, Neoprene Bearings

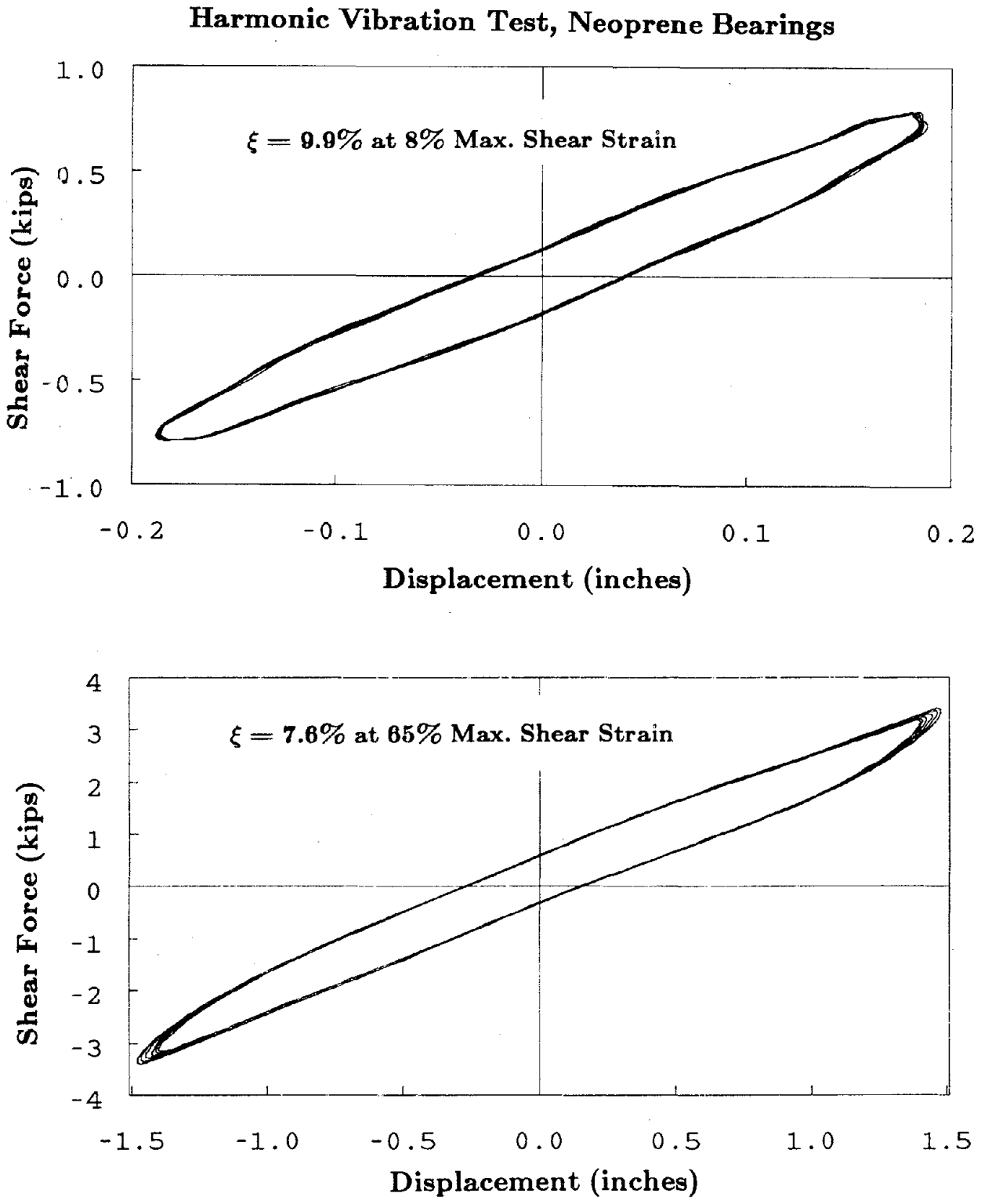

Figure 5.4 Bearing Shear Hysteresis Loops

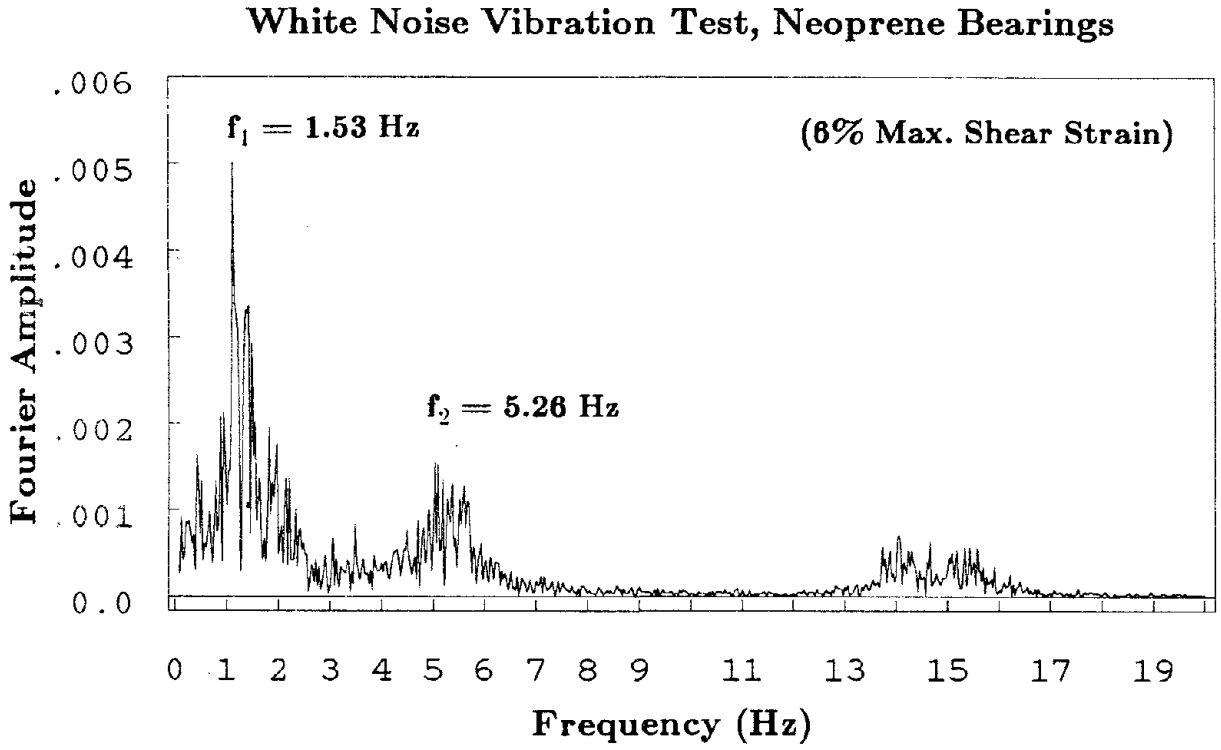

Figure 5.5 Fourier Amplitude Plot of Roof Acceleration

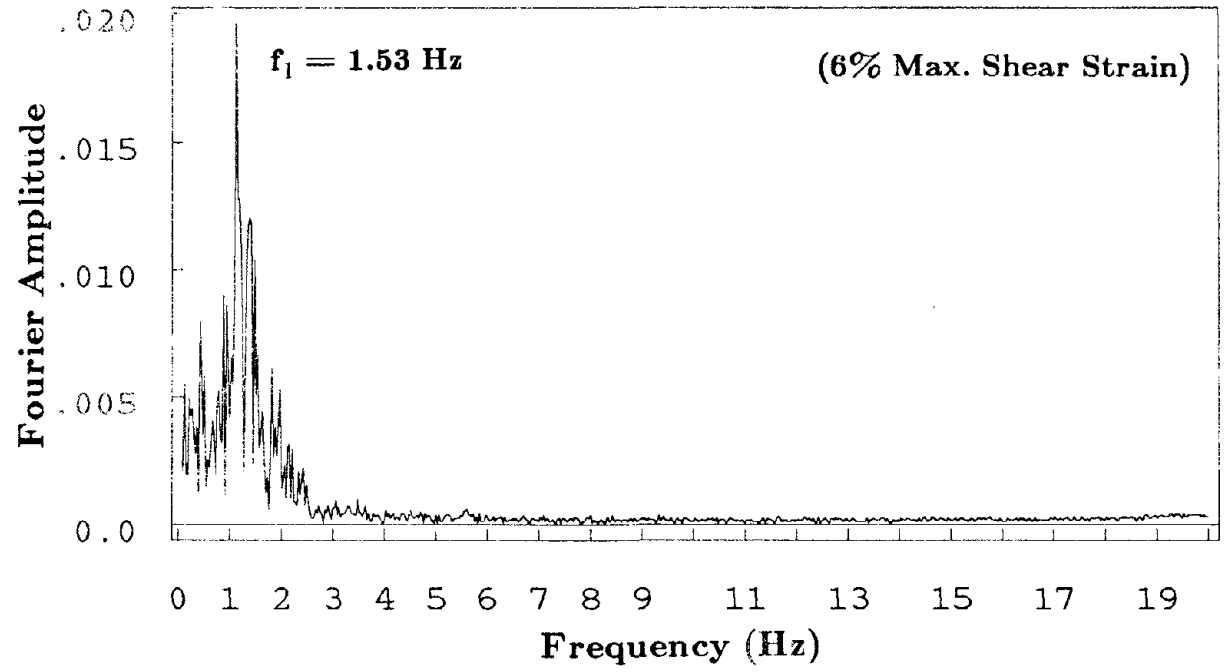

Figure 5.6 Fourier Amplitude Plot of Bearing Displacement

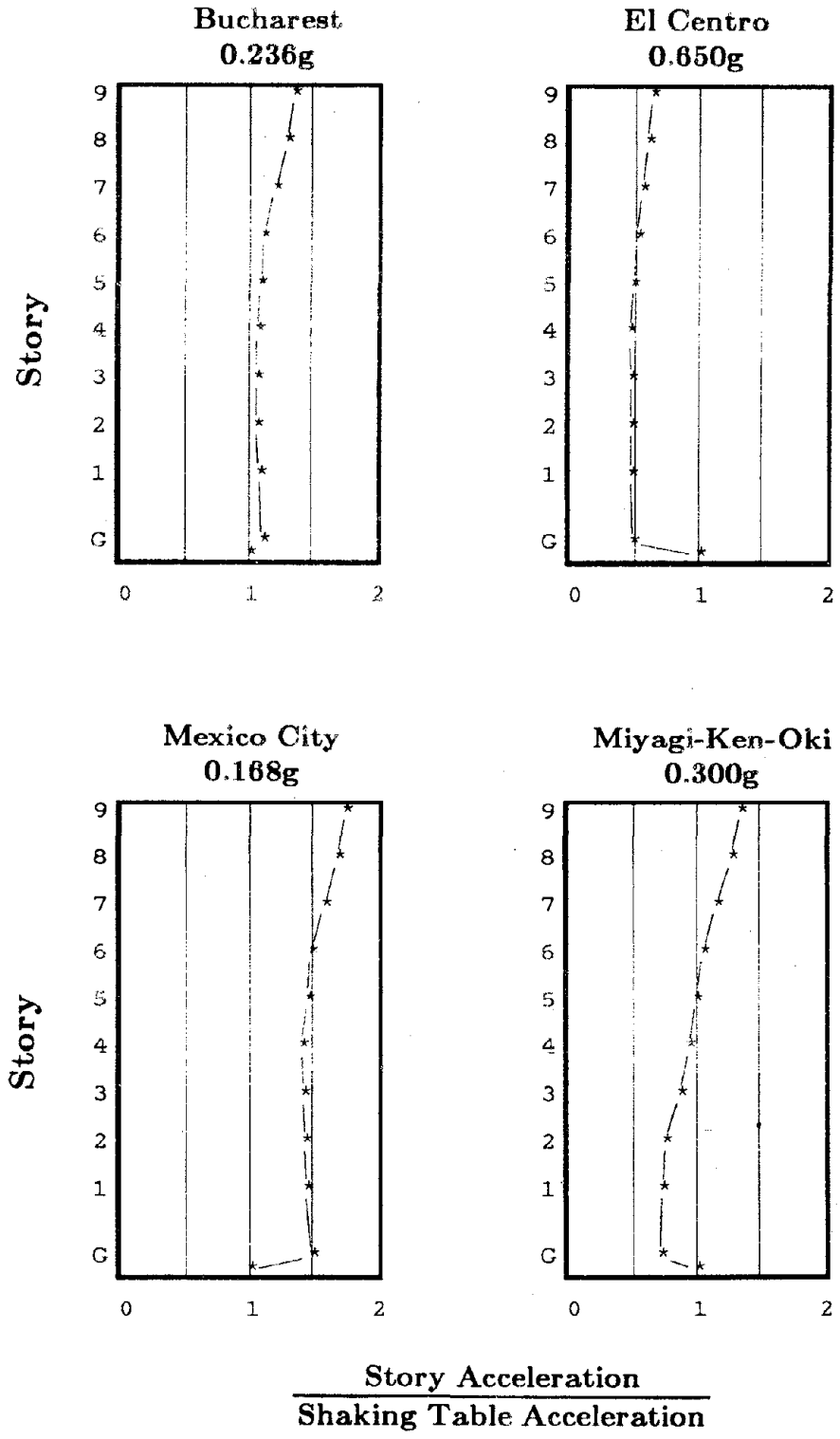

Figure 5.7 Story Acceleration Profiles, Neoprene Bearings

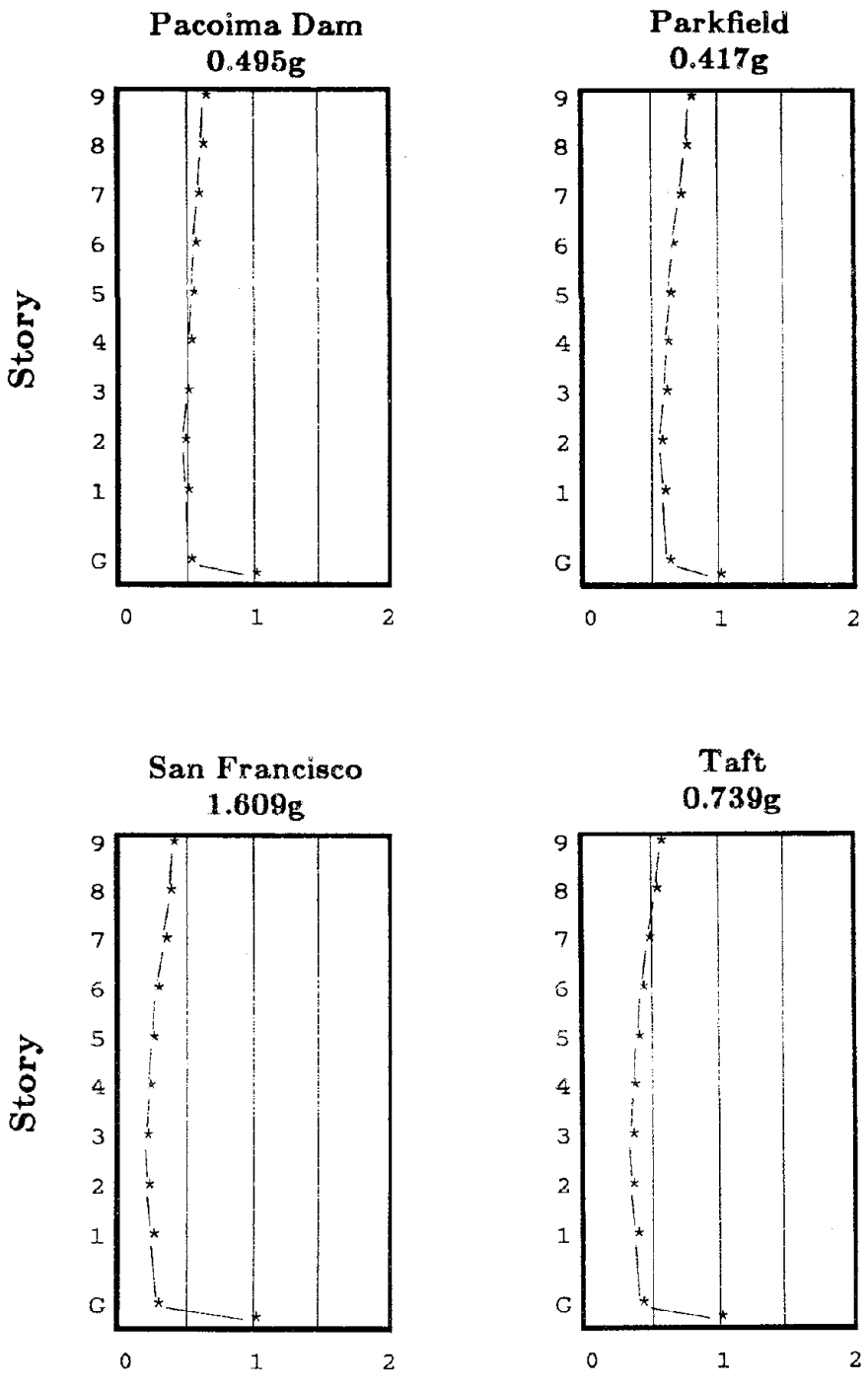

Figure 5.7 Continued

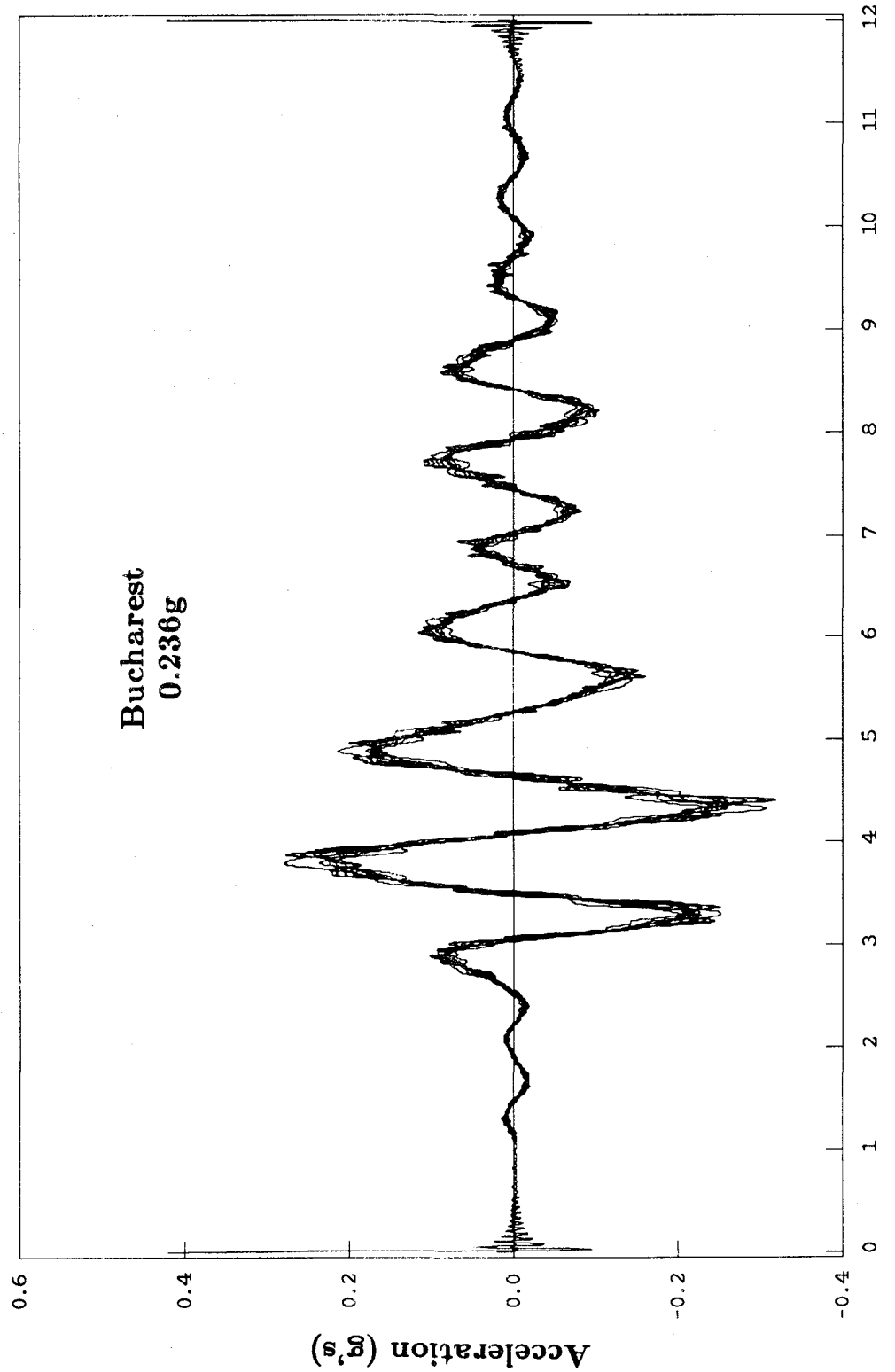

Figure 5.8 Superimposed Story Acceleration Time Series Plots, Neoprene Bearings

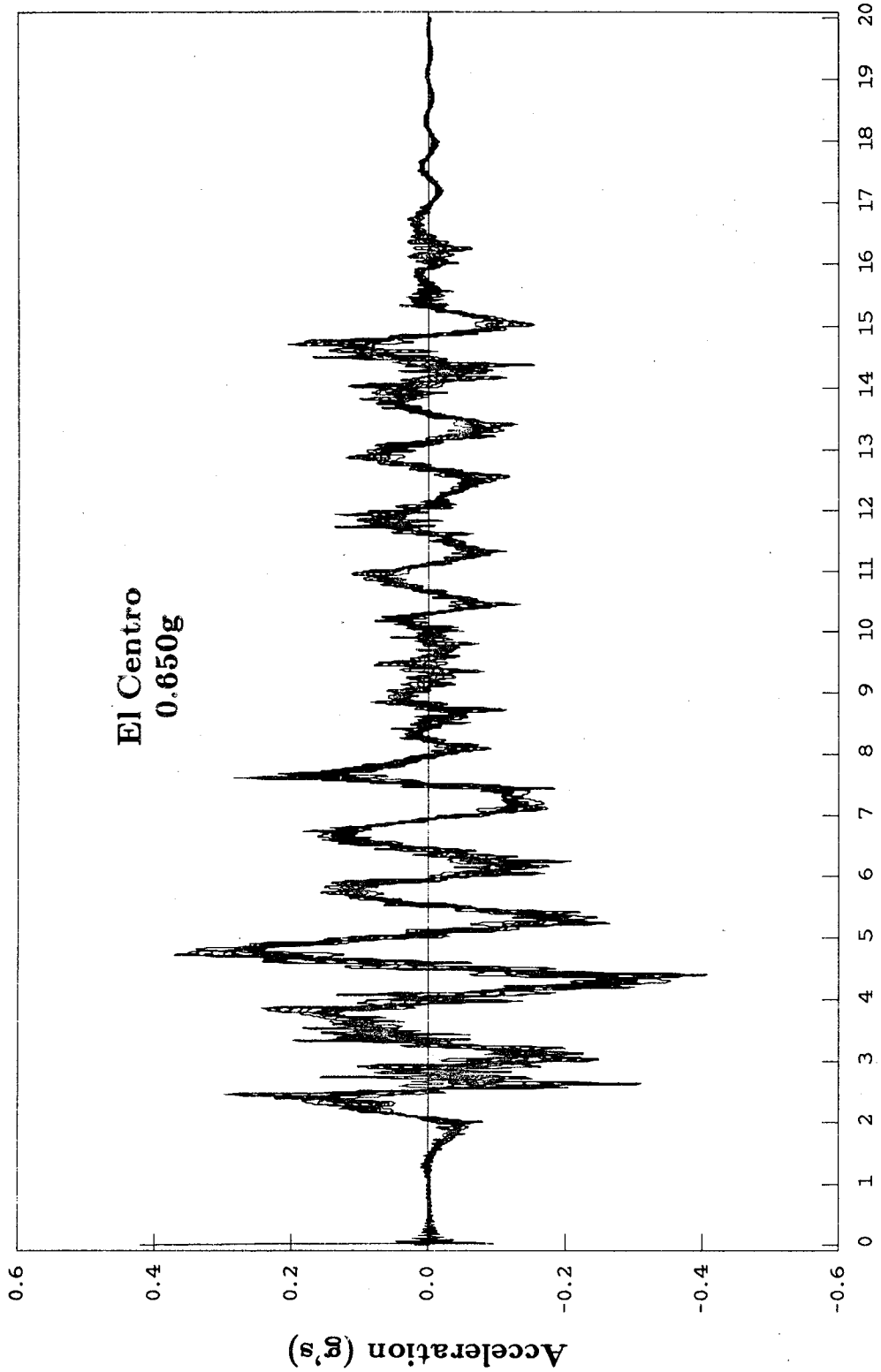

Figure 5.8 Continued

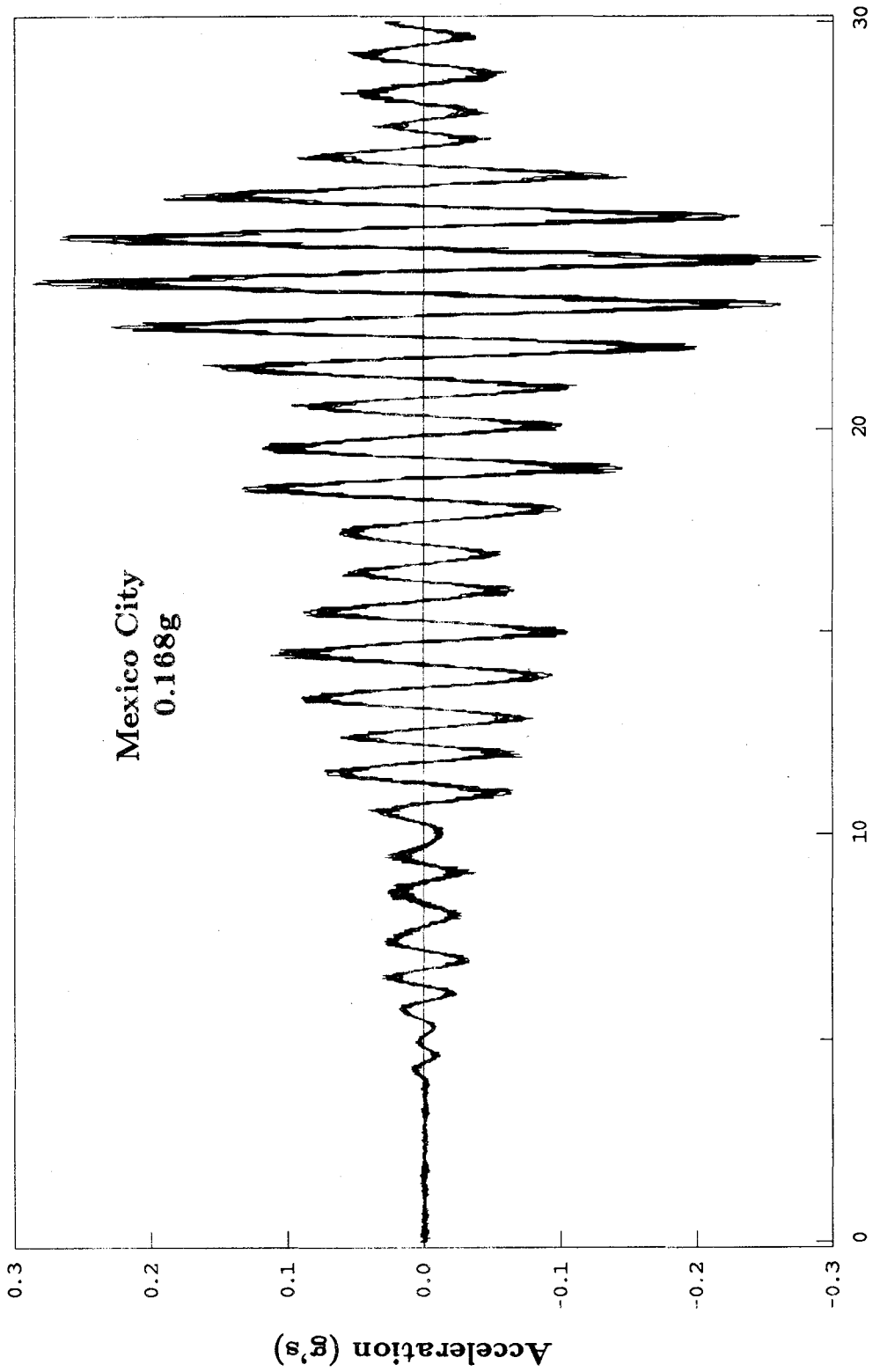

Figure 5.8 Continued

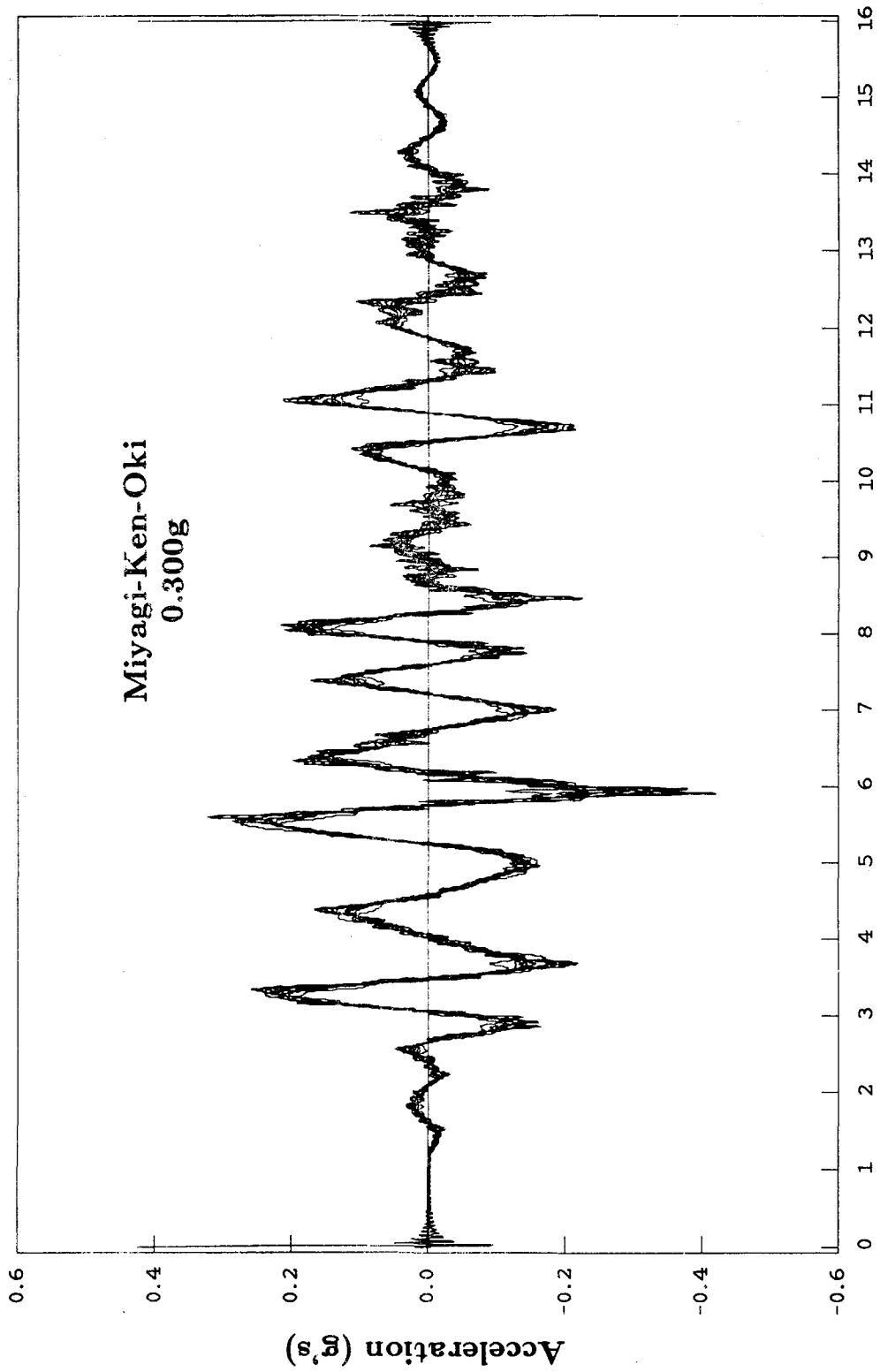

Figure 5.8 Continued

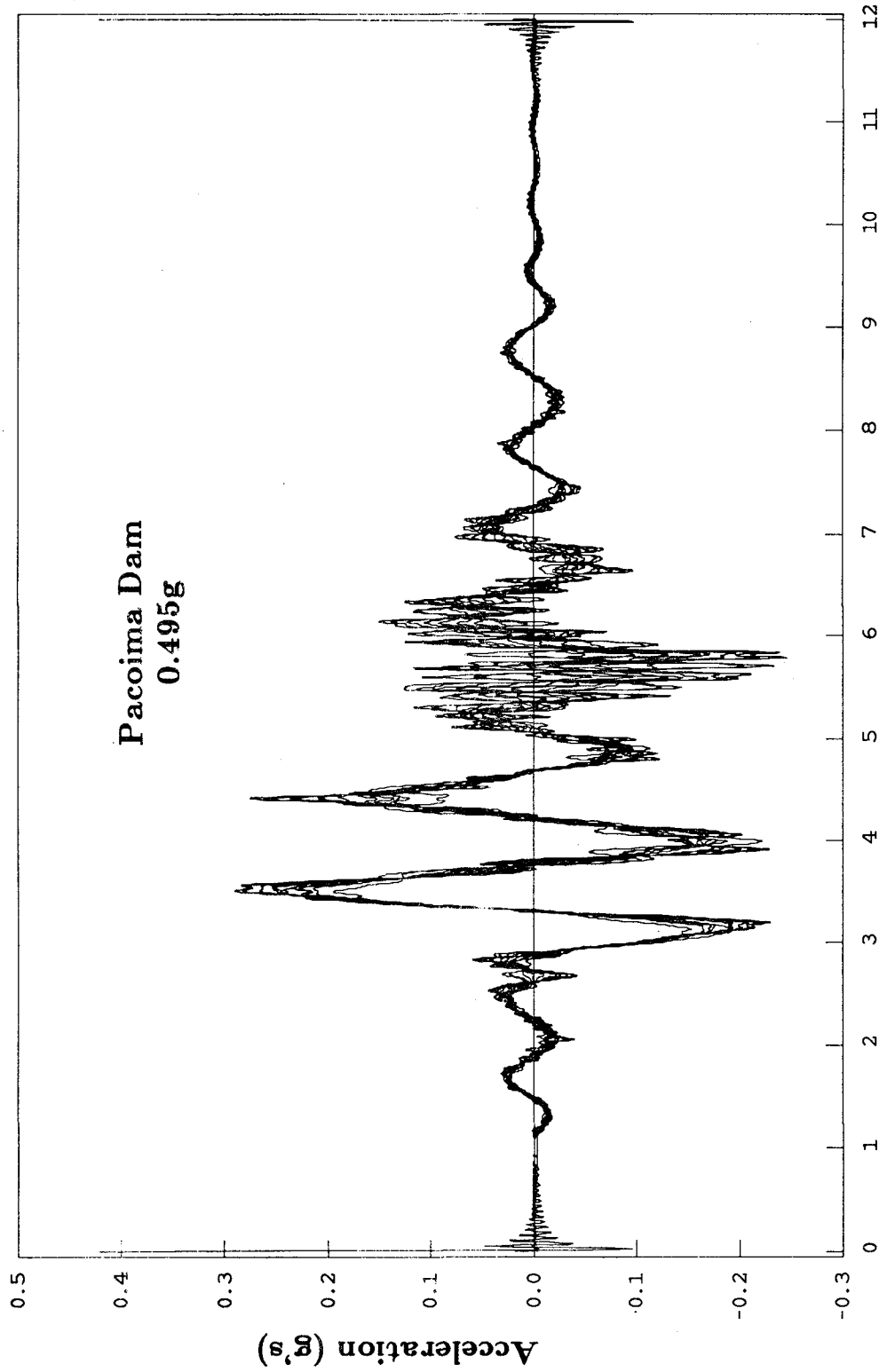

Figure 5.8 Continued

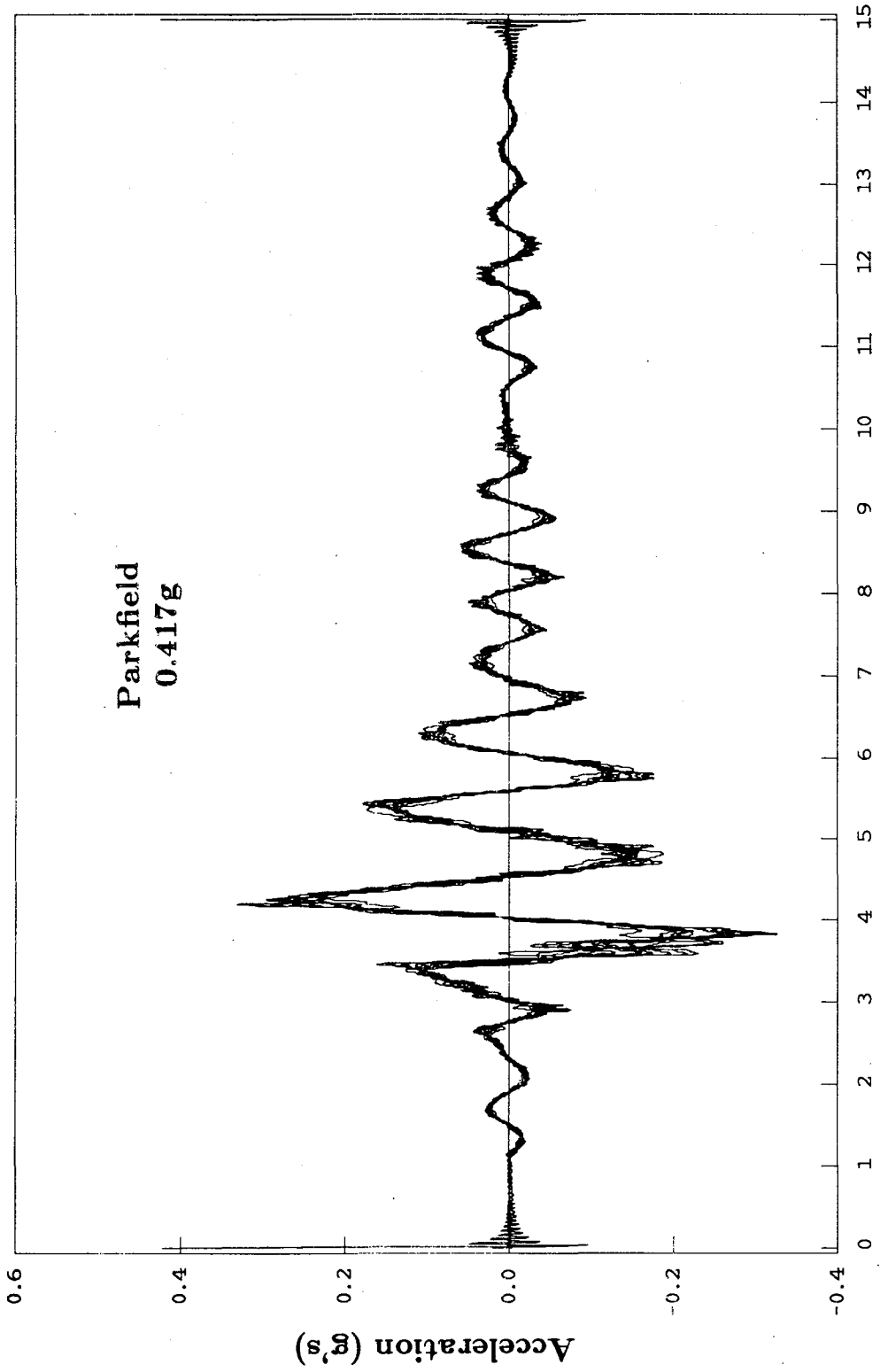

Figure 5.8 Continued

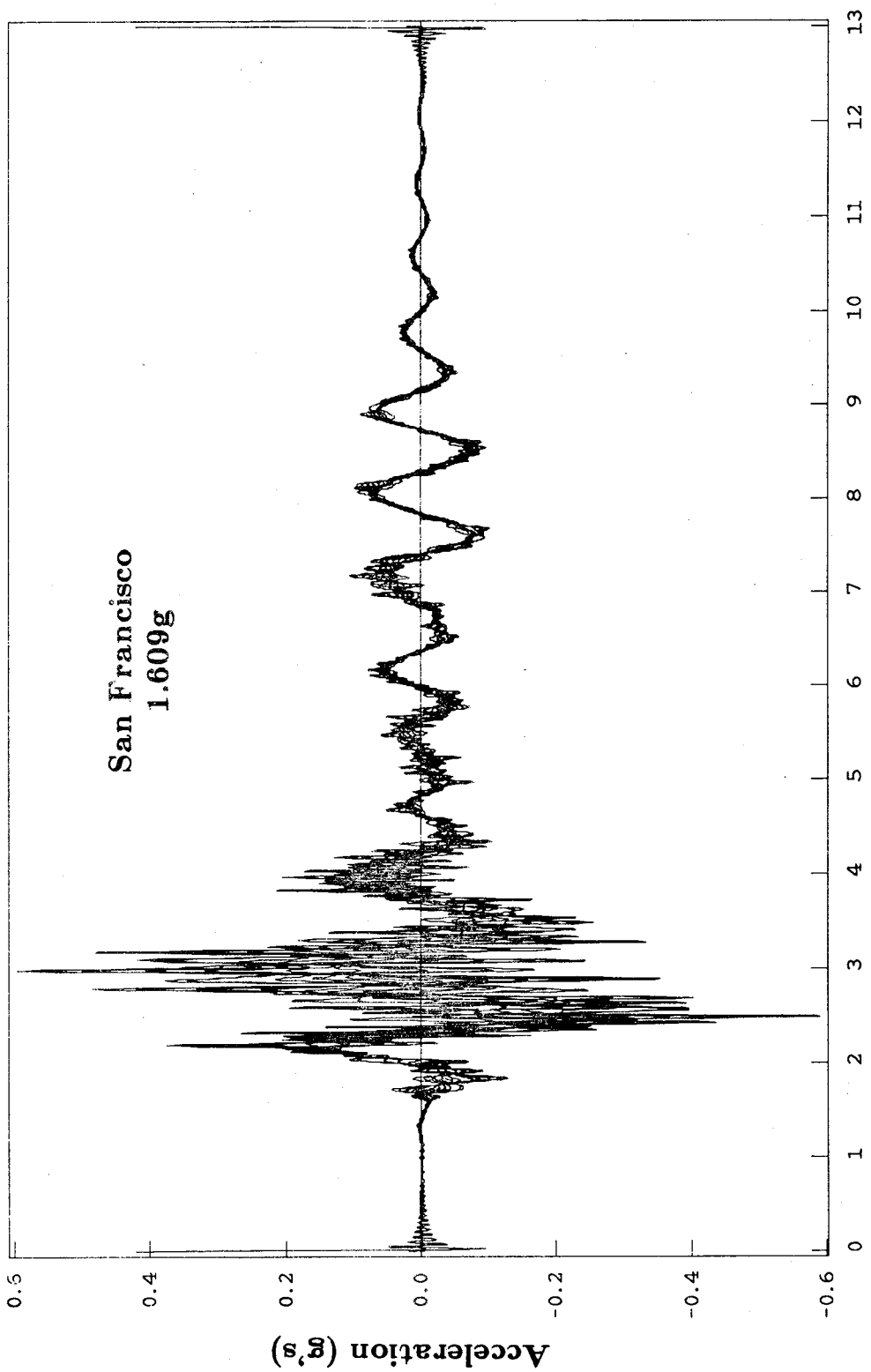

Figure 5.8 Continued

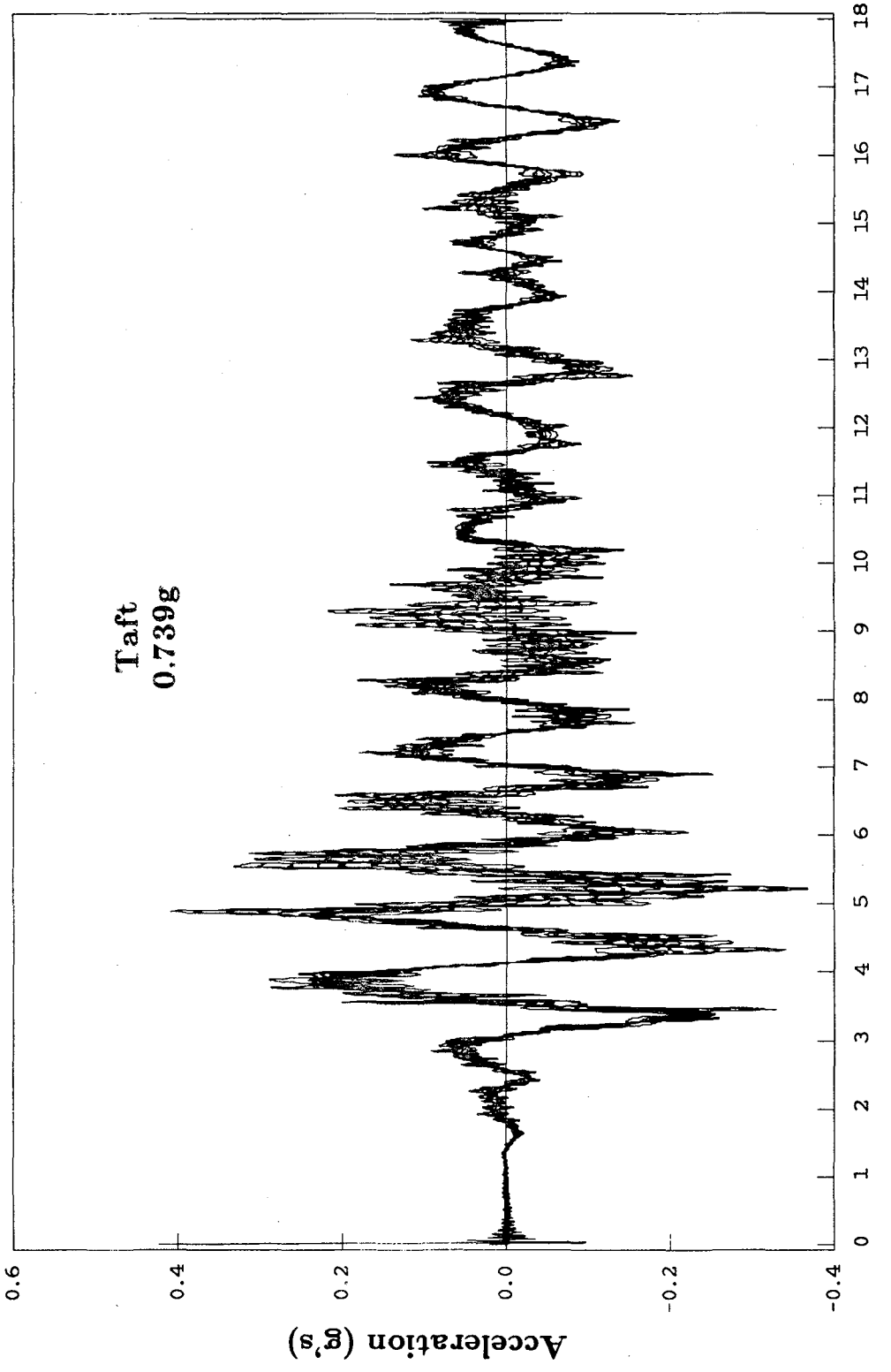

Figure 5.8 Continued

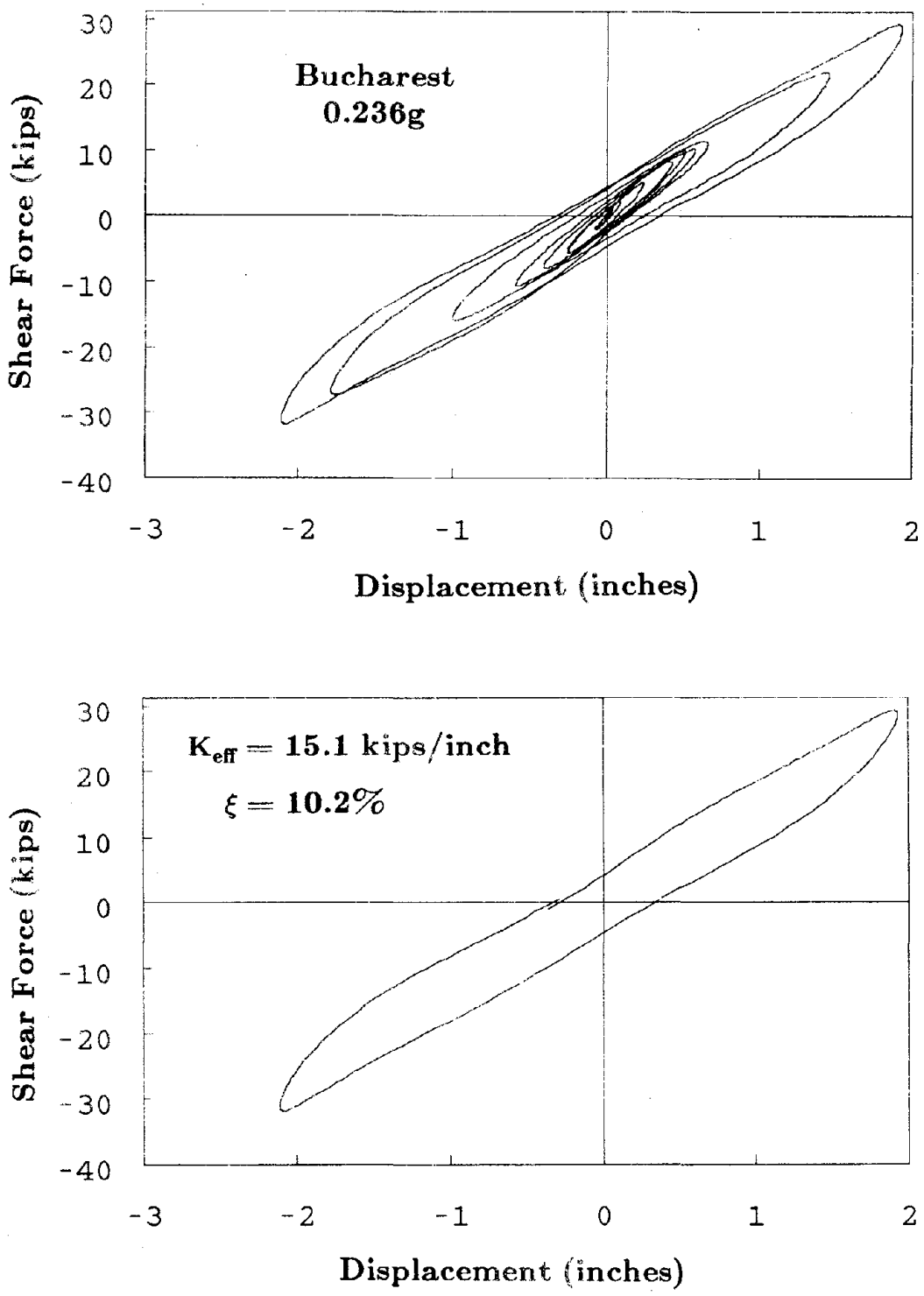

Figure 5.9 Isolation System Hysteresis Loops During Earthquake Tests, Neoprene Bearings

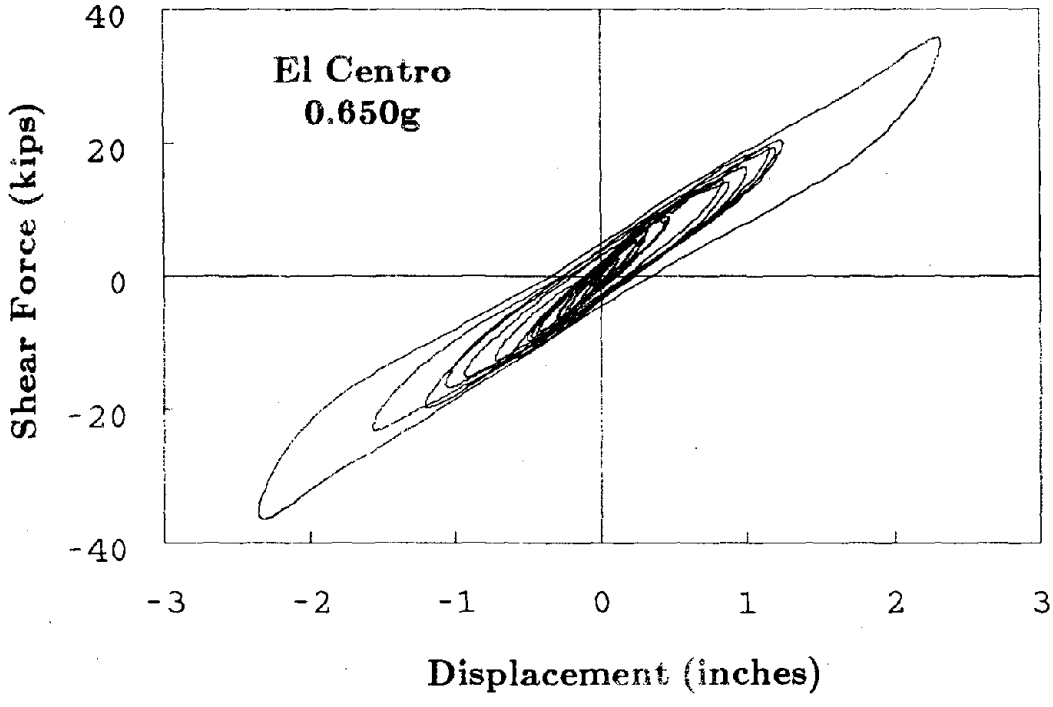

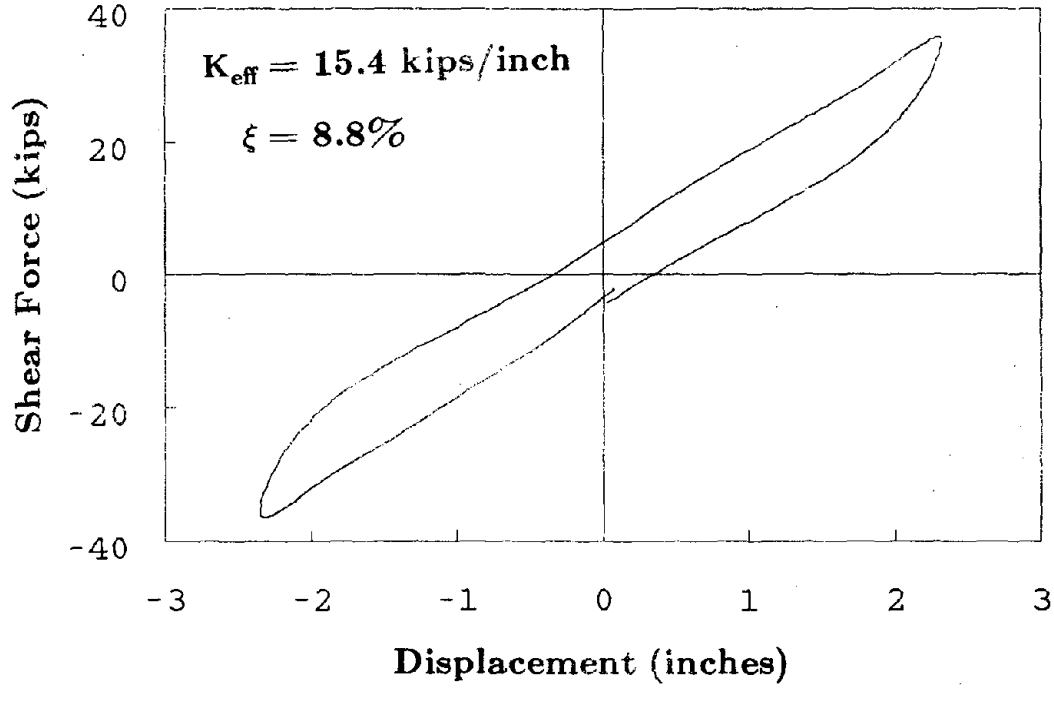

Figure 5.9 Continued

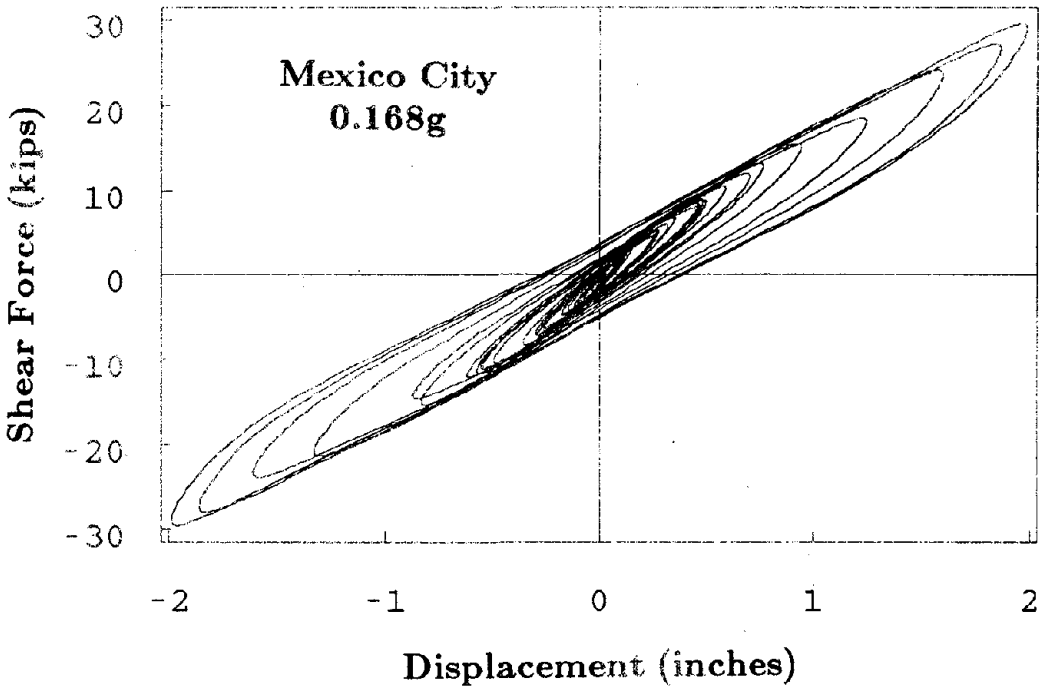

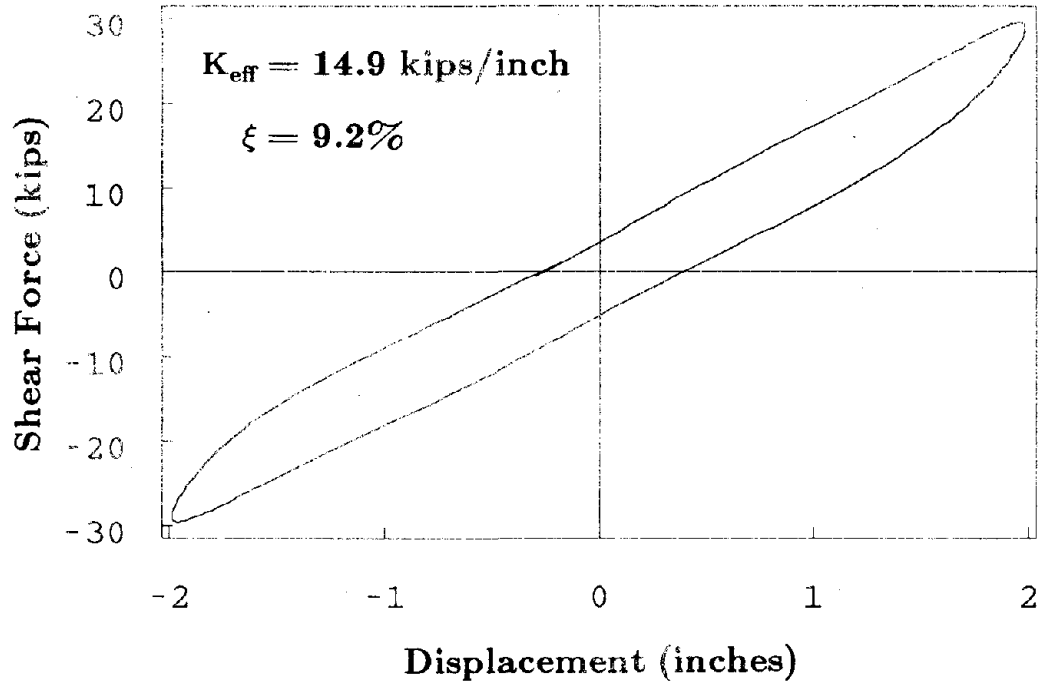

Figure 5.9 Continued

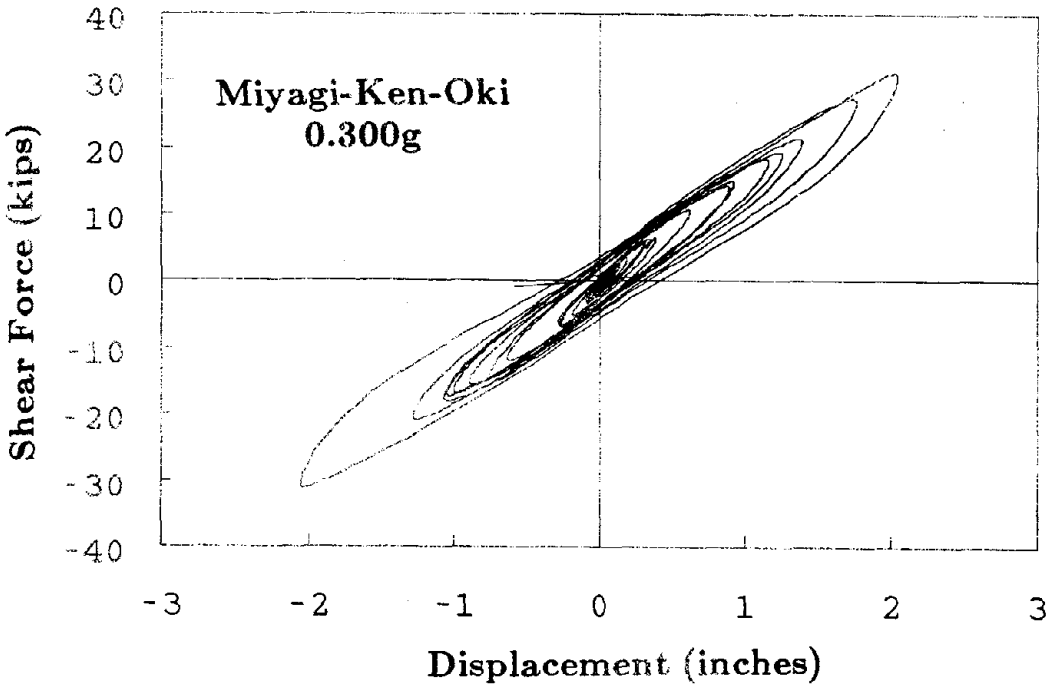

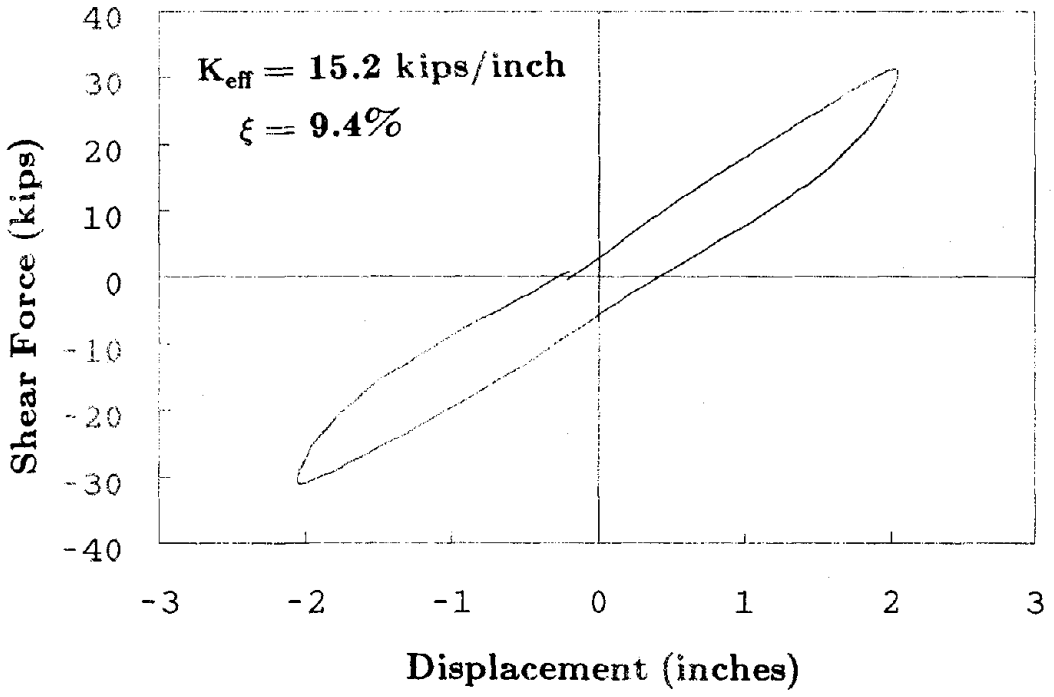

Figure 5.9 Continued

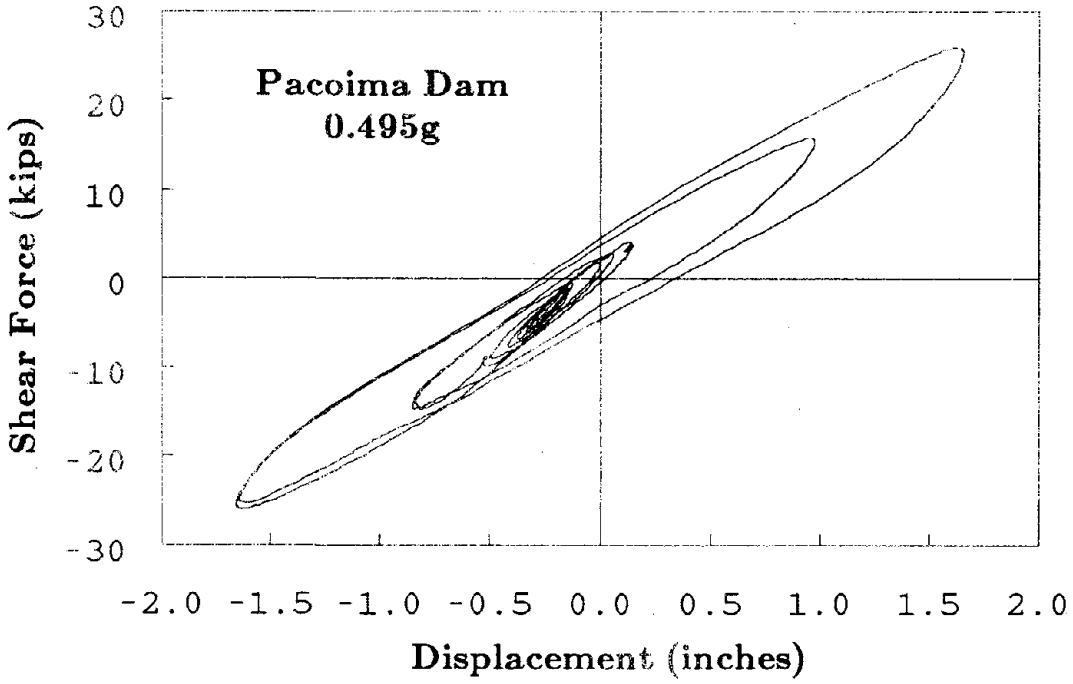

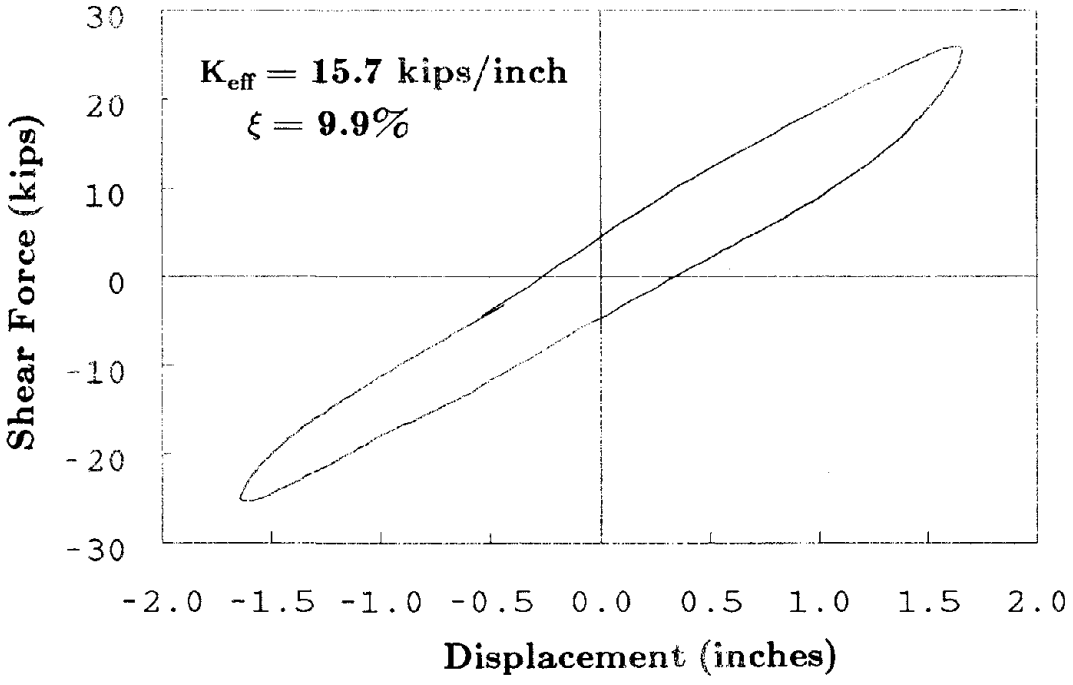

Figure 5.9 Continued

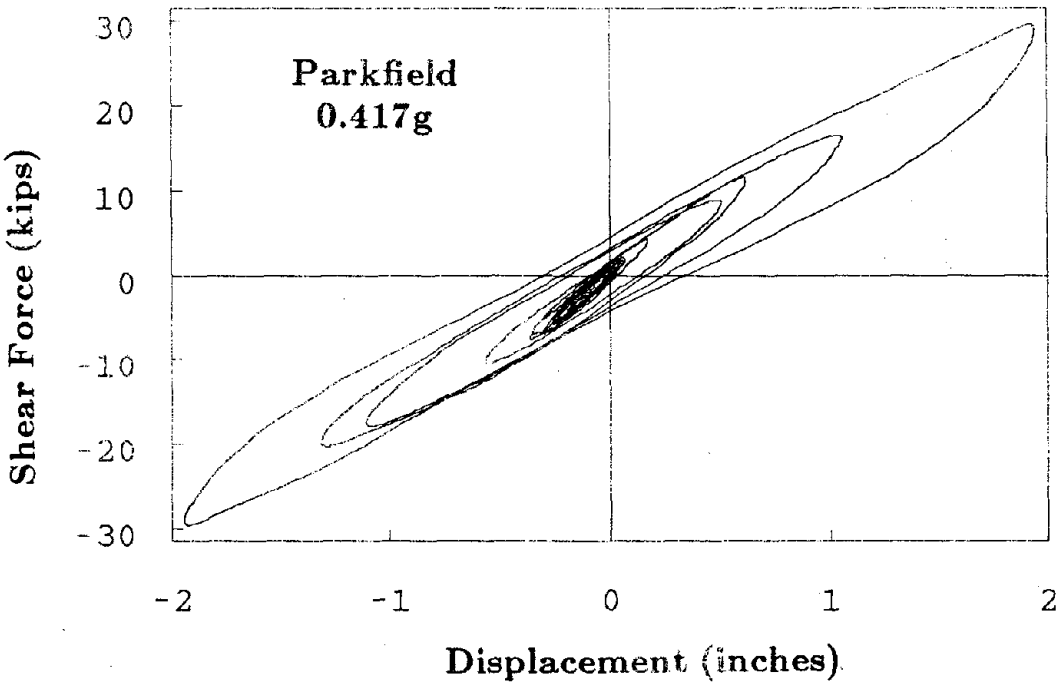

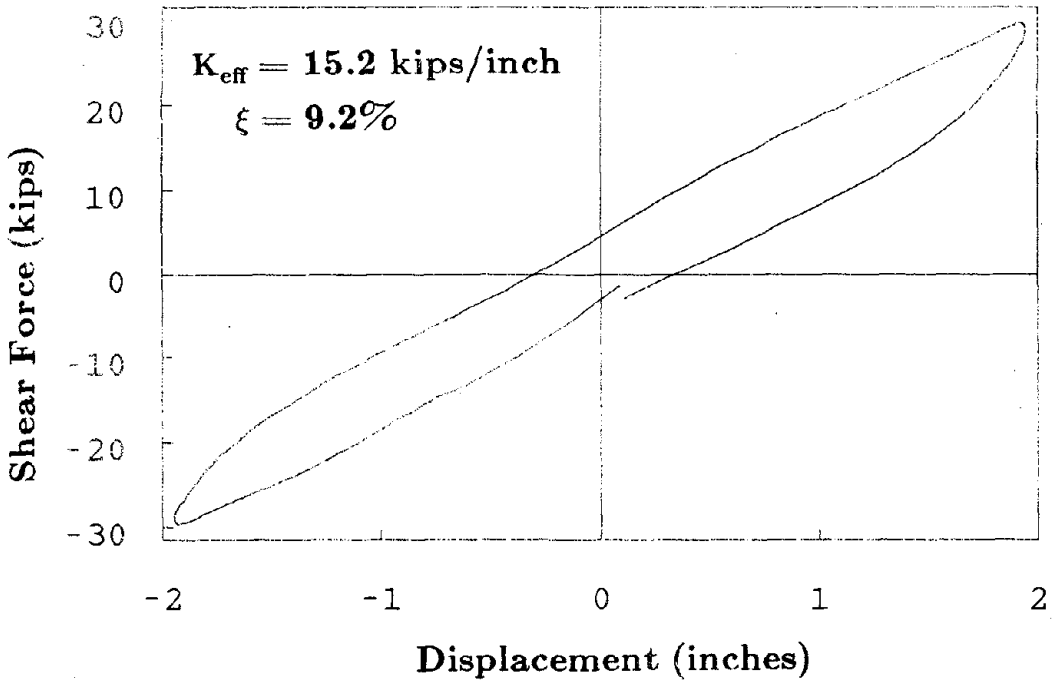

Figure 5.9 Continued

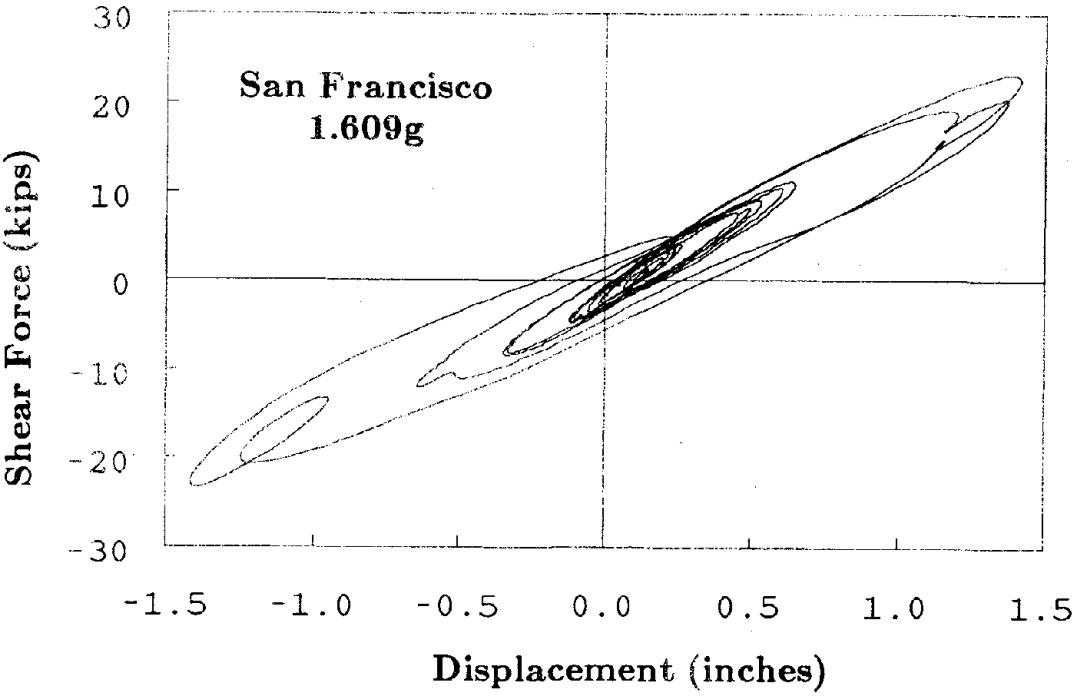

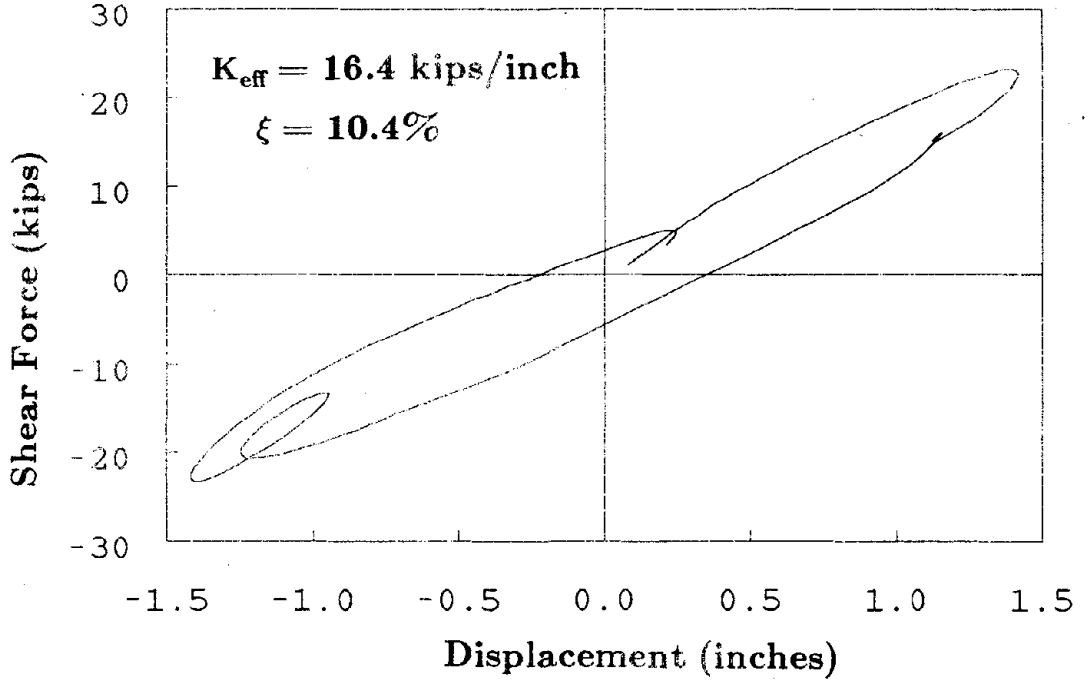

Figure 5.9 Continued

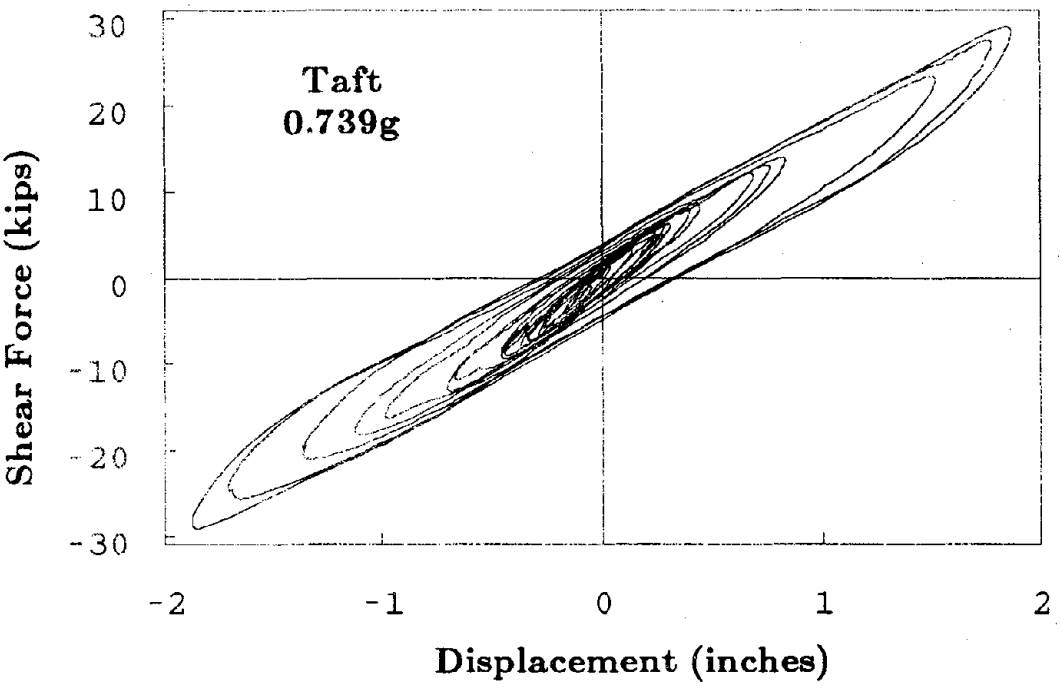

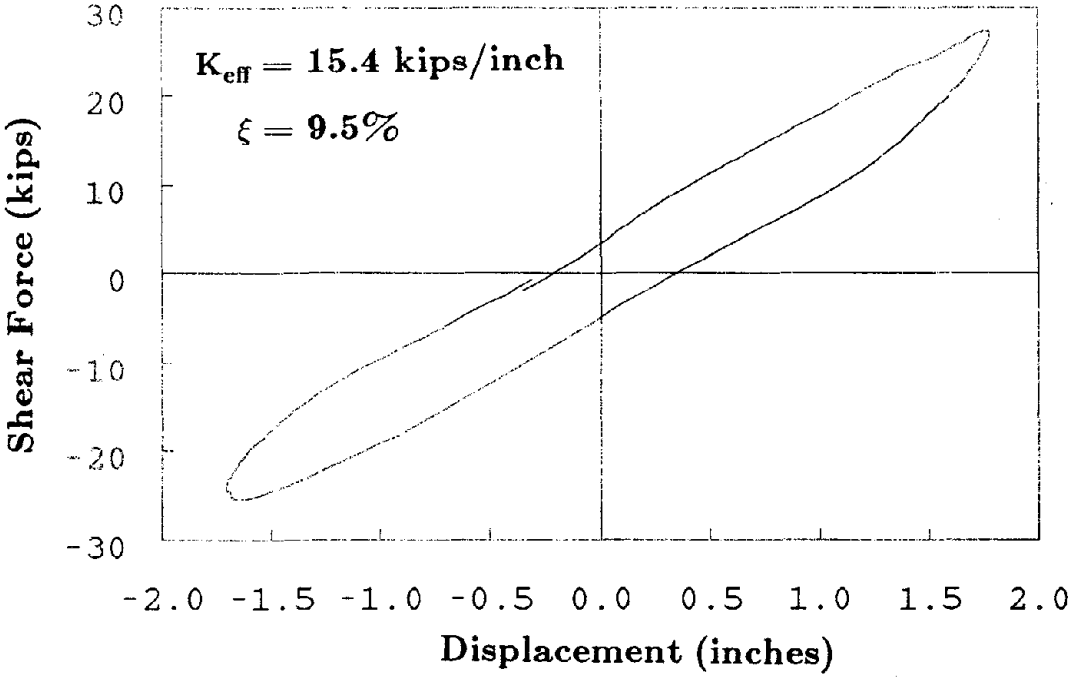

Figure 5.9 Continued

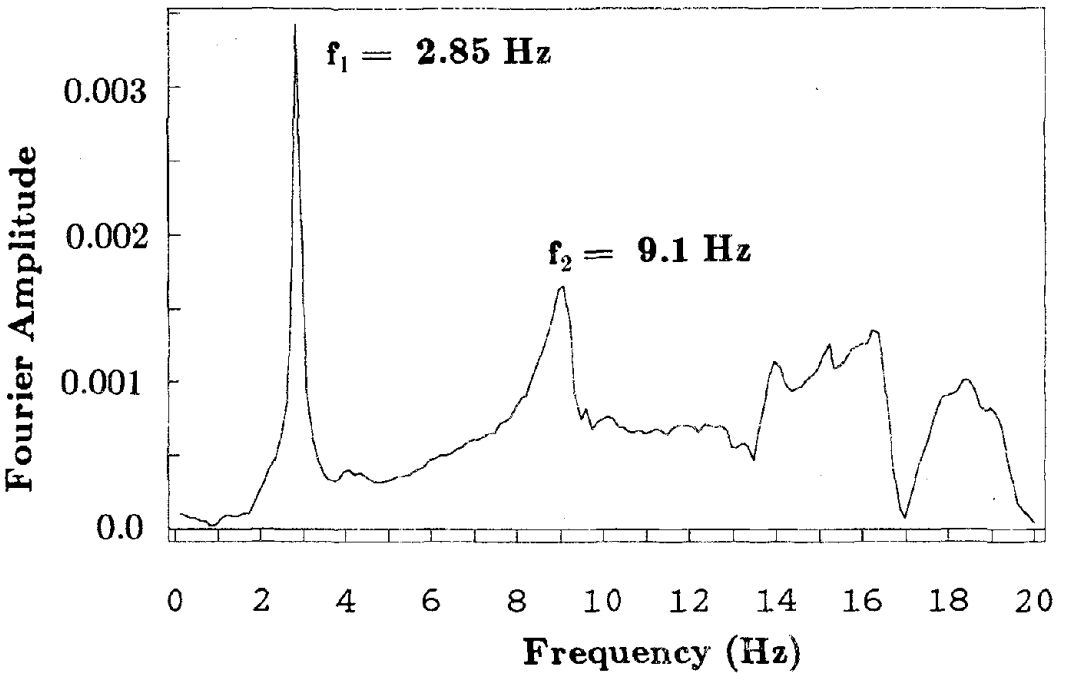

Figure 6.1 Fourier Amplitude Plot of Roof Acceleration Free-Vibration Test, Lead-Plug Bearings

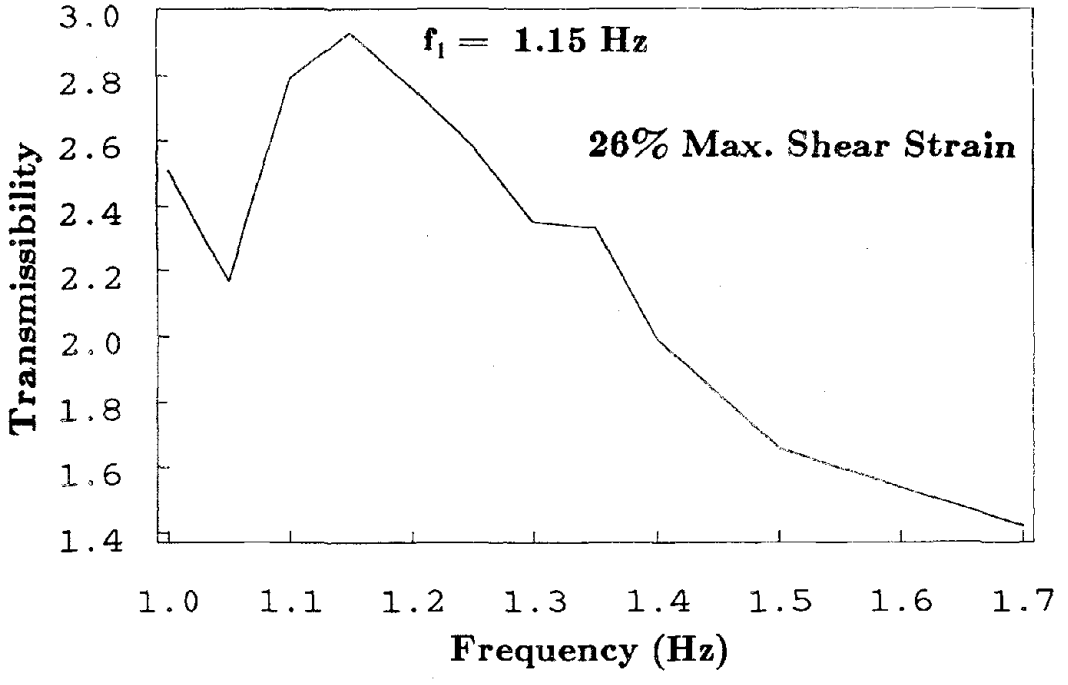

Figure 6.2 Transmissibility Plot for Roof Acceleration Harmonic Vibration Test, Lead-Plug Bearings

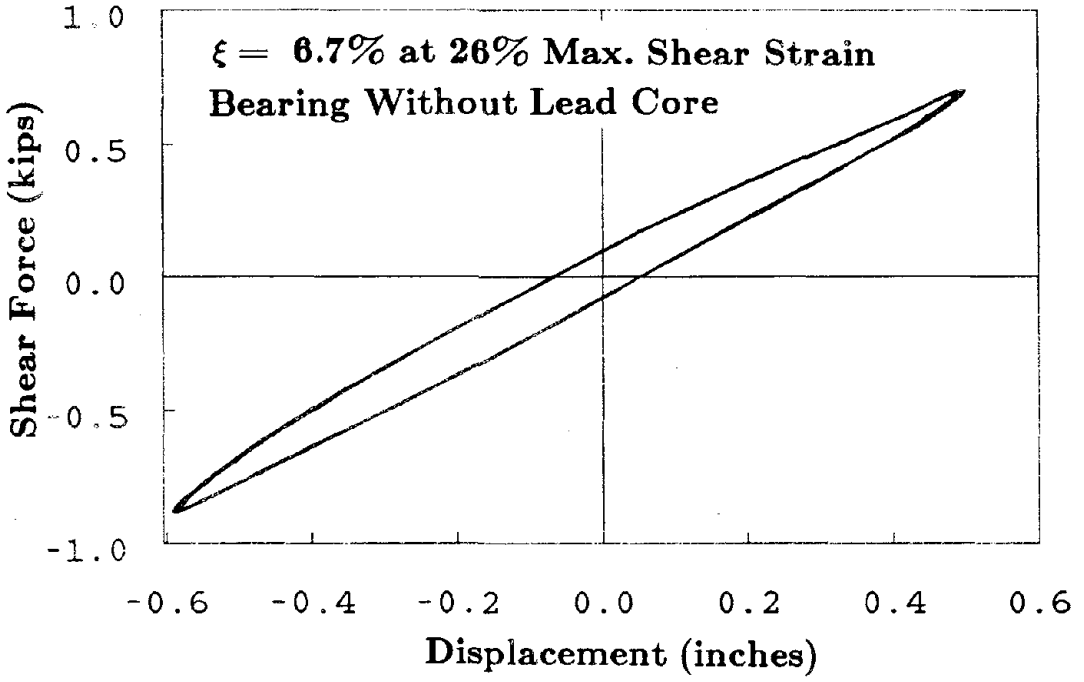

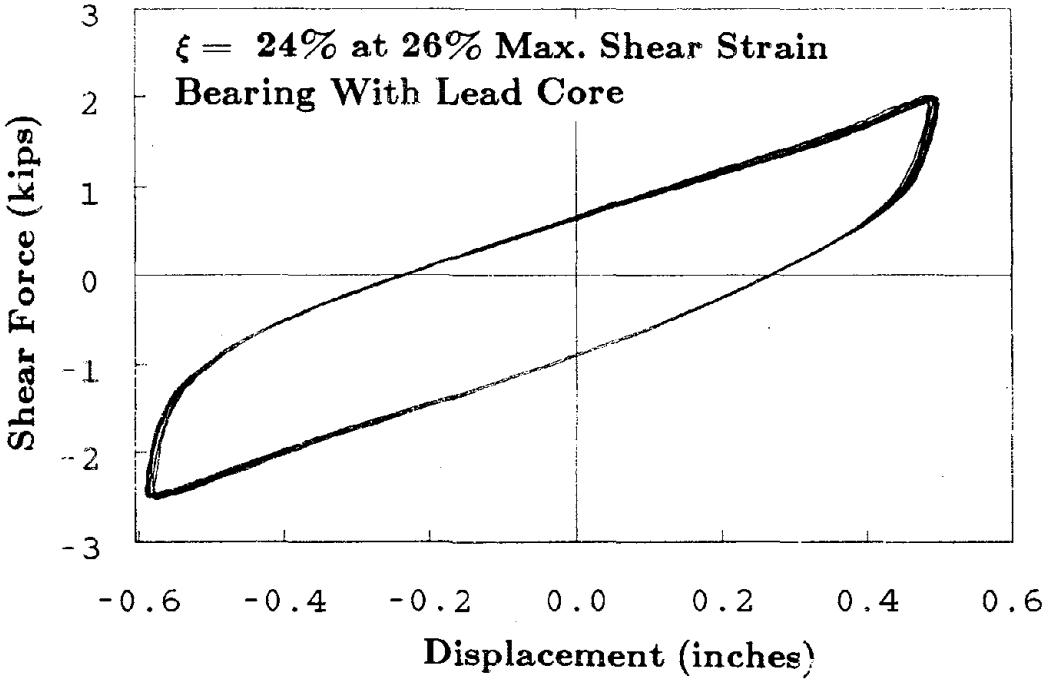

Figure 6.3 Bearing Shear Hysteresis Loops
Harmonic Vibration Test, Lead-Plug Bearings

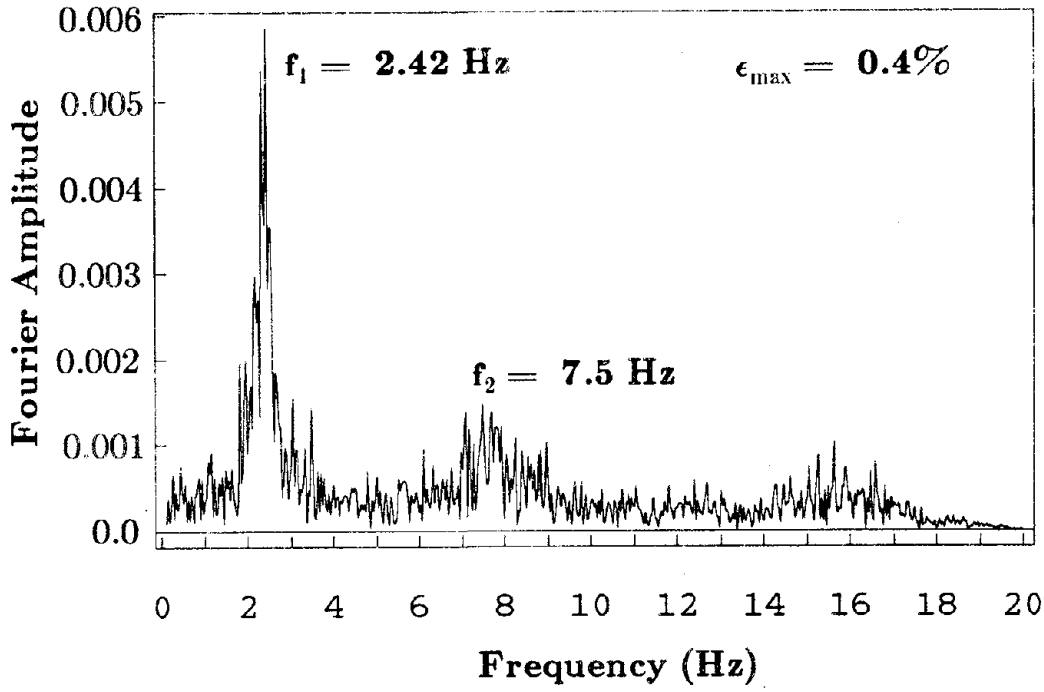

Figure 6.4 Fourier Amplitude Plot of Roof Acceleration White Noise Vibration Test, Lead-Plug Bearings

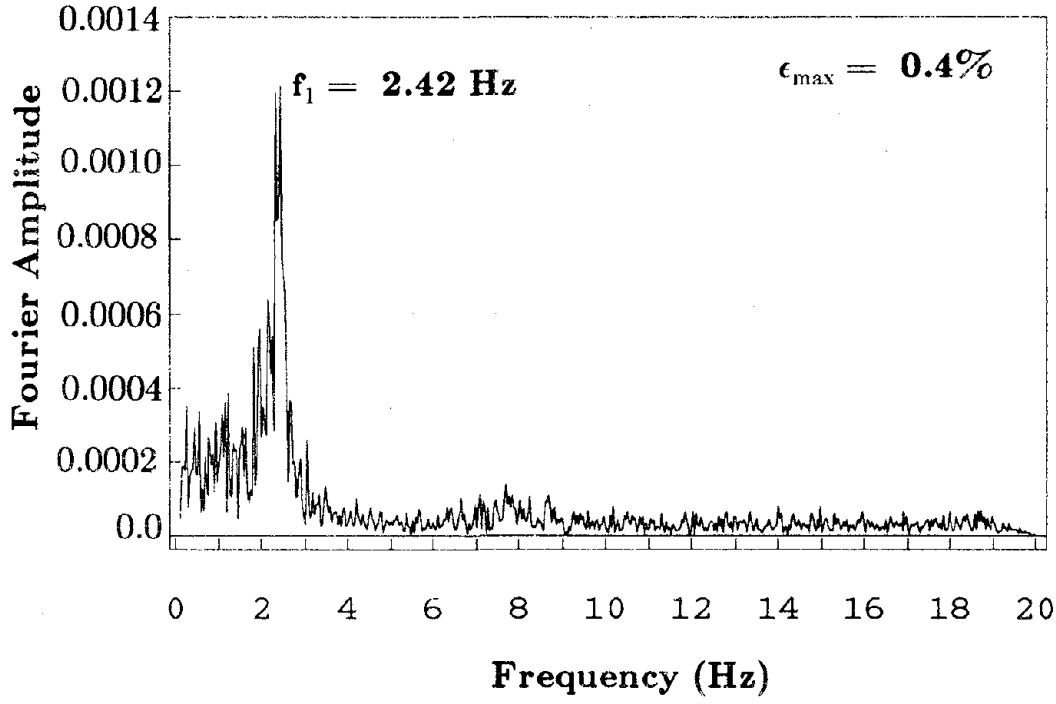

Figure 6.5 Fourier Amplitude Plot of Bearing Displacement White Noise Vibration Test, Lead-Plug Bearings

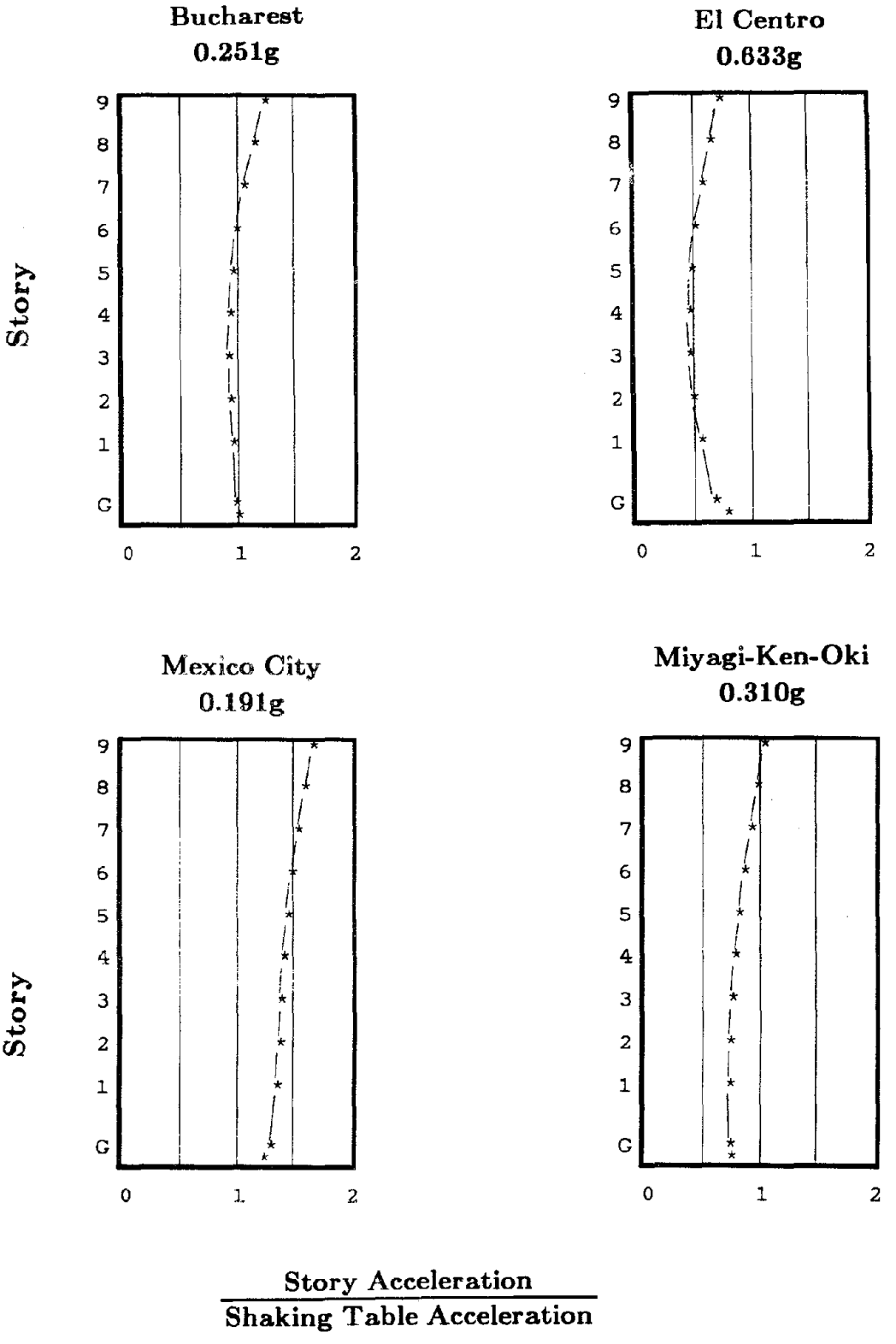

Figure 6.6 Story Acceleration Profiles, Lead-Plug Bearings

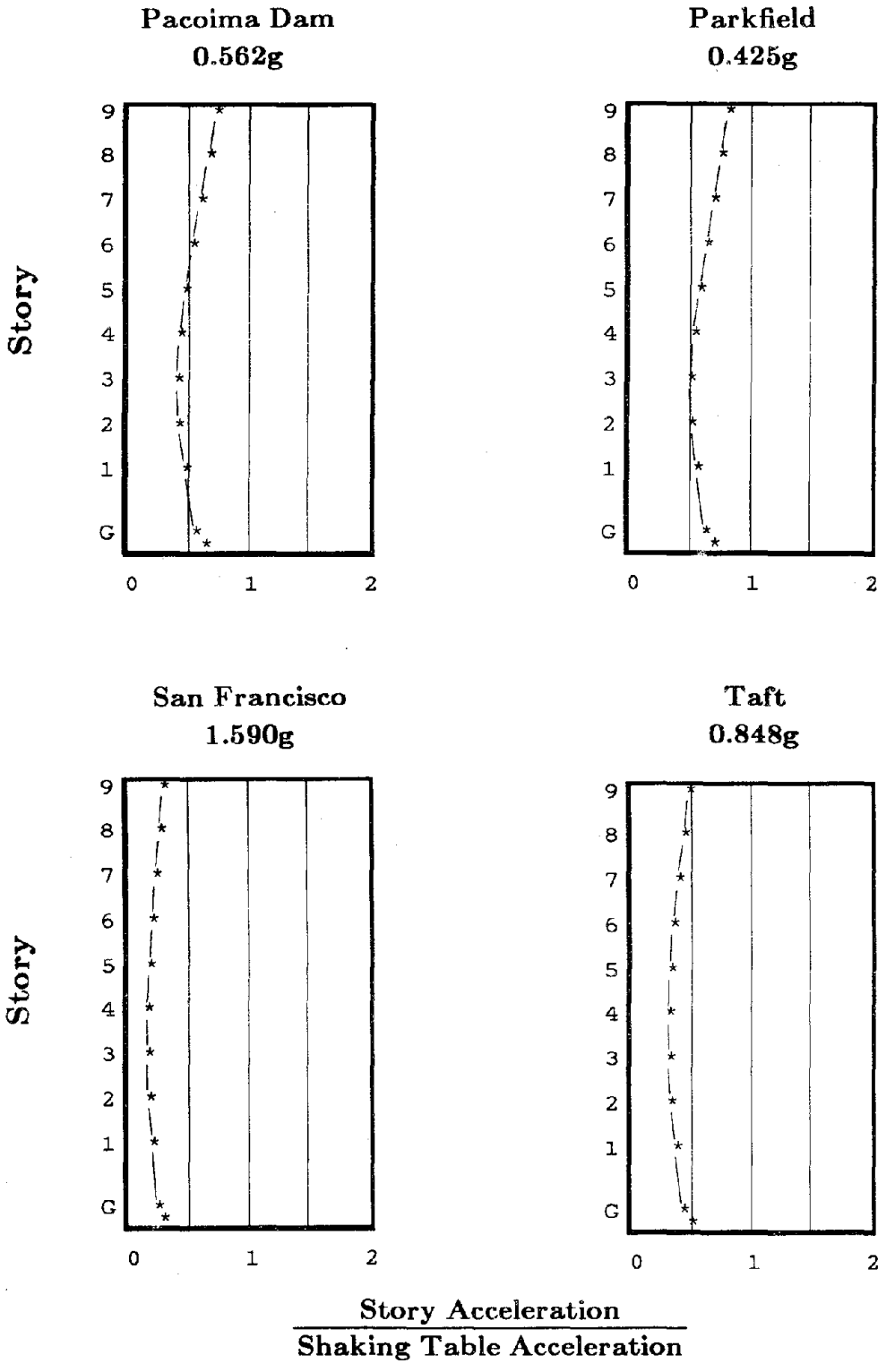

Figure 6.6 Continued

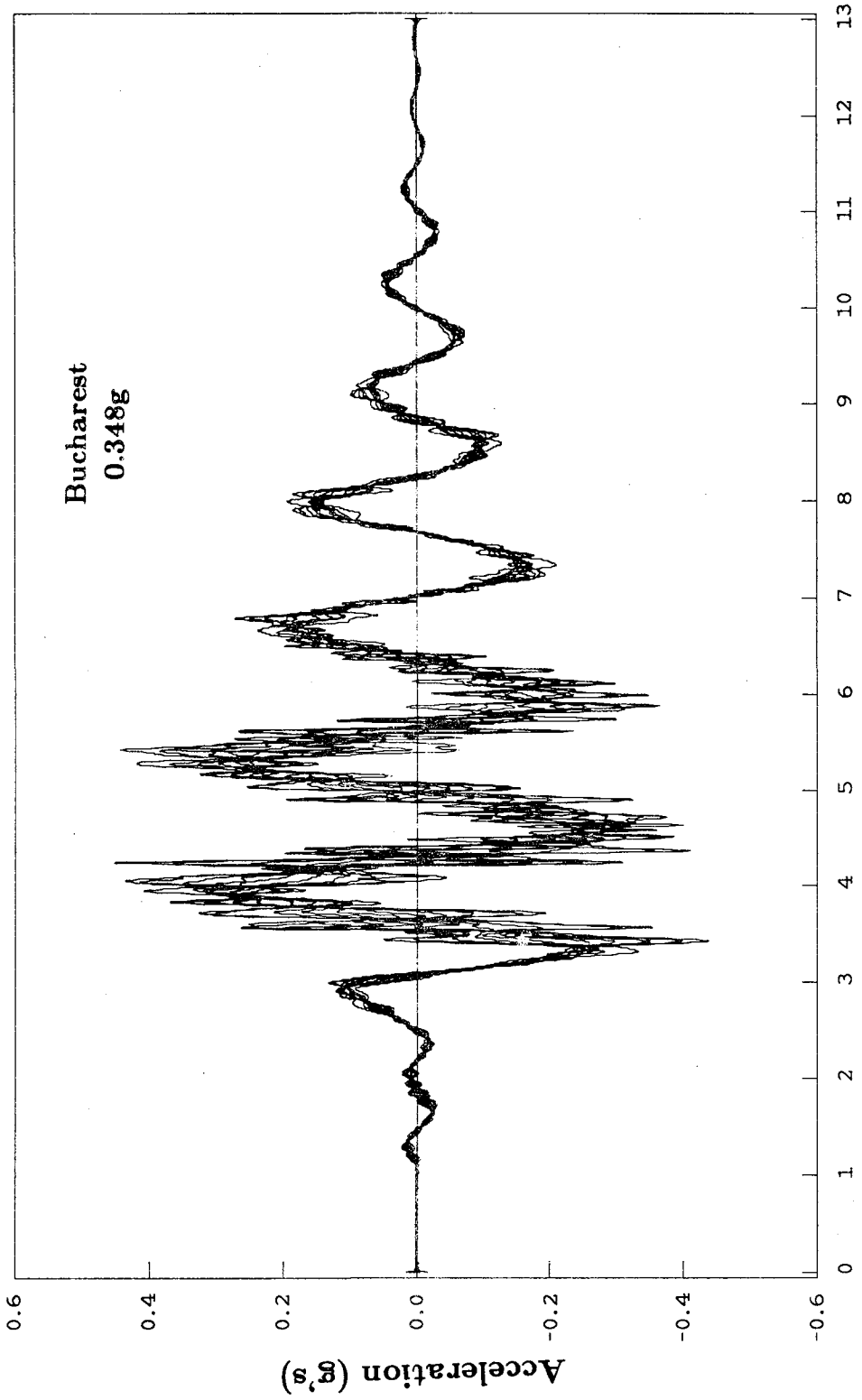

Figure 6.7 Superimposed Story Acceleration Time Series Plots, Lead-Plug Bearings

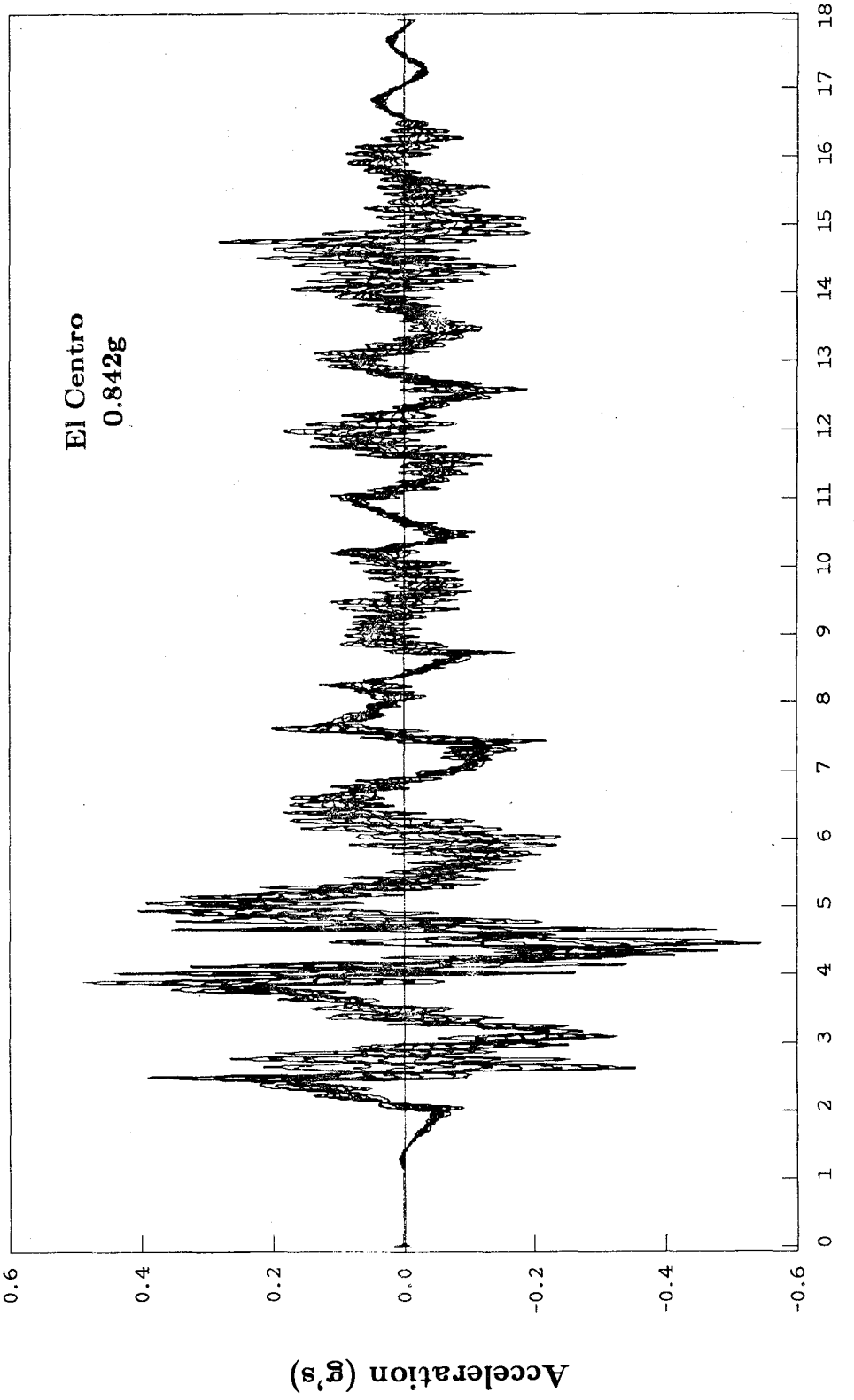

Figure 6.7 Continued

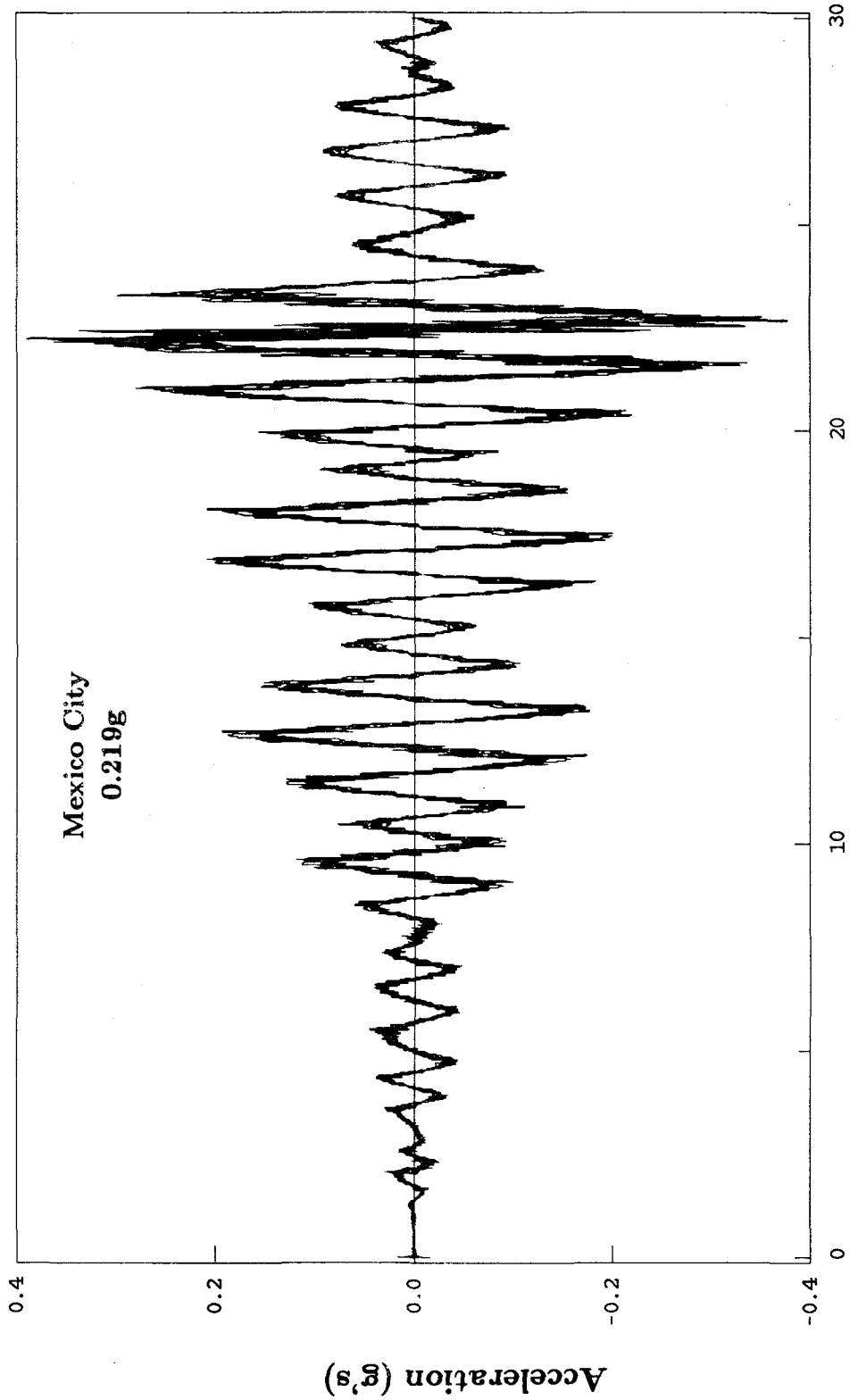

Figure 6.7 Continued

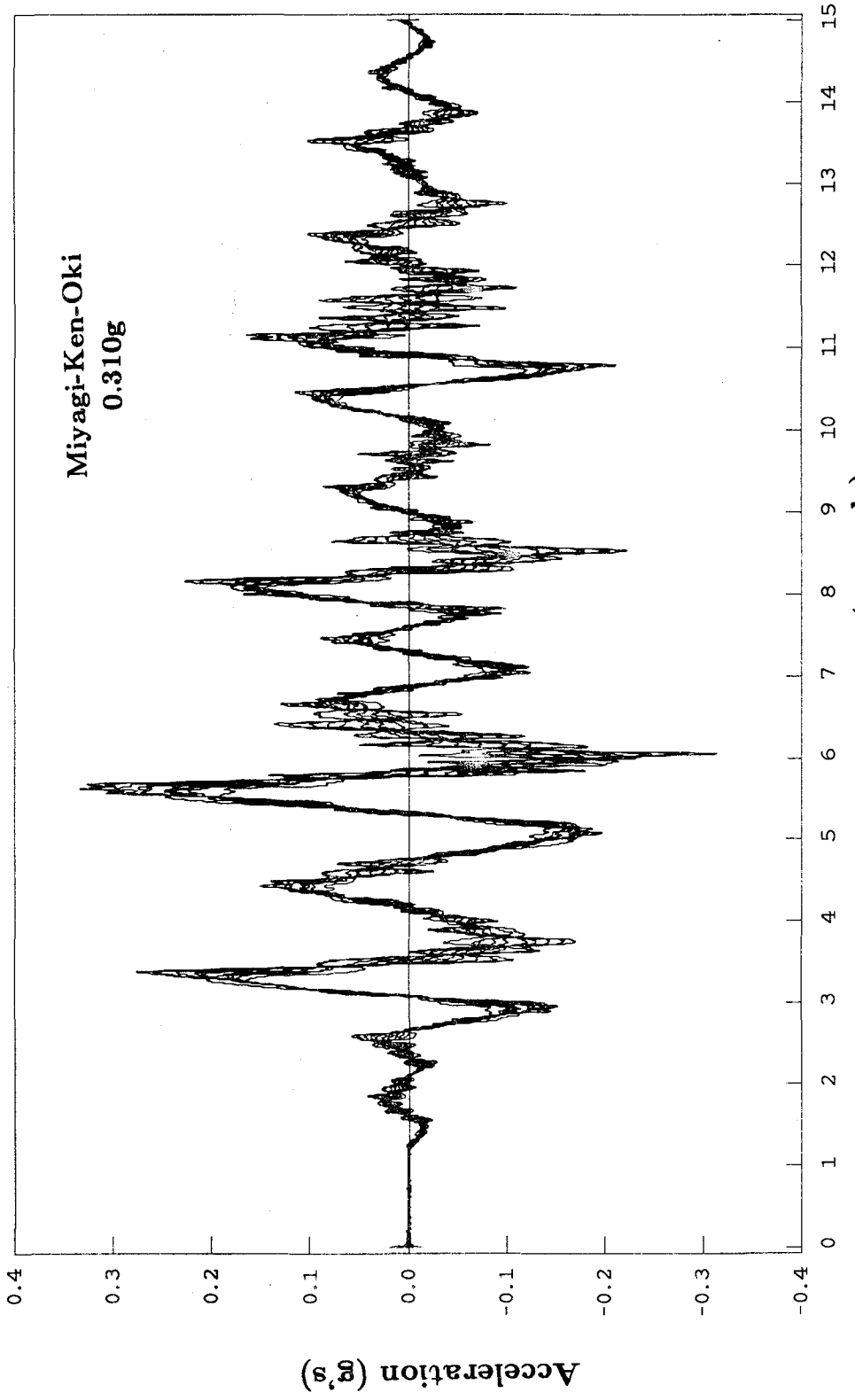

Figure 6.7 Continued

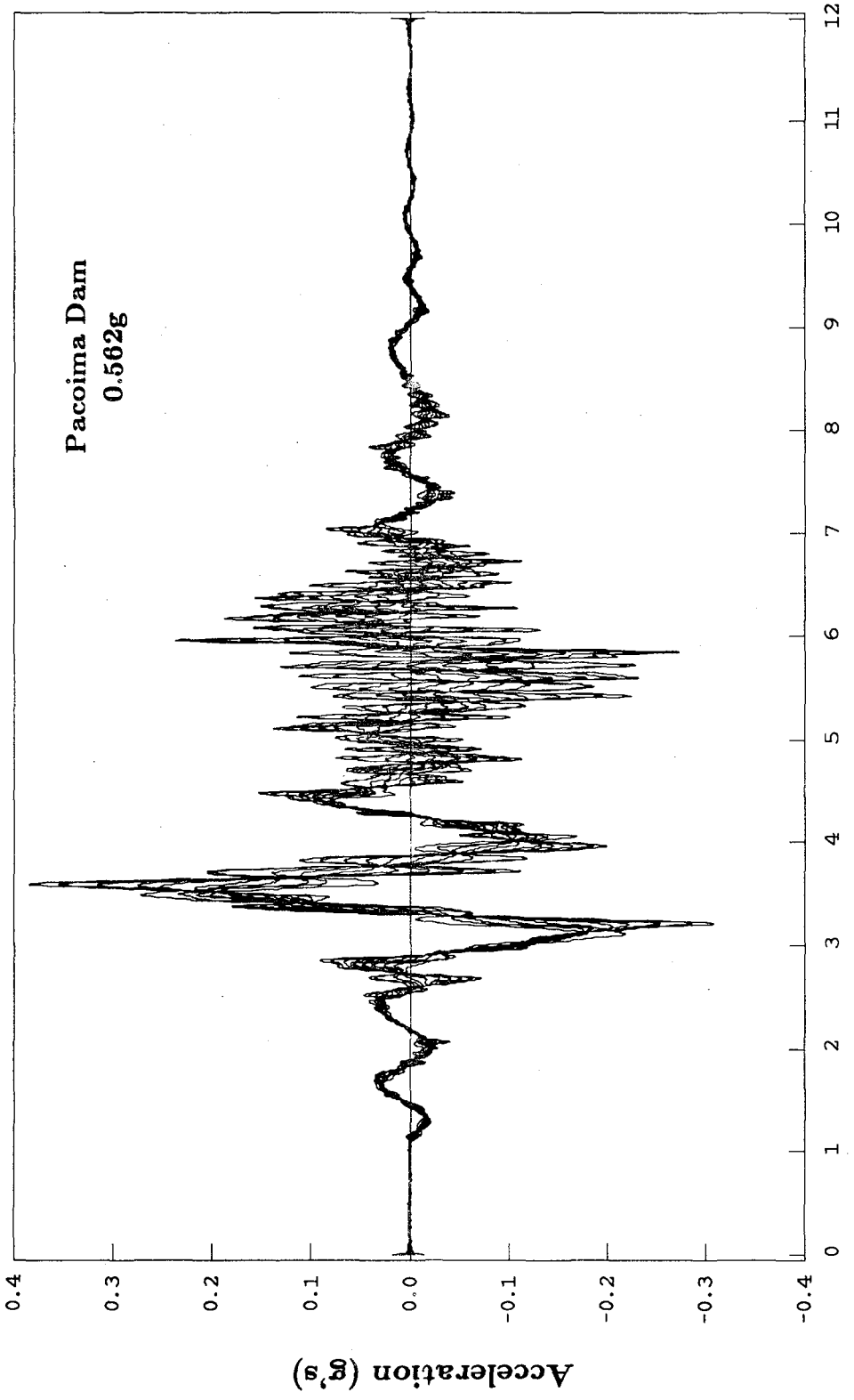

Figure 6.7 Continued

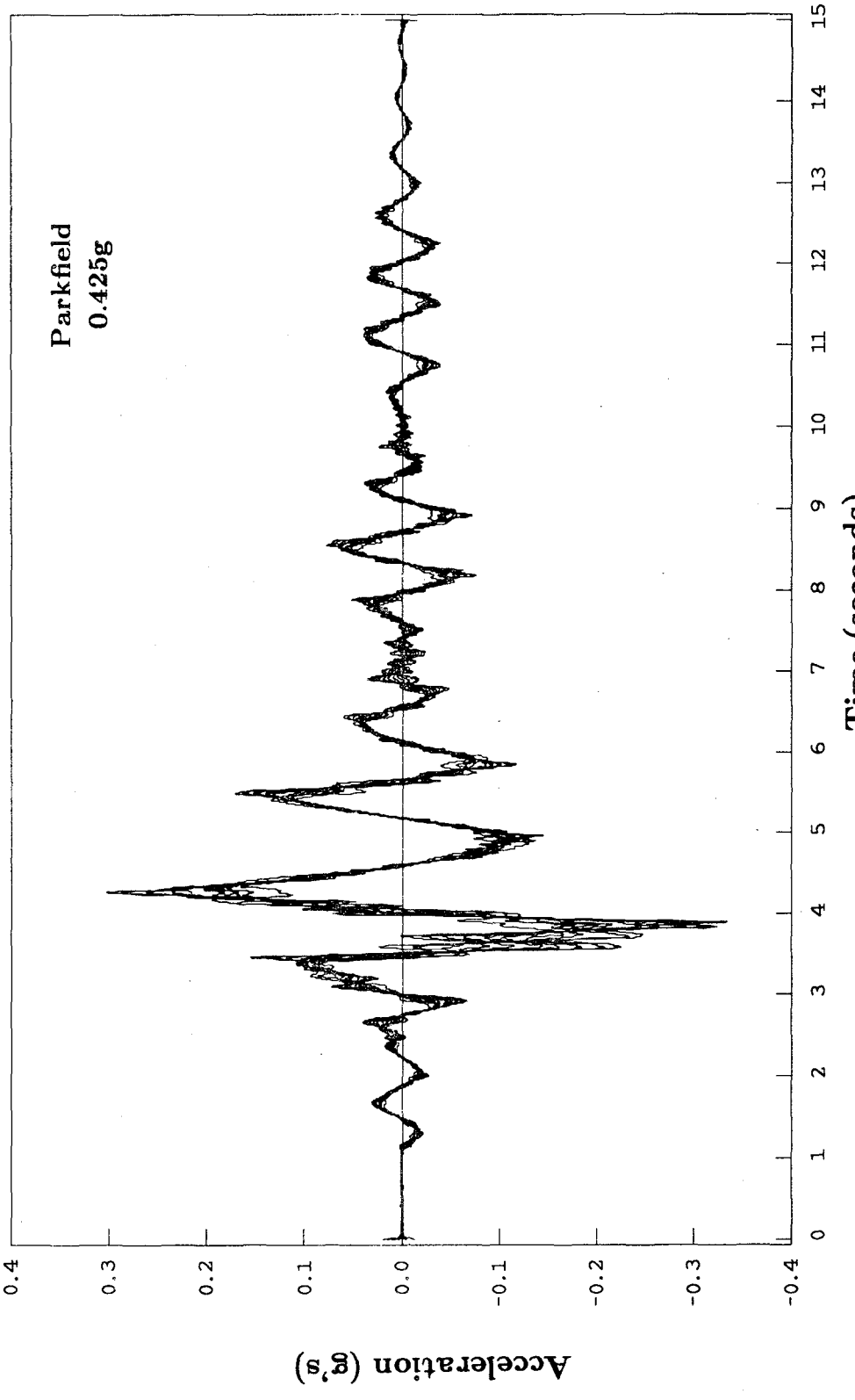

Figure 6.7 Continued

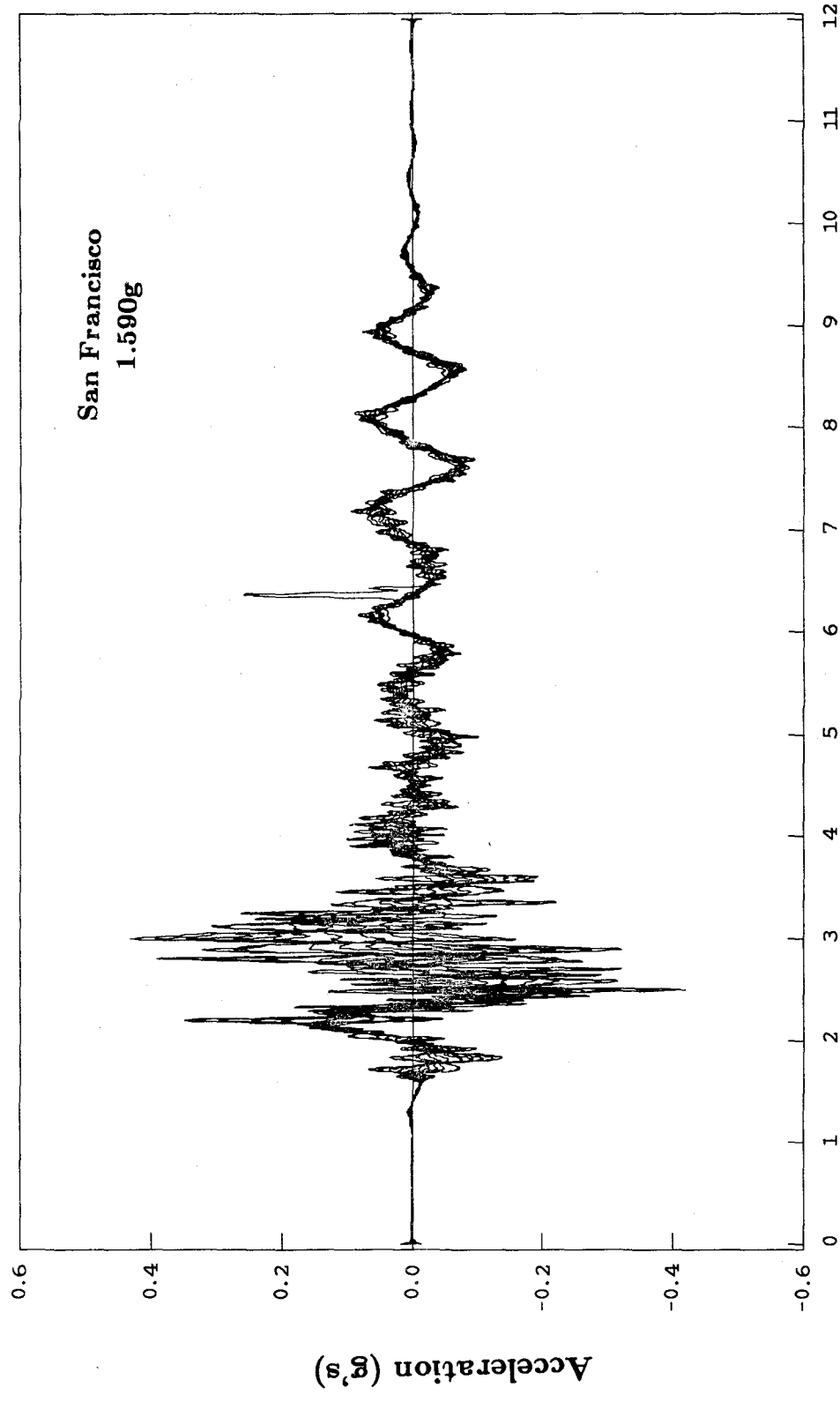

Figure 6.7 Continued

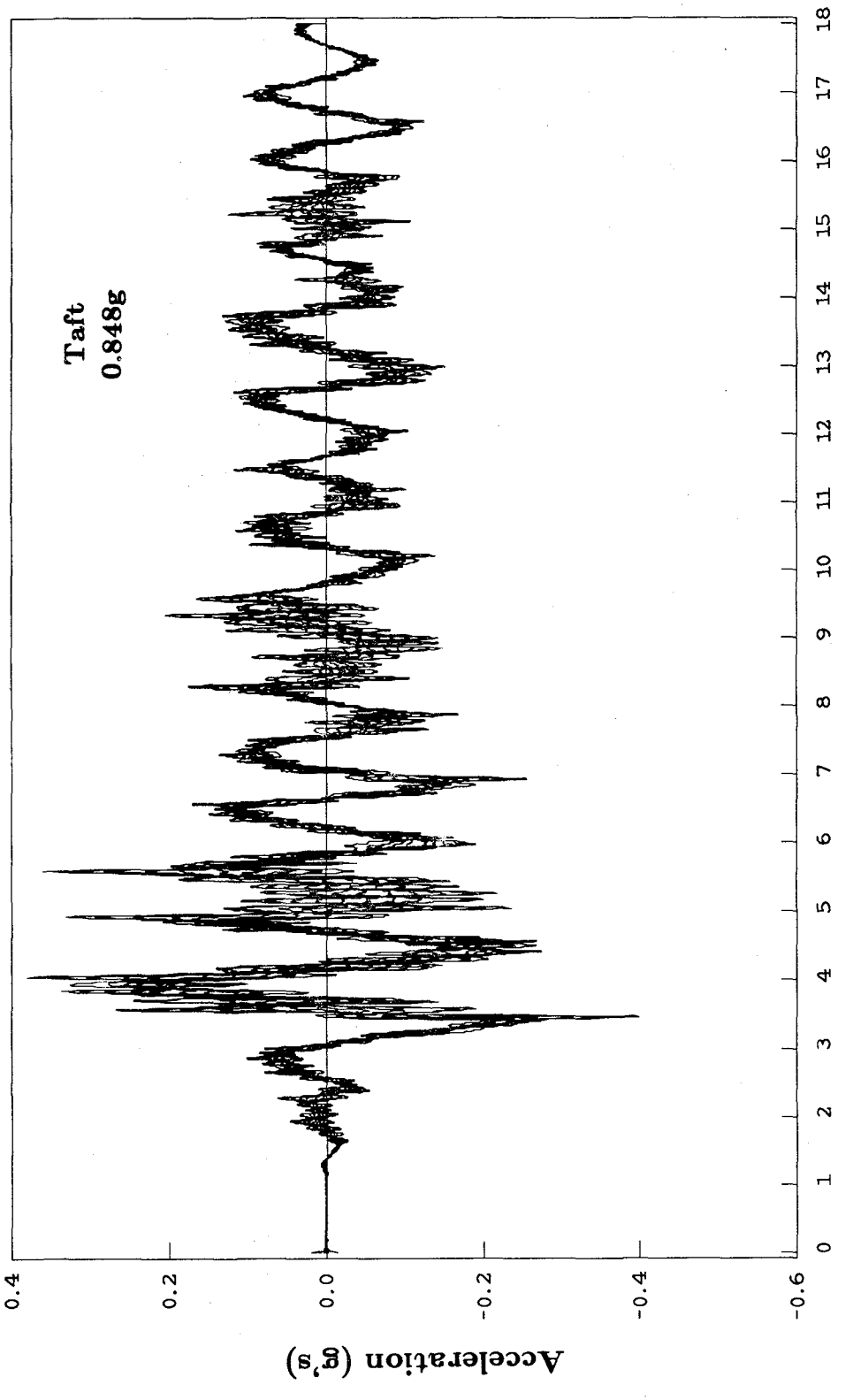

Figure 6.7 Continued

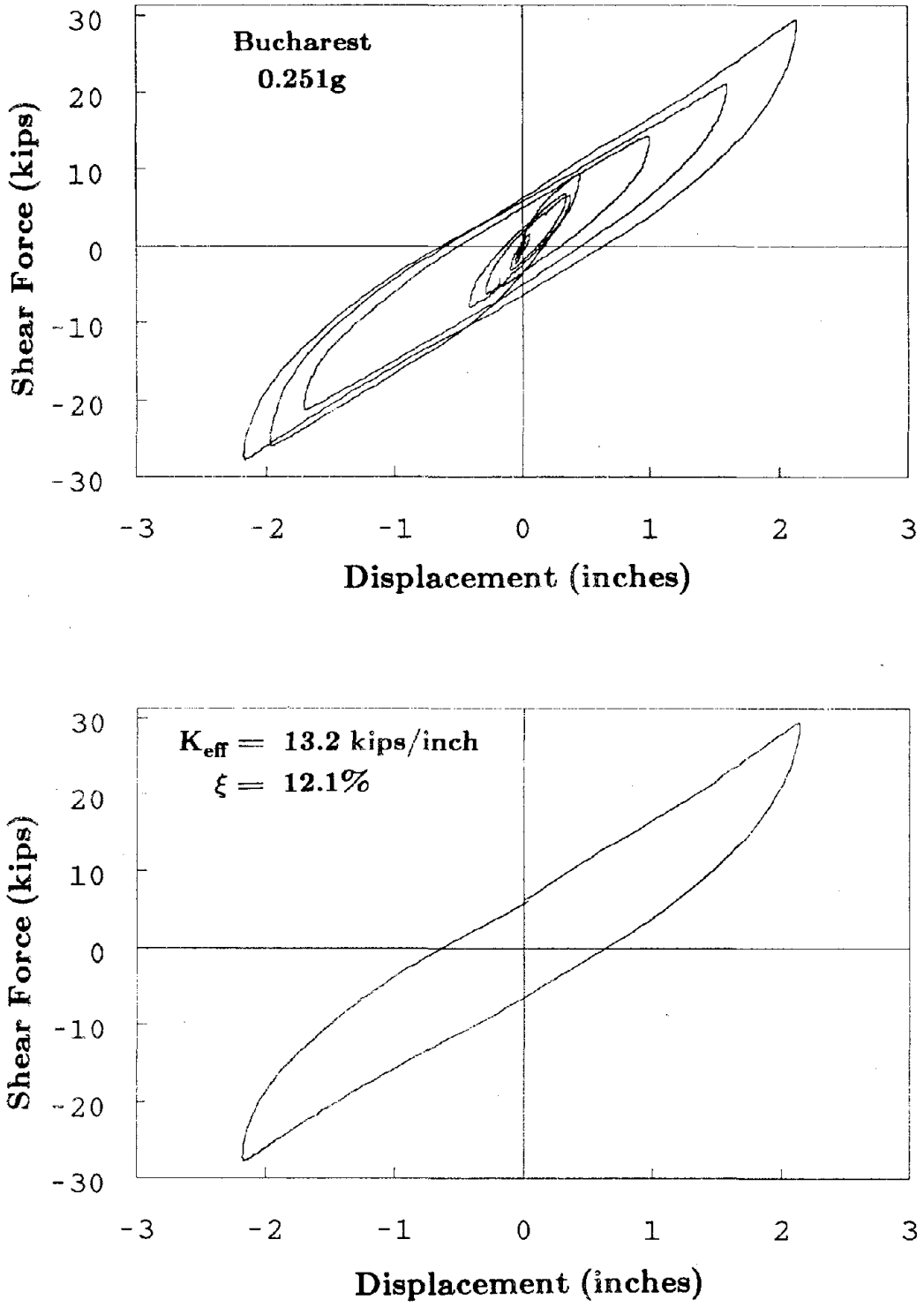

Figure 6.8 Isolation System Shear Hysteresis Loops During Earthquake Tests, Lead-Plug Bearings

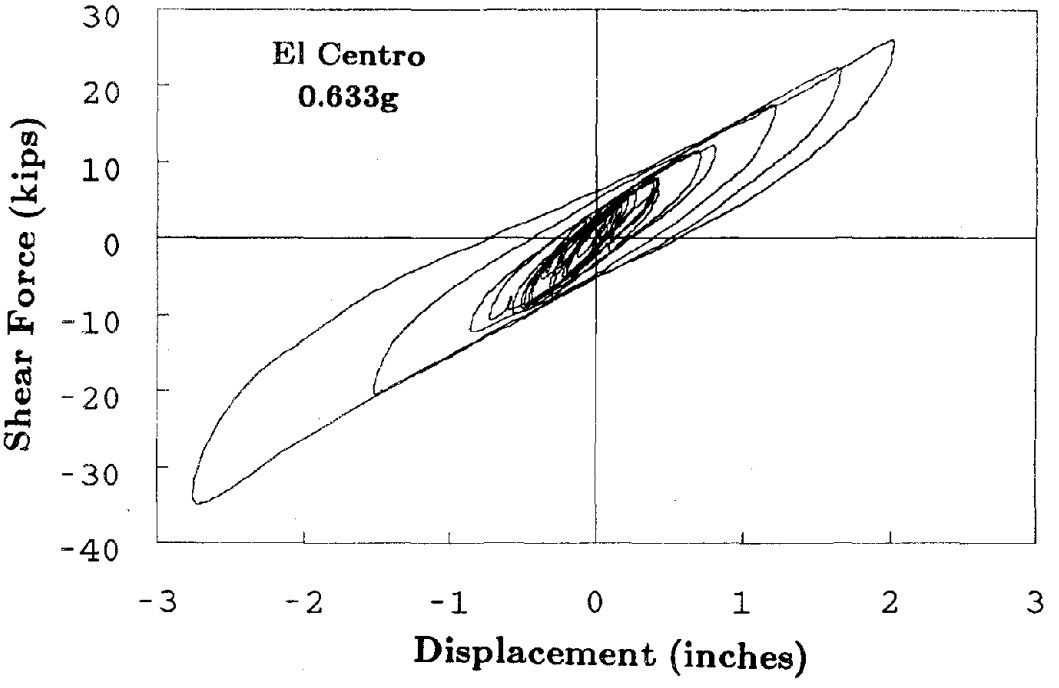

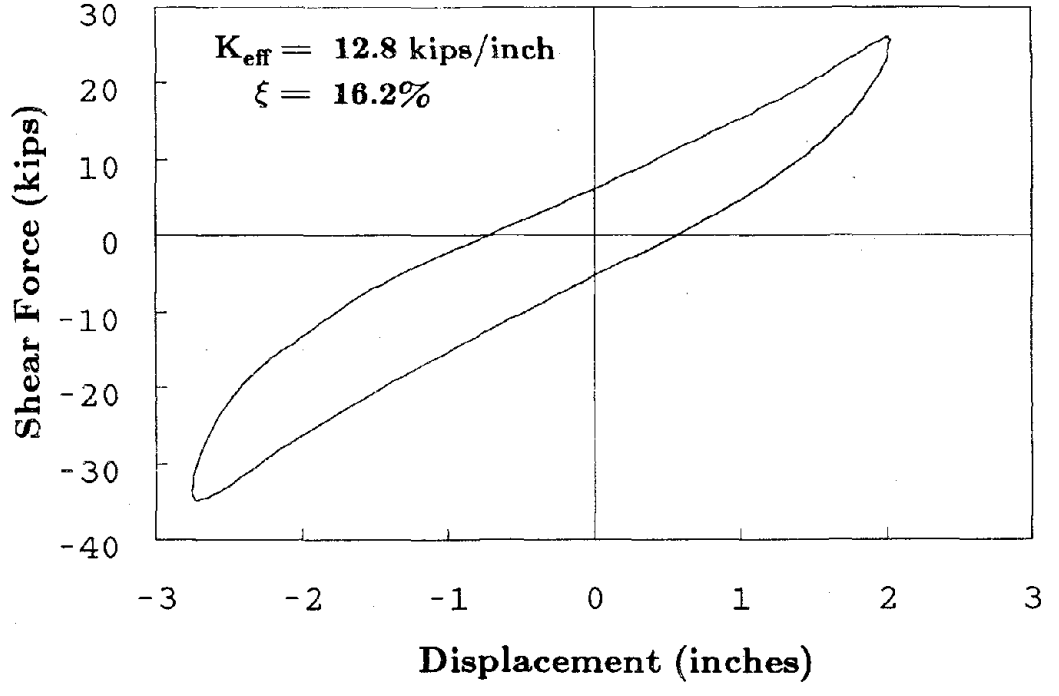

Figure 6.8 Continued

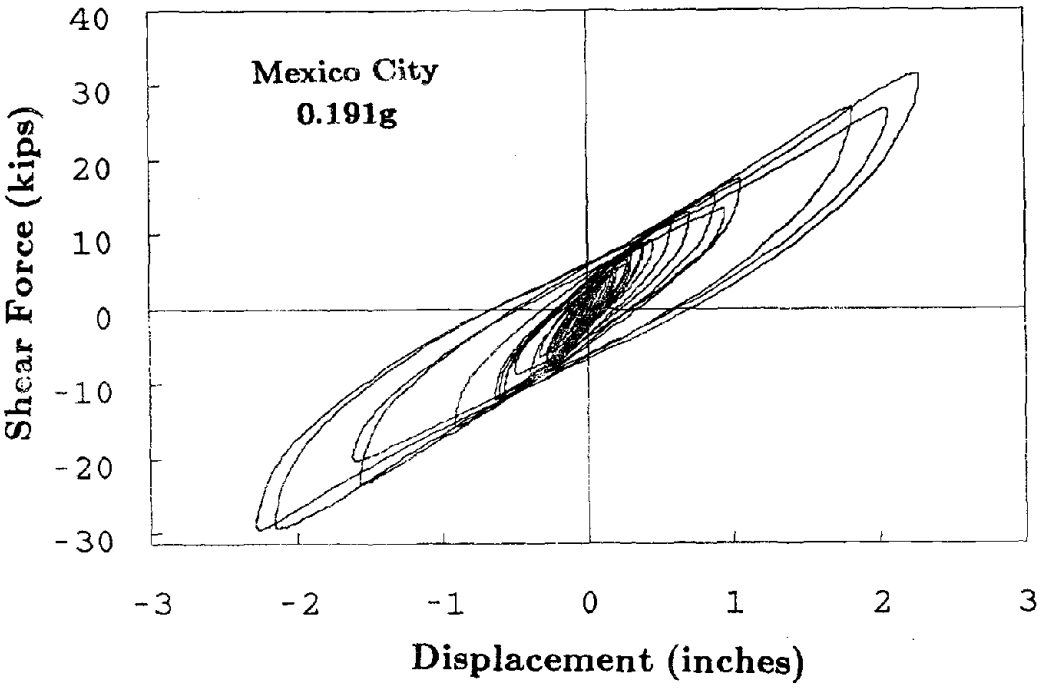

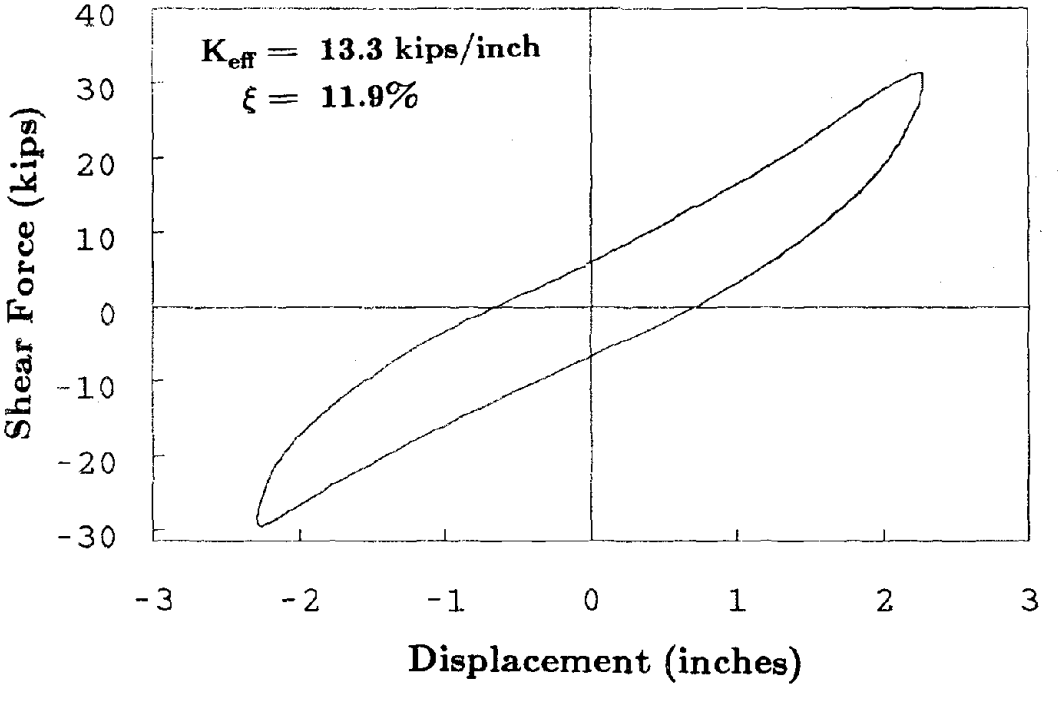

Figure 6.8 Continued

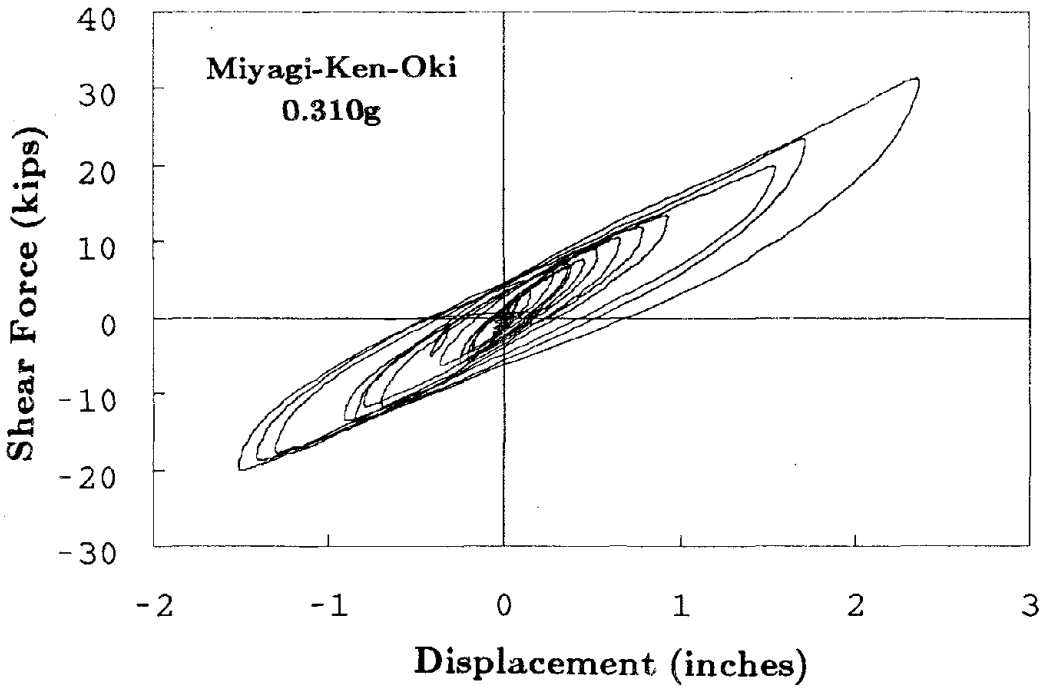

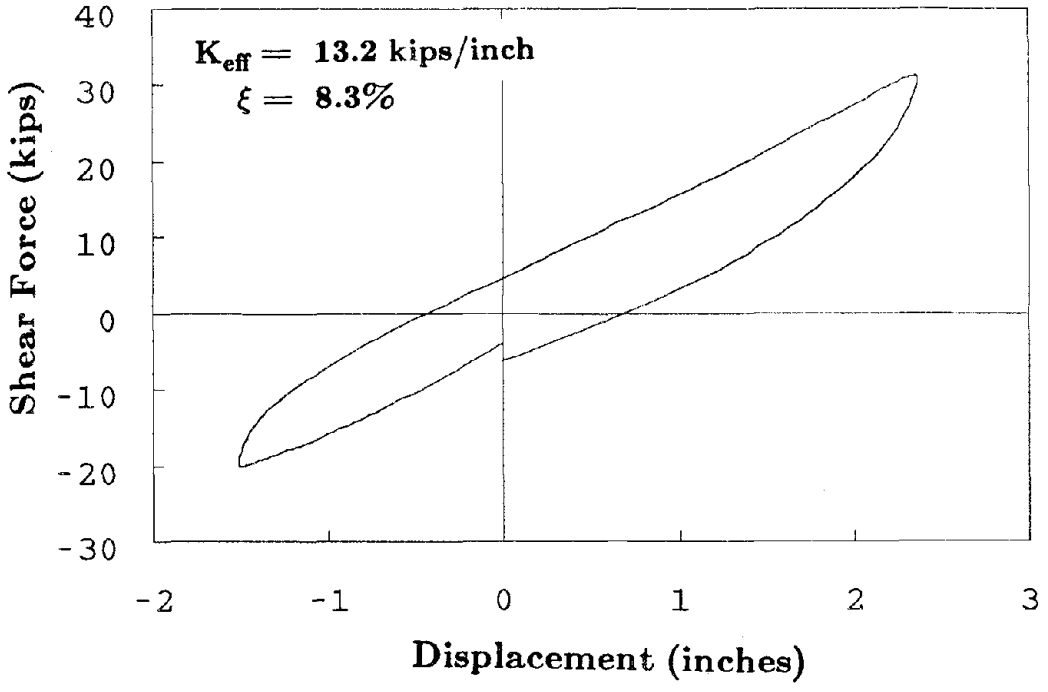

Figure 6.8 Continued

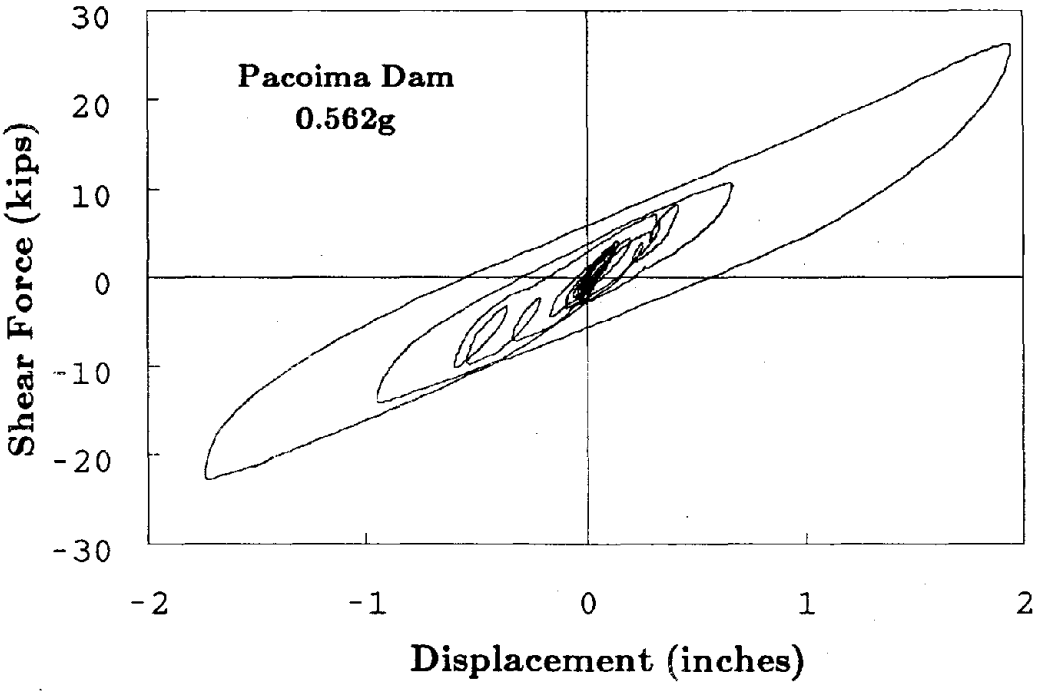

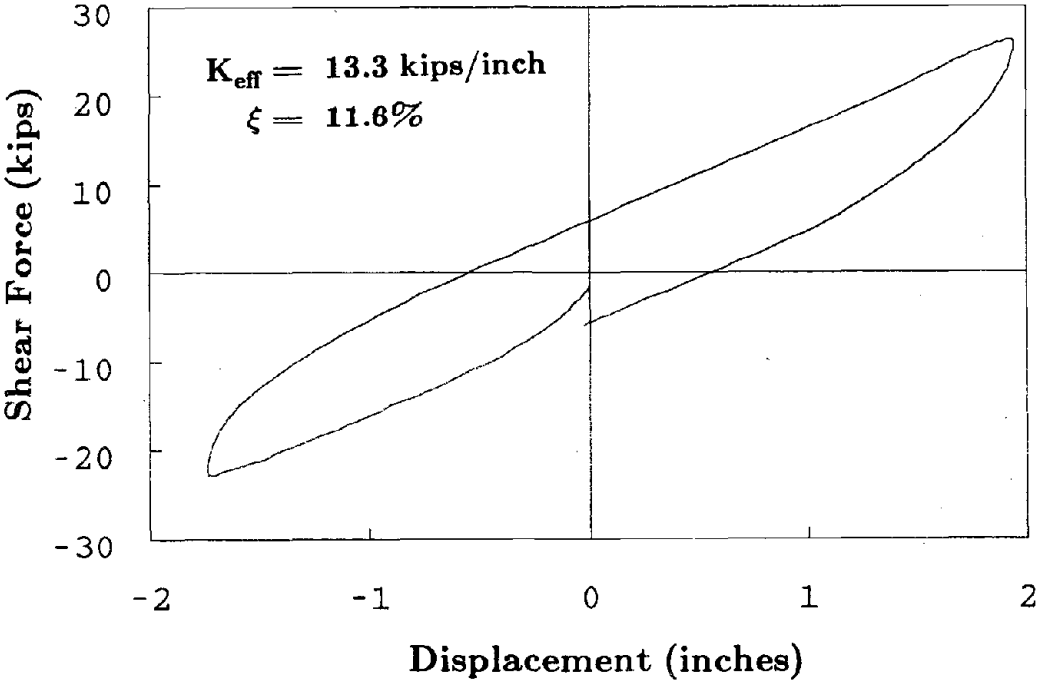

Figure 6.8 Continued

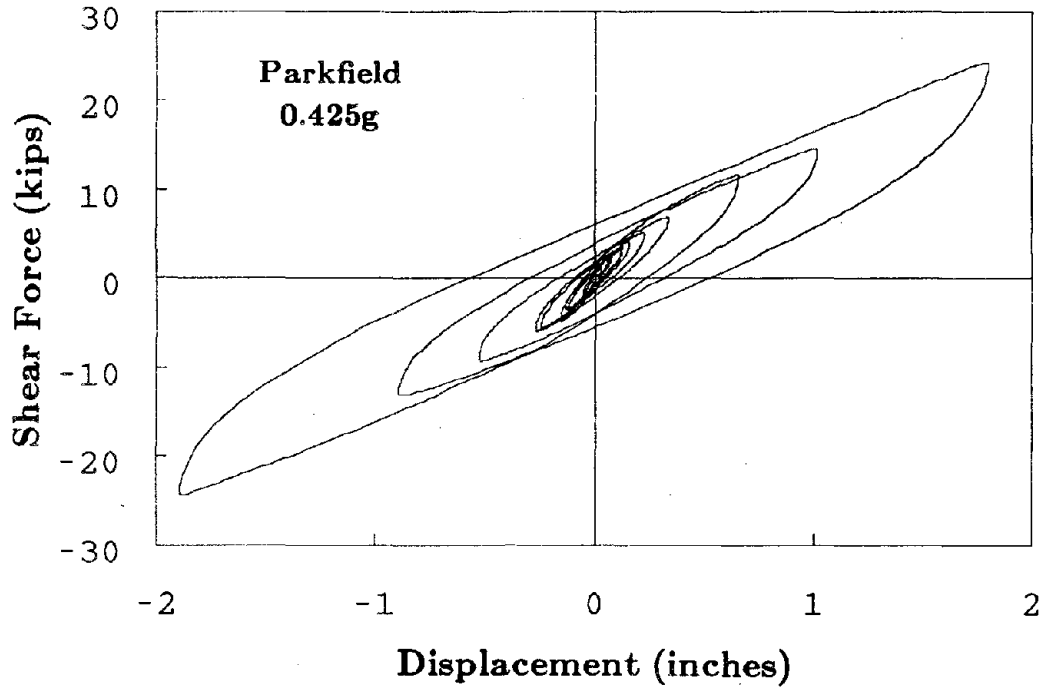

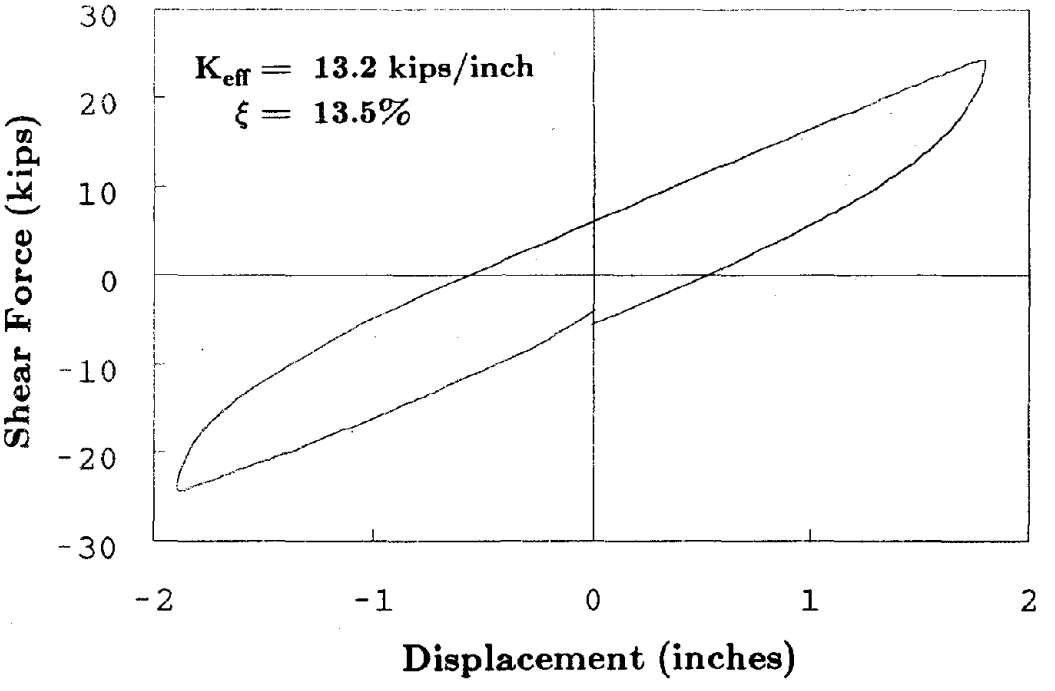

Figure 6.8 Continued

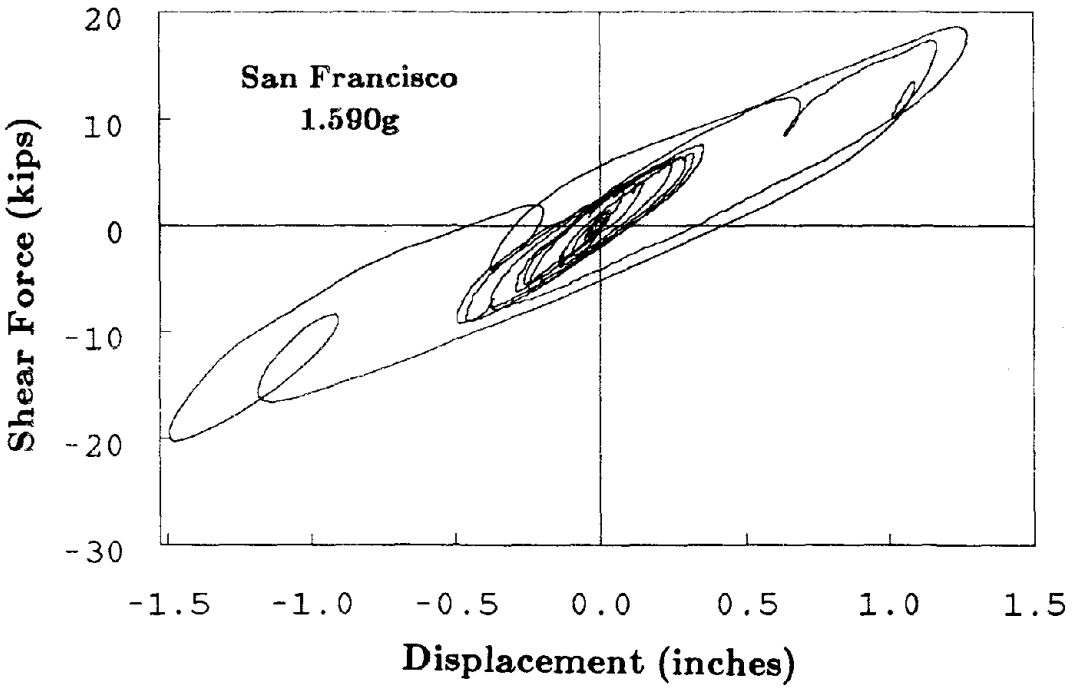

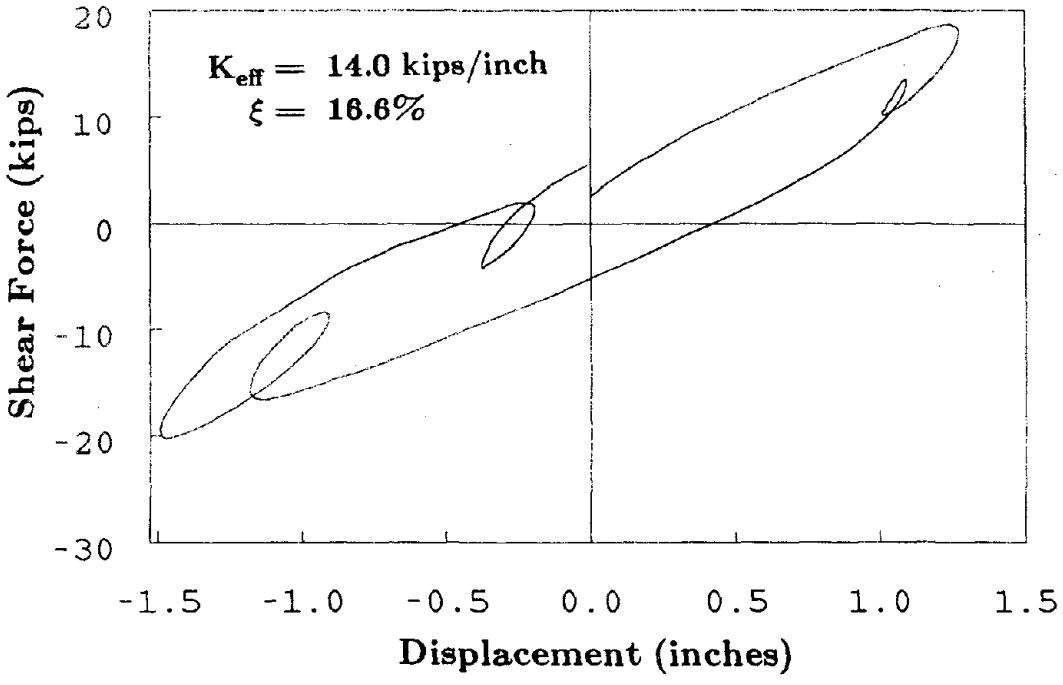

Figure 6.8 Continued

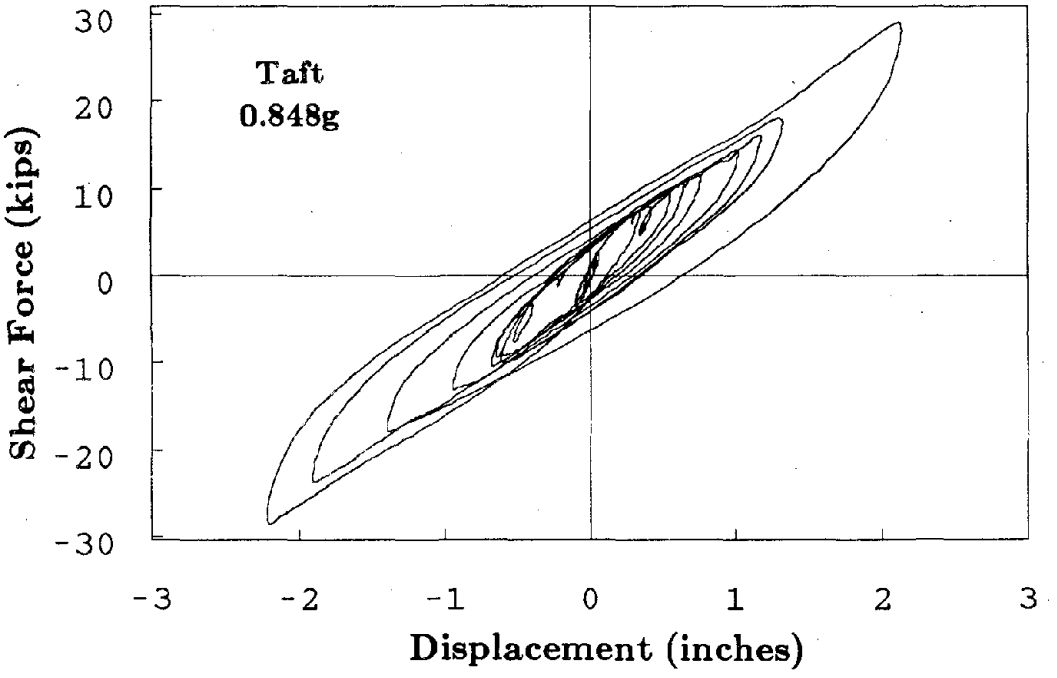

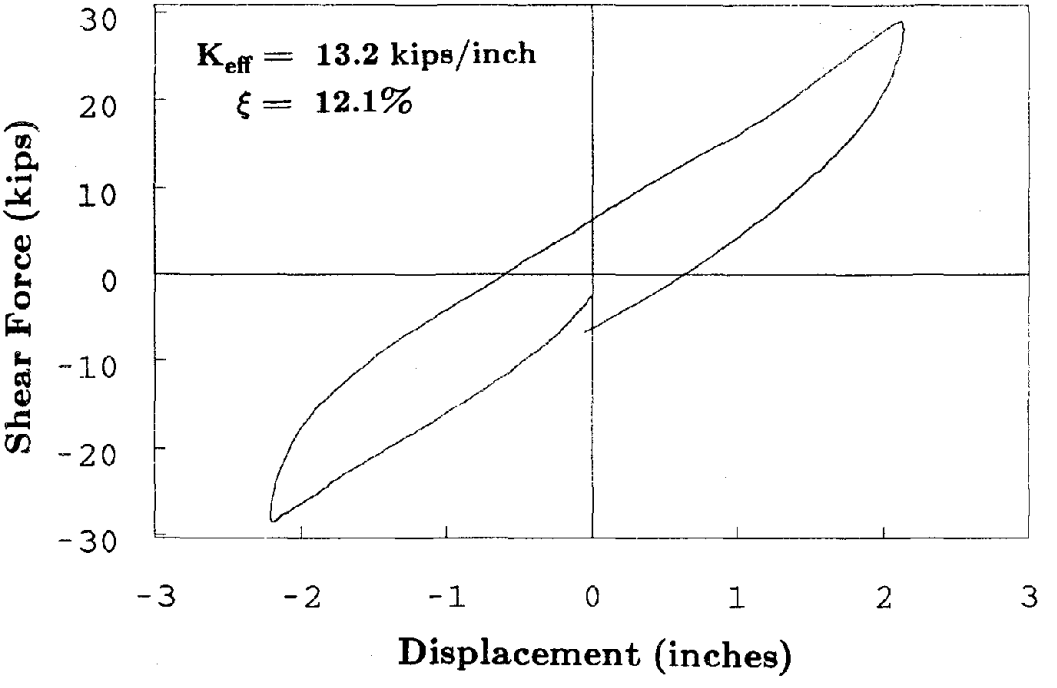

Figure 6.8 Continued

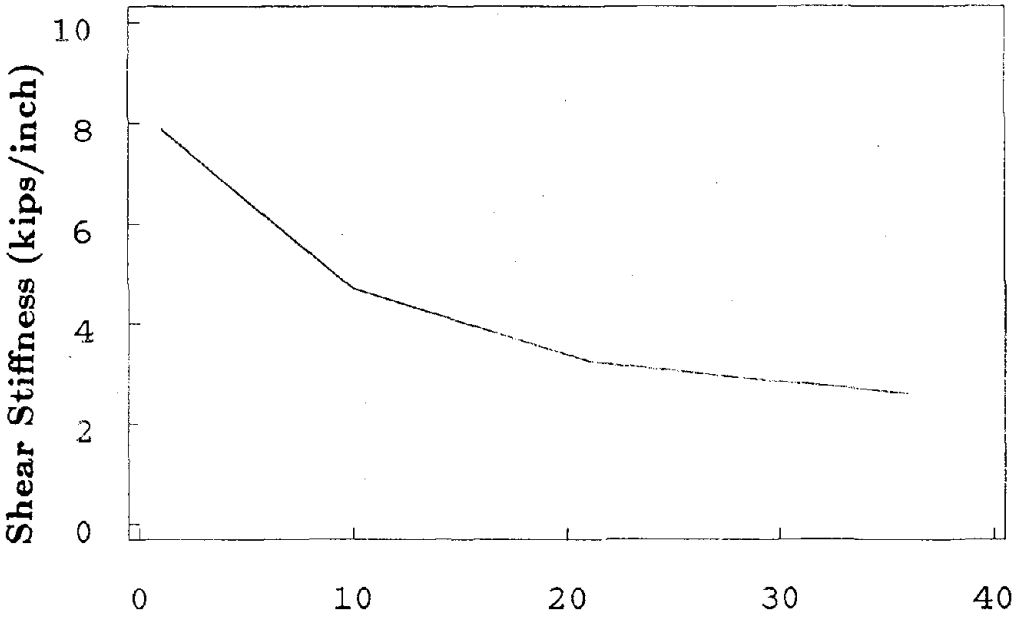

Figure 6.9 Effect of Earthquake Tests on Lead-Plug Bearing Dynamic Shear Stiffness

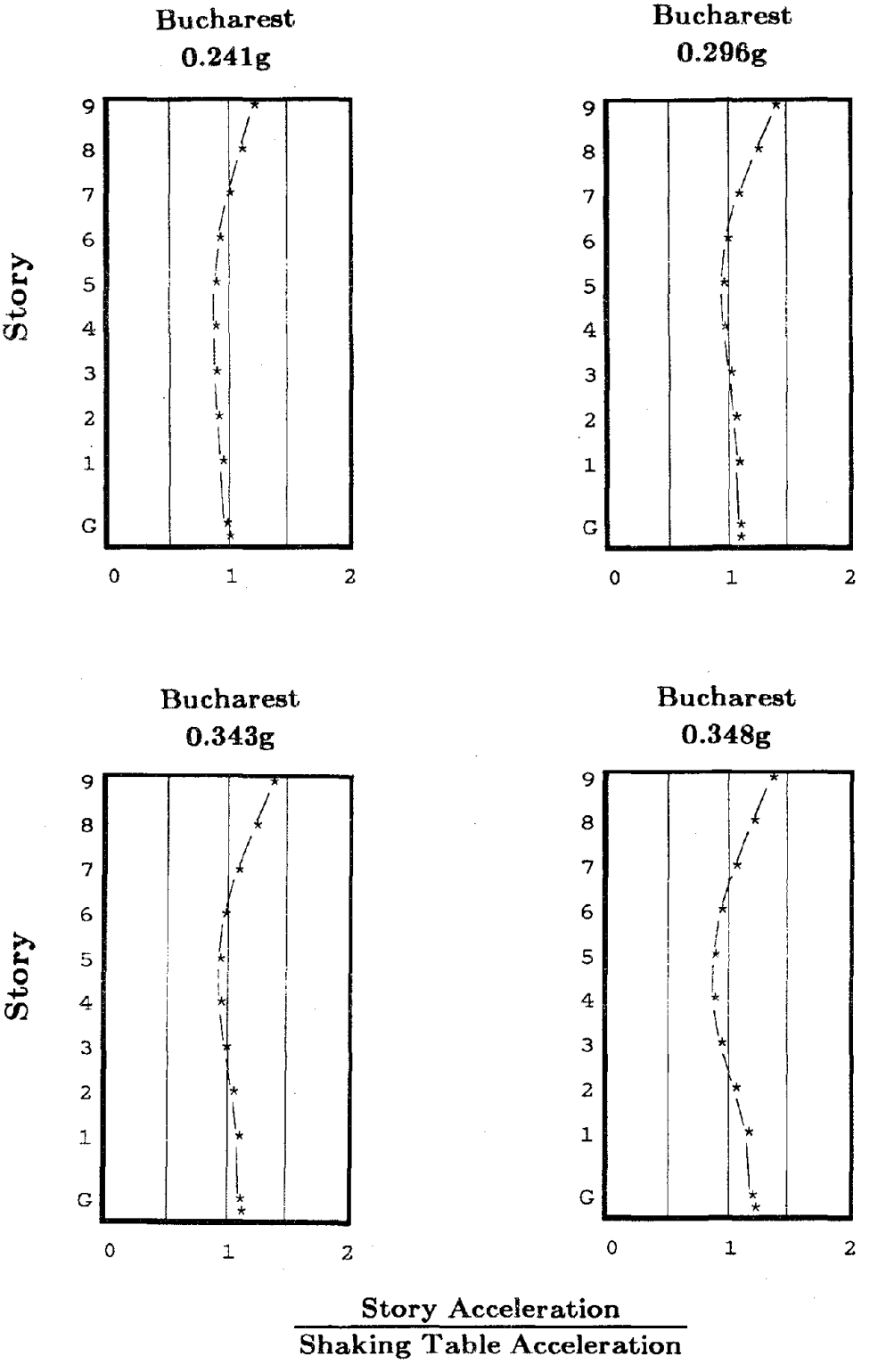

Figure 6.10 Bucharest Story Acceleration Profiles Lead-Plug Bearings

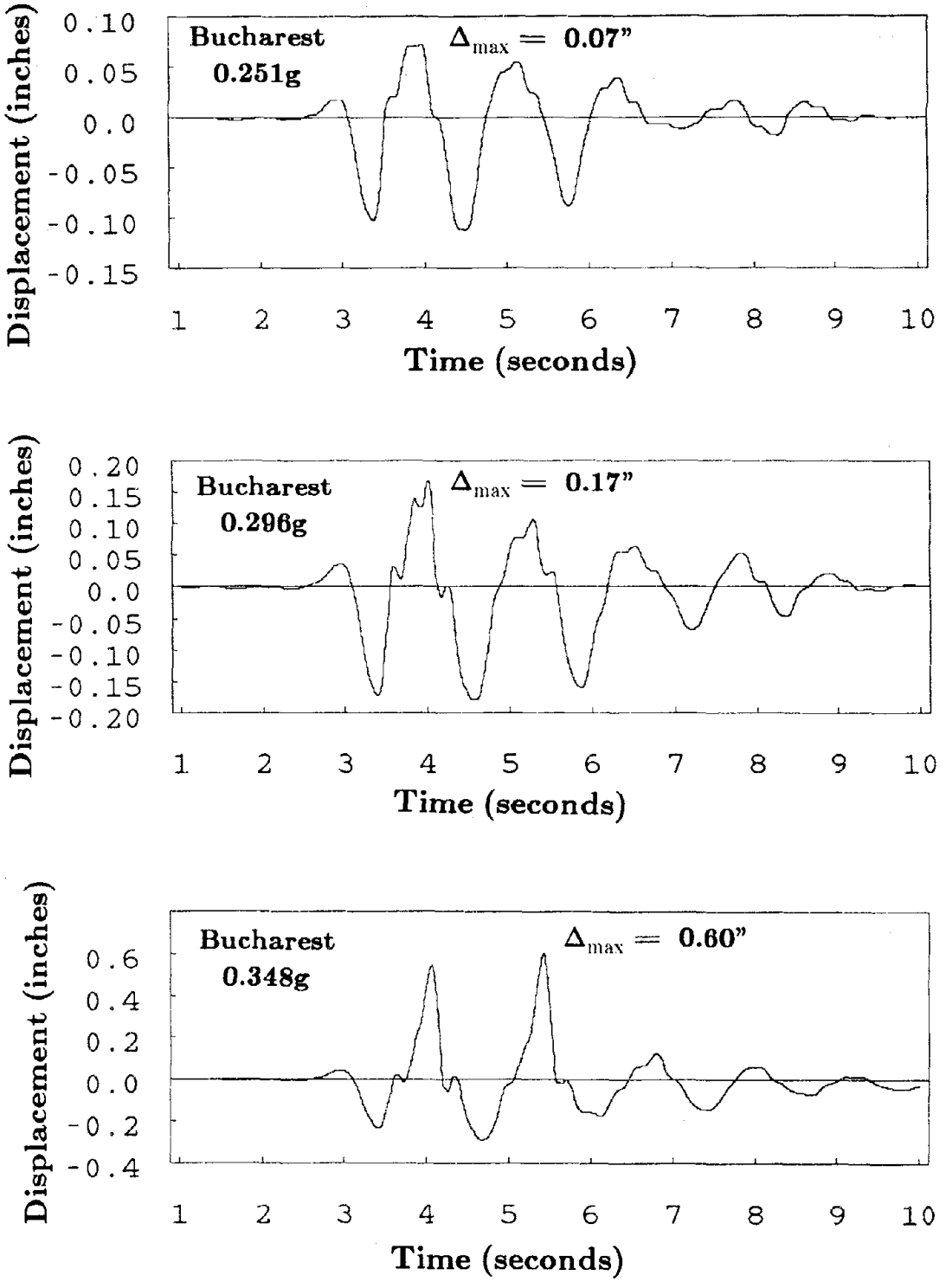

Figure 6.11 Column Uplift Displacement Time Histories, Lead-Plug Bearings

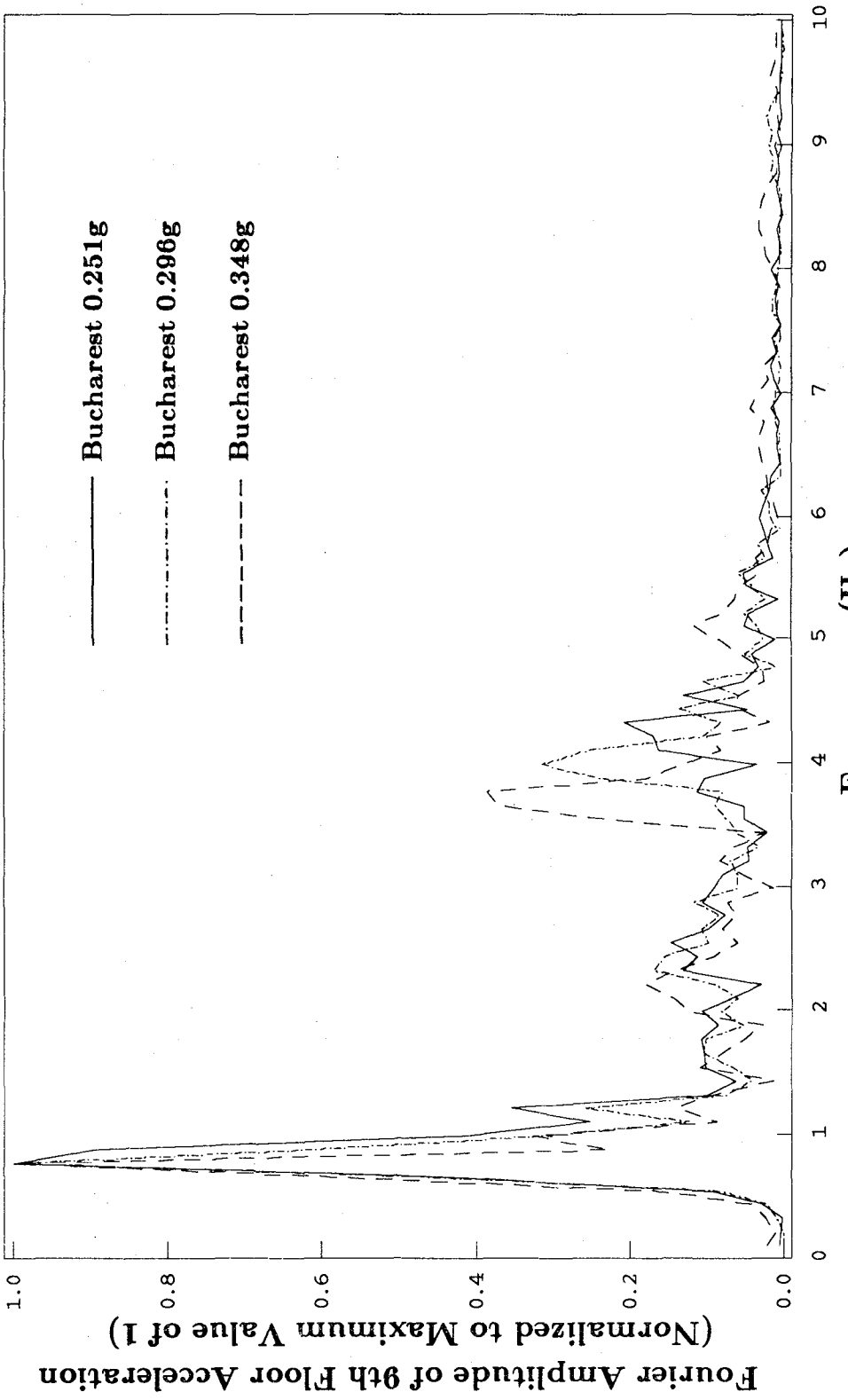

Figure 6.12 Fourier Amplitude Plots of Roof Acceleration During Bucharest Tests, Lead-Plug Bearings

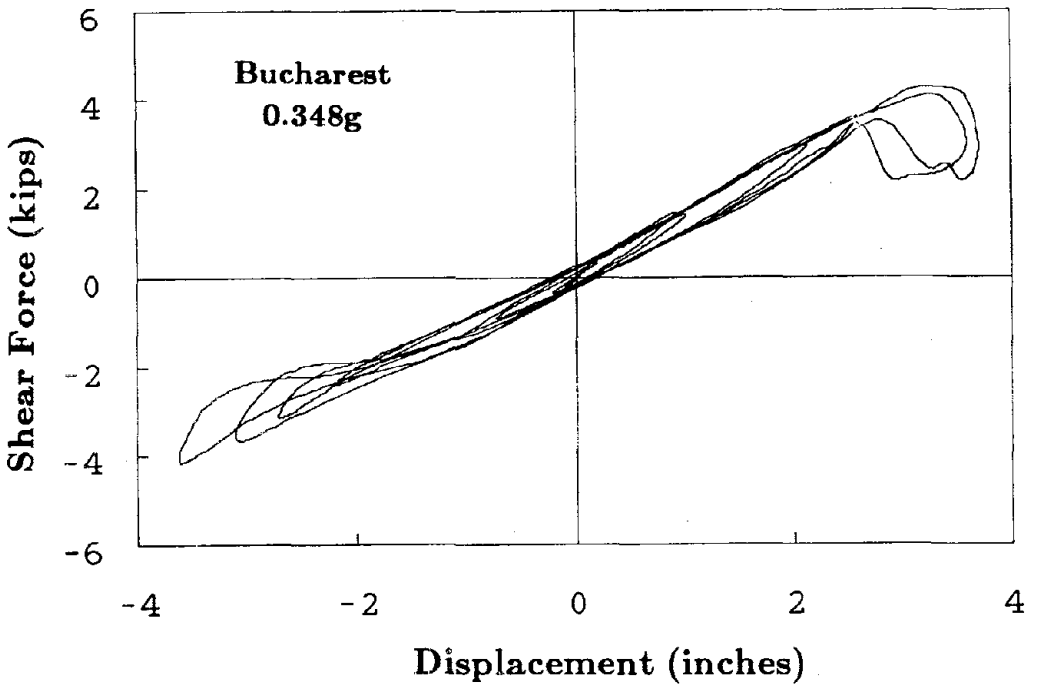

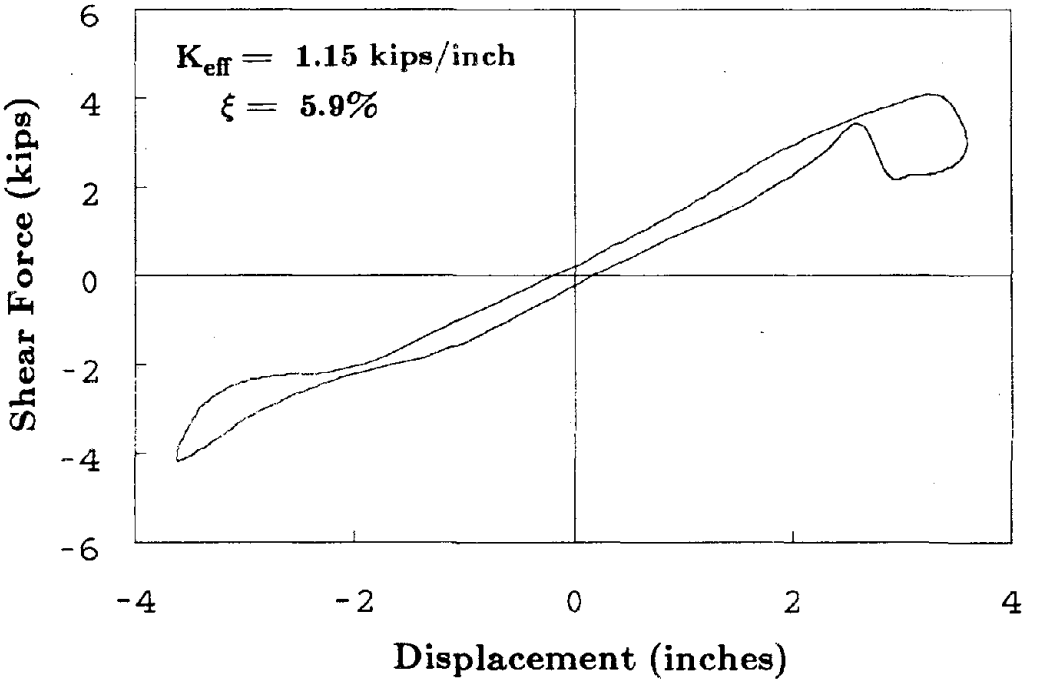

Figure 6.13 Individual Bearing Hysteresis Loops With Column Uplift, Lead-Plug Bearings

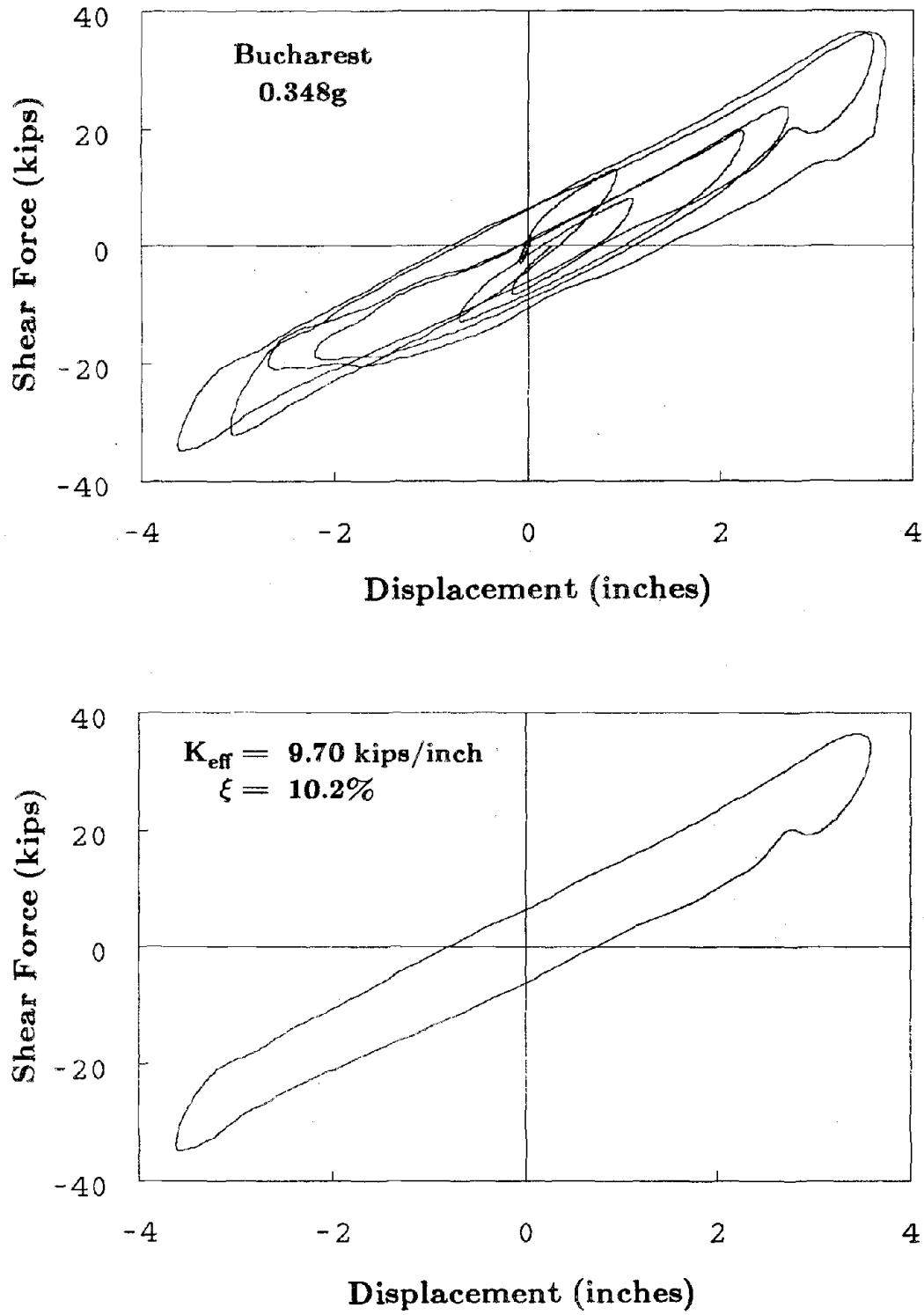

Figure 6.14 Isolation System Hysteresis Loops With Column Uplift, Lead-Plug Bearings

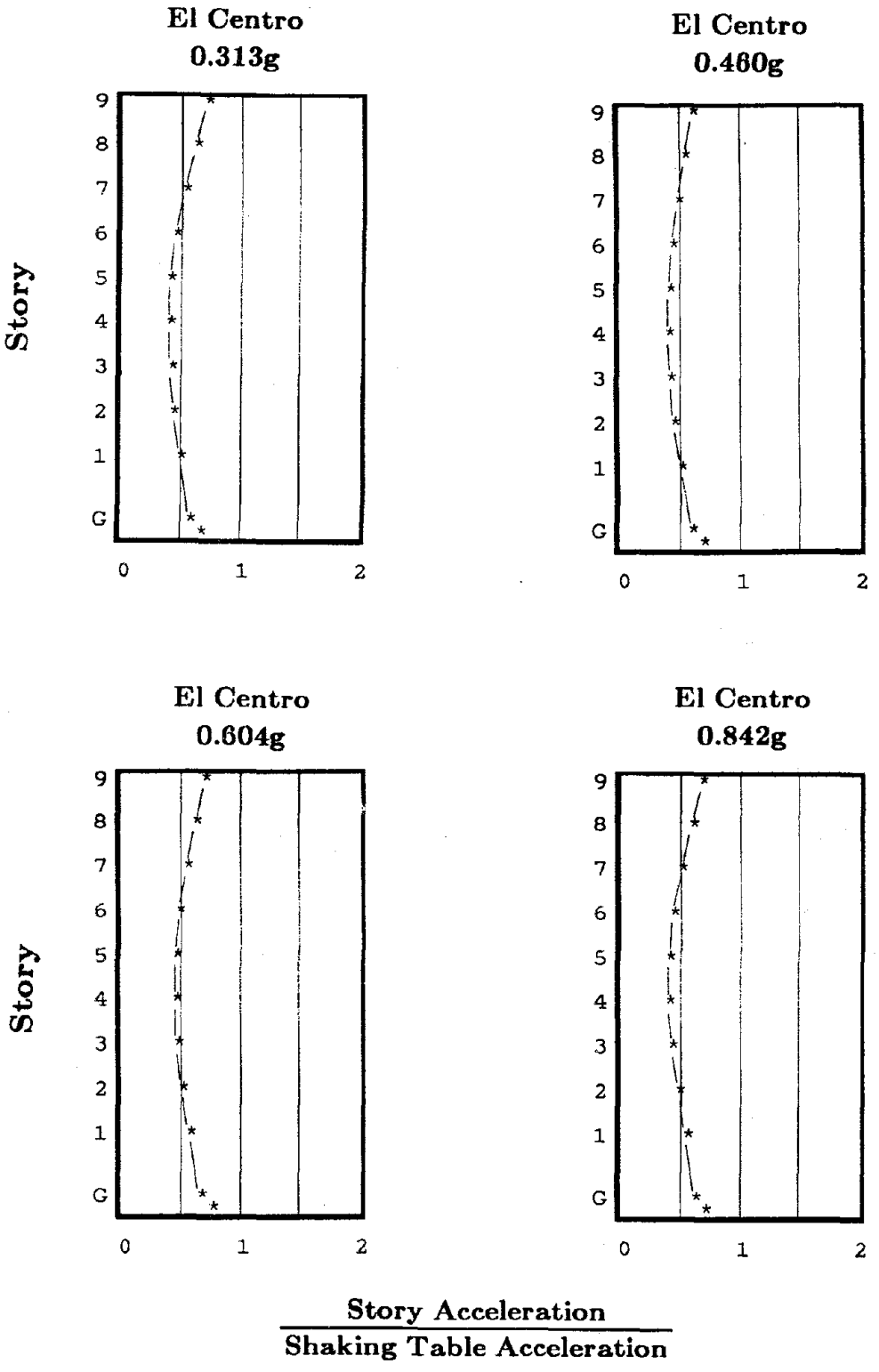

Figure 6.15 El Centro Story Acceleration Profiles, Lead-Plug Bearings

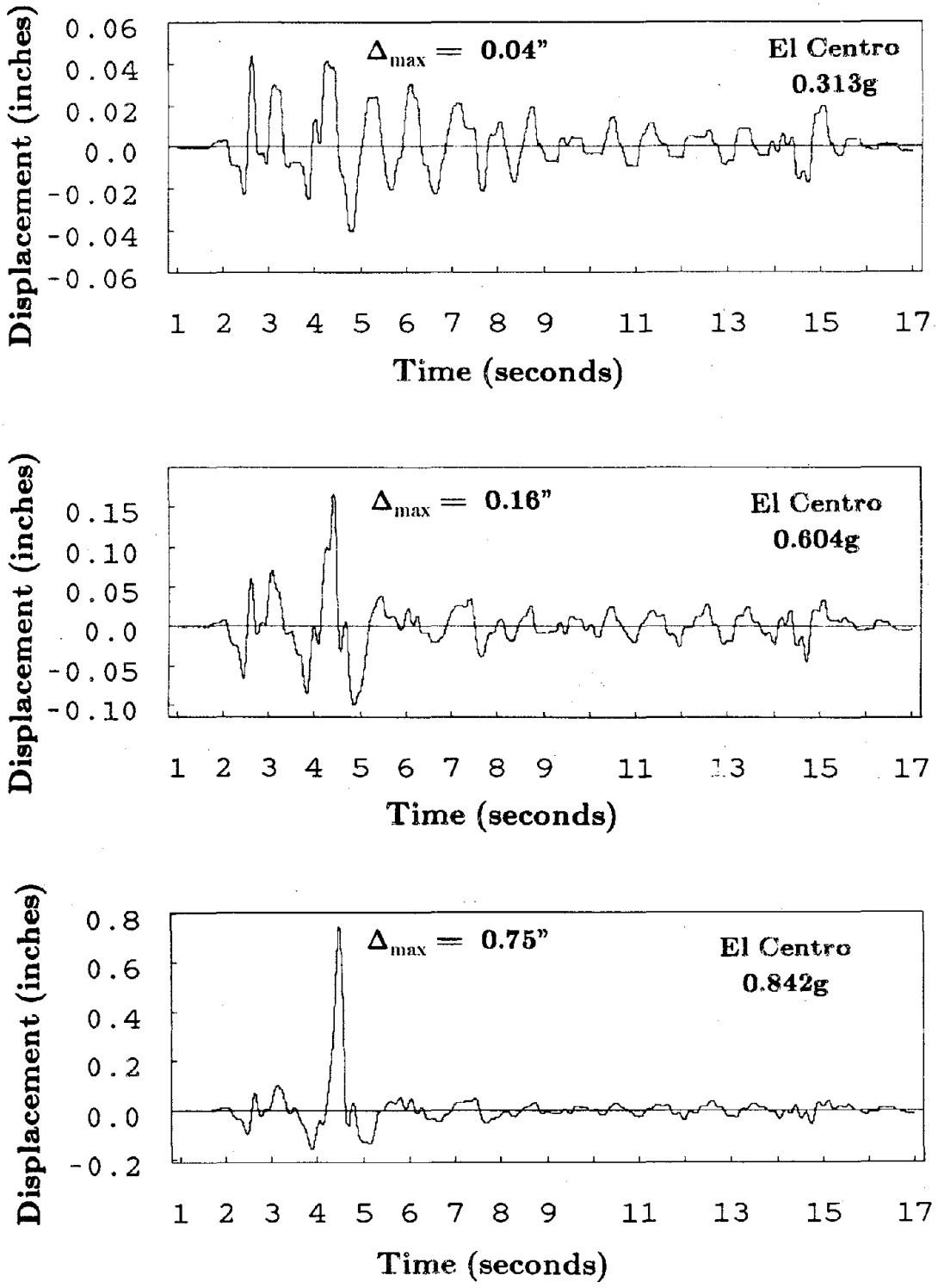

Figure 6.16 Column Uplift Displacement Time Histories, Lead-Plug Bearings

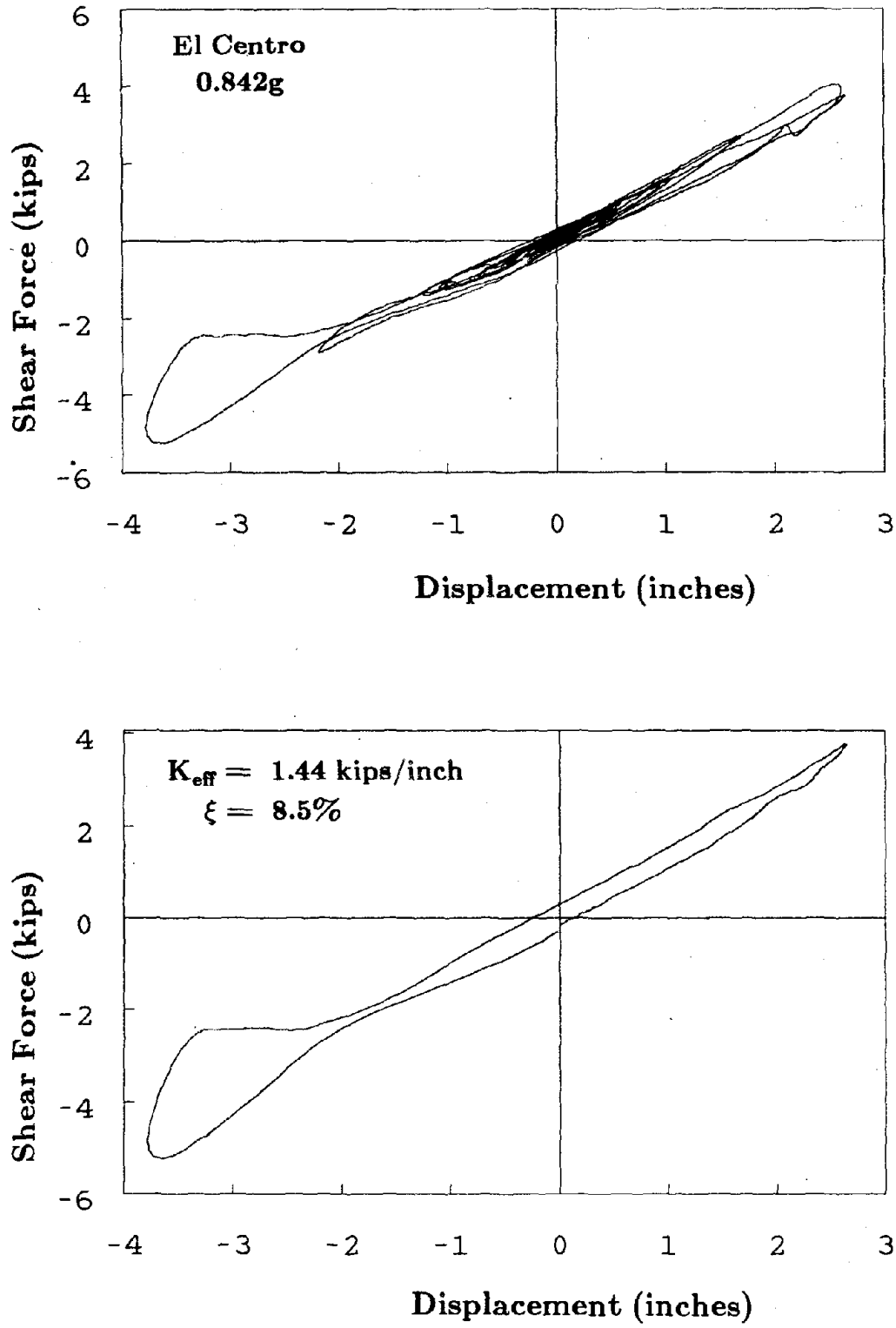

Figure 6.17 Individual Bearing Hysteresis Loops With Column Uplift, Lead-Plug Bearings

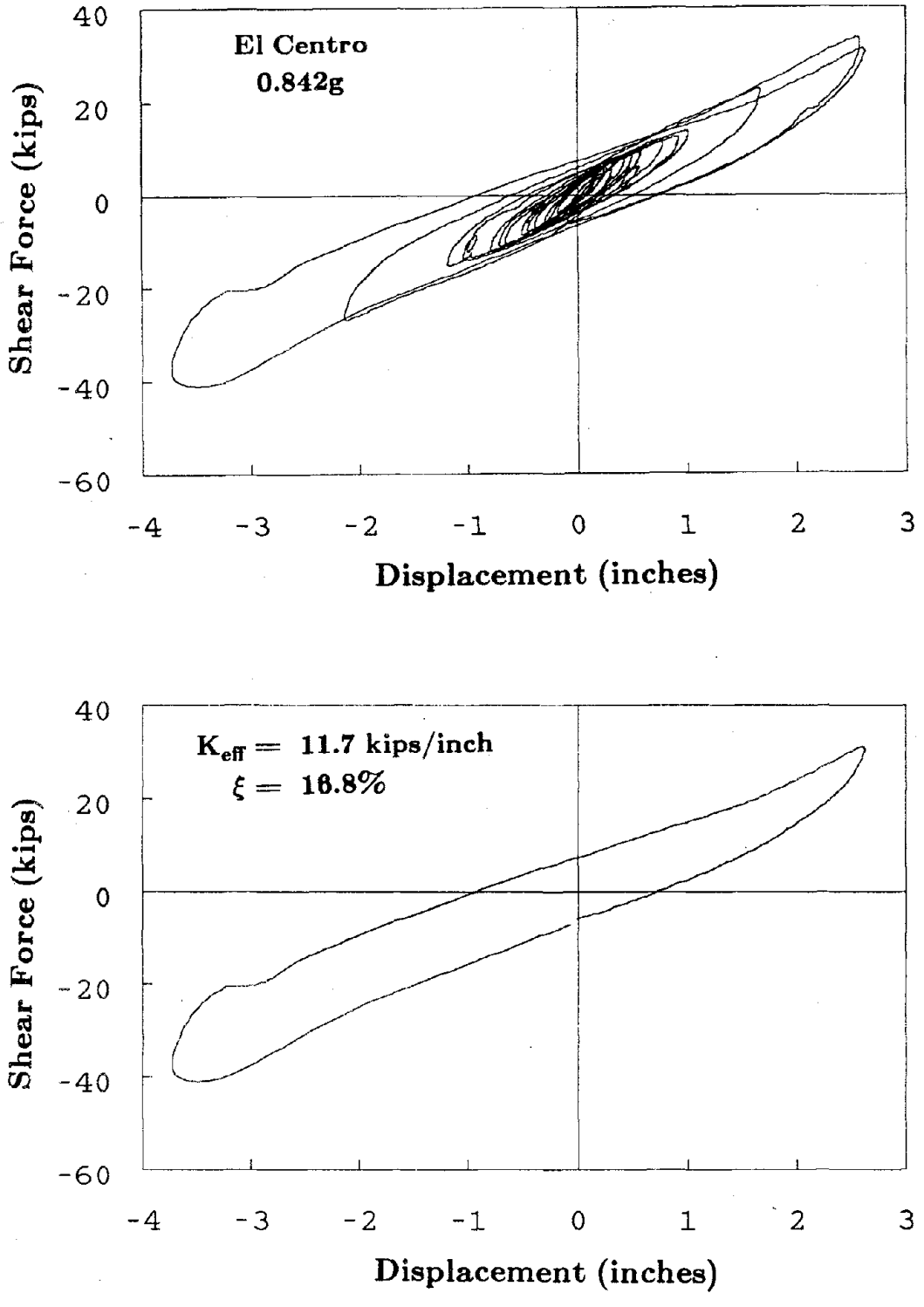

Figure 6.18 Isolation System Hysteresis Loops With Column Uplift, Lead-Plug Bearings

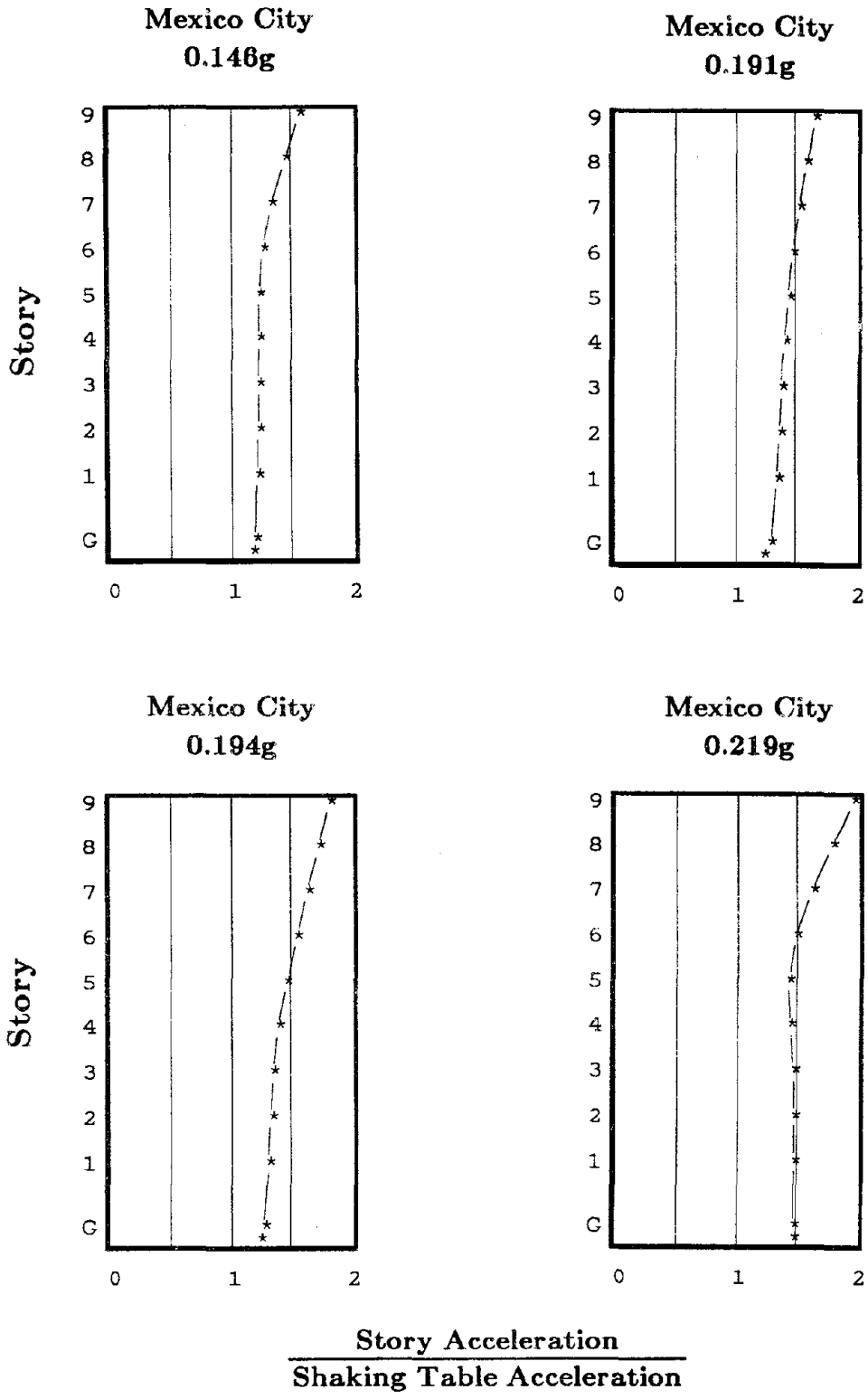

Figure 6.19 Mexico City Story Acceleration Profiles, Lead-Plug Bearings

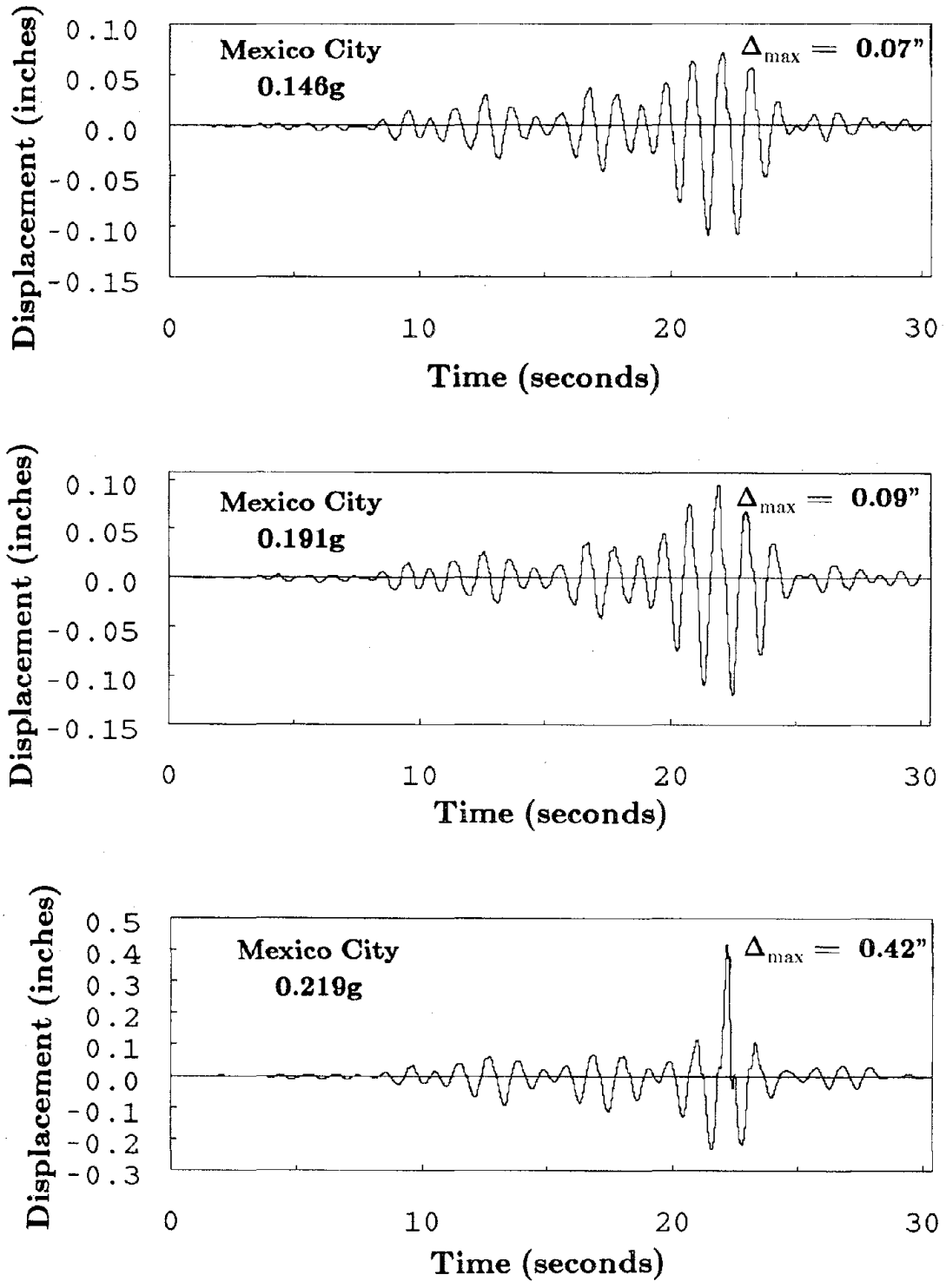

Figure 6.20 Column Uplift Displacement Time Histories, Lead-Plug Bearings

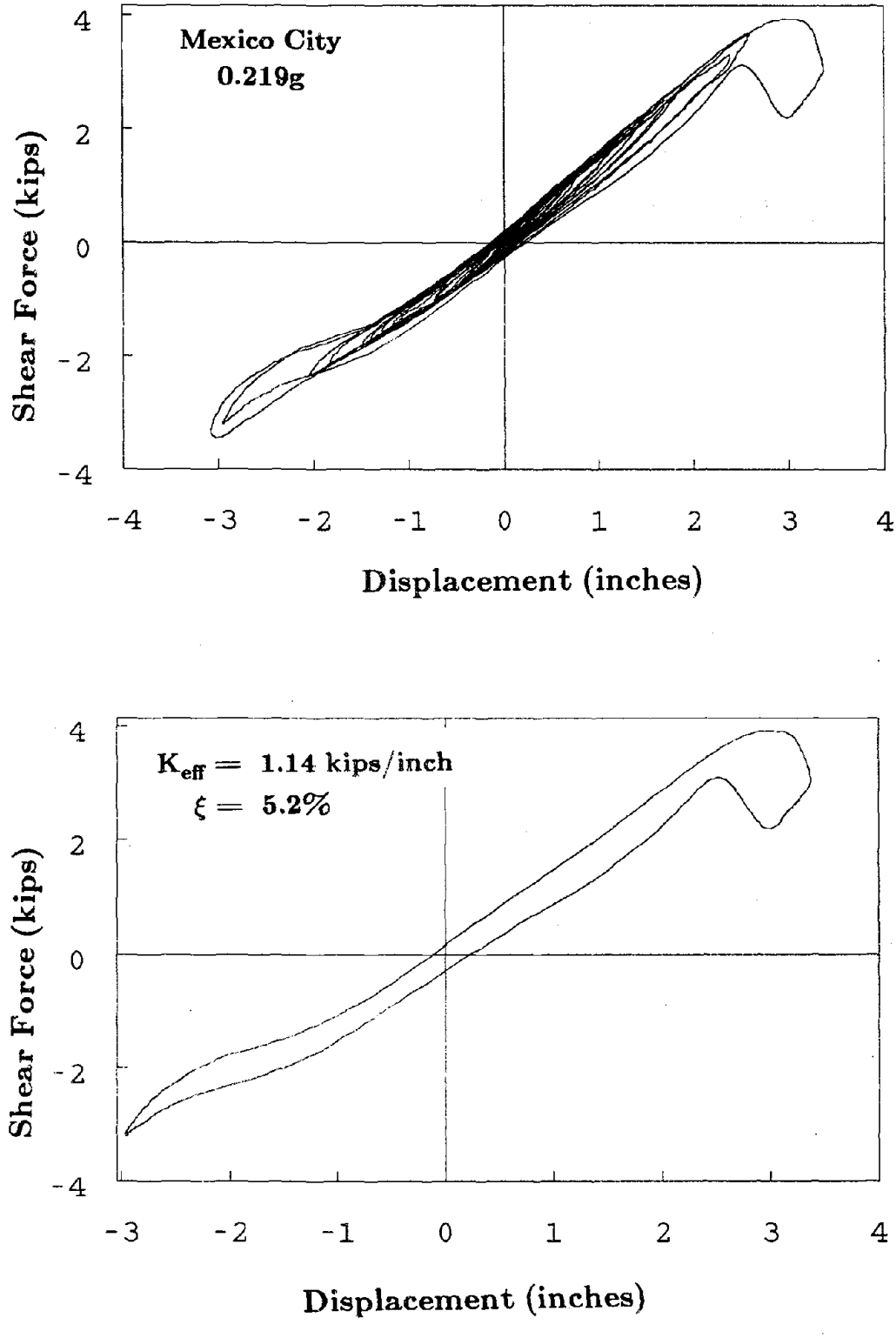

Figure 6.21 Individual Bearing Hysteresis Loops With Column Uplift, Lead-Plug Bearings

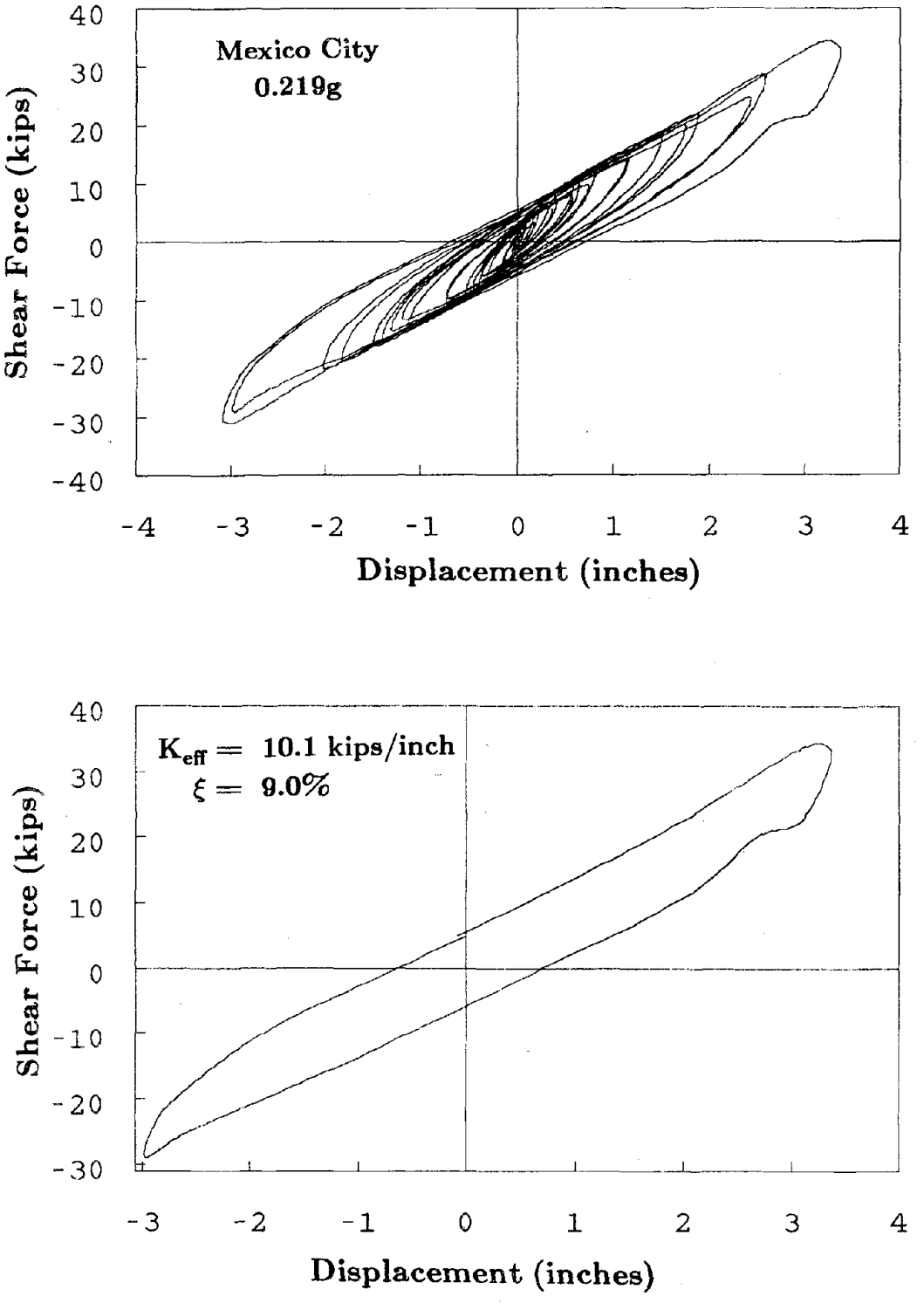

Figure 6.22 Isolation System Hysteresis Loops With Column Uplift, Lead-Plug Bearings

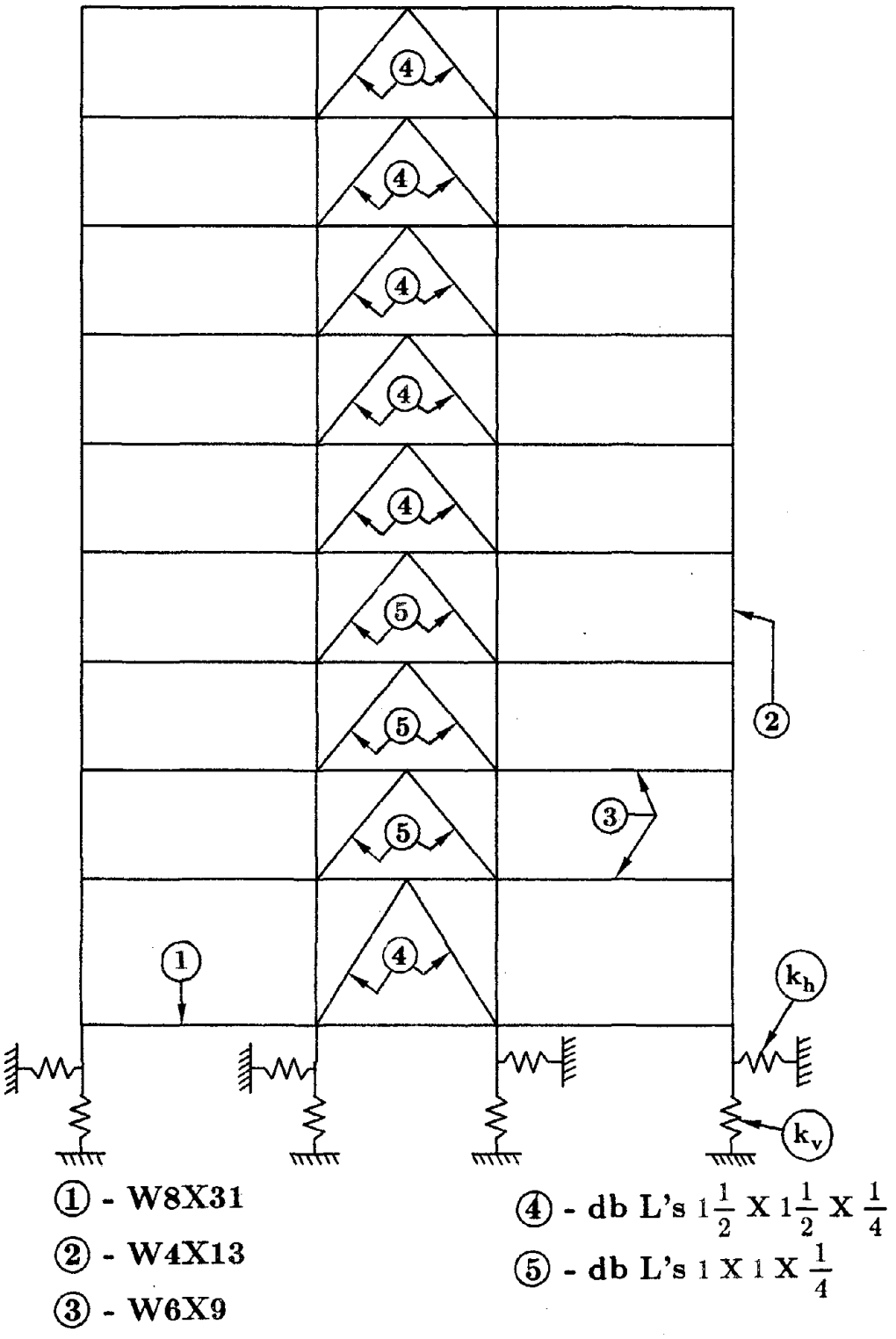

Figure 7.1 Finite Element Model for Braced Steel Frame

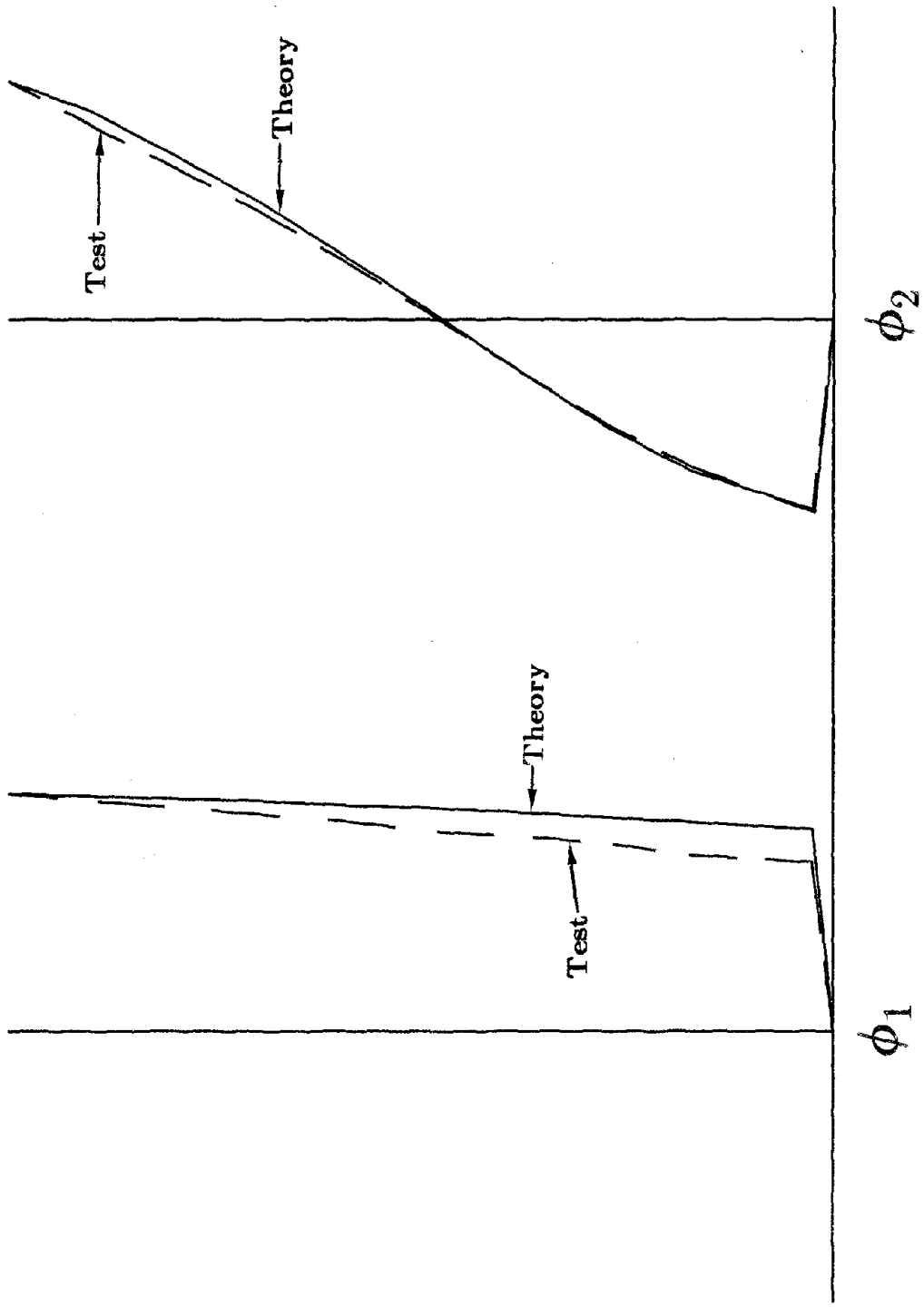

Figure 7.2 Experimental and Analytical Mode Shapes

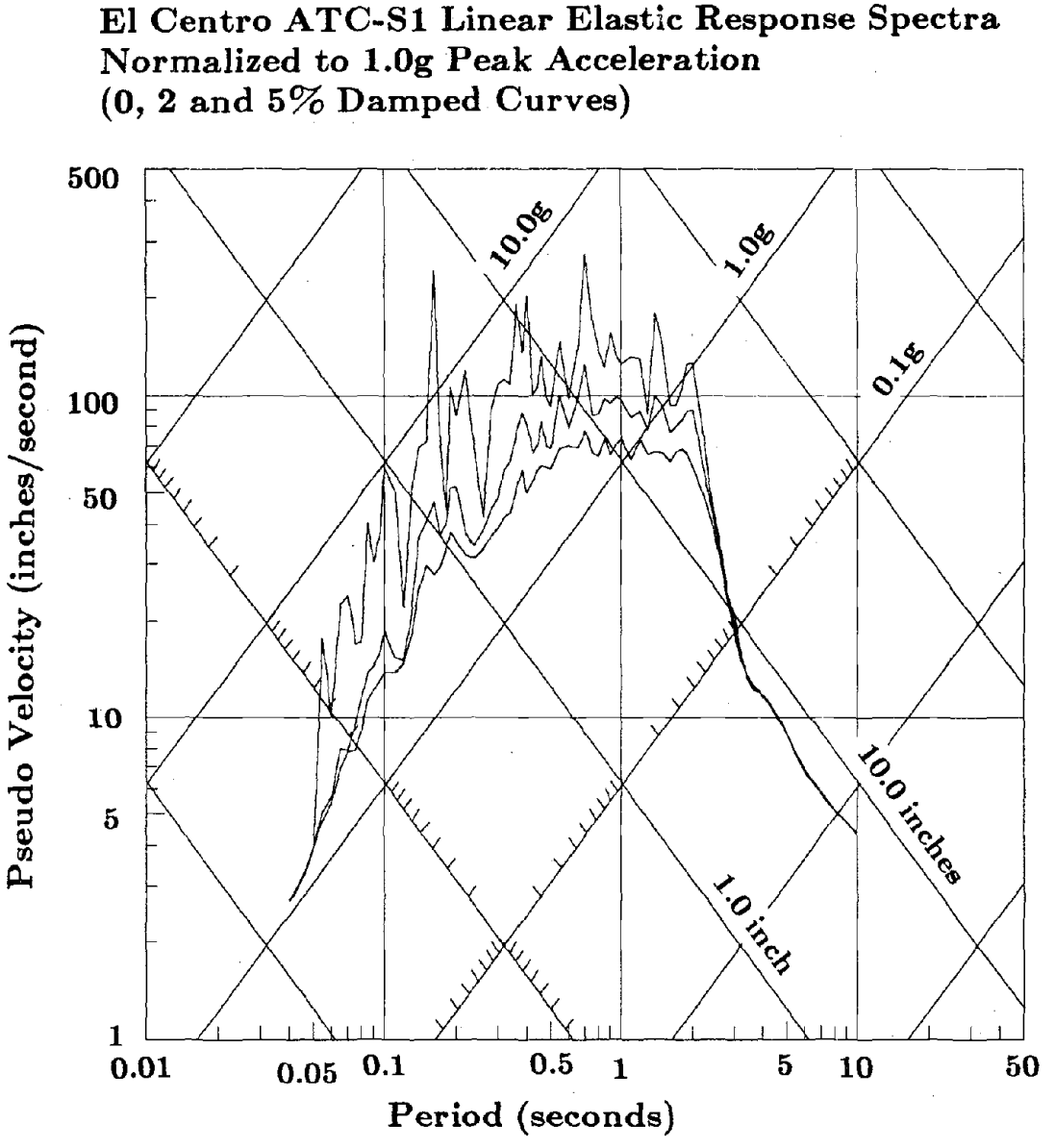

Figure 8.1 Response Spectrum of Modified El Centro Ground Motion (Time-Scaled)

EARTHQUAKE ENGINEERING RESEARCH CENTER REPORT SERIES

EERC reports are available from the National Information Service for Earthquake Engineering(NISEE) and from the National Technical Information Service(NTIS). Numbers in parentheses are Accession Numbers assigned by the National Technical Information Service; these are followed by a price code. Contact NTIS, 5285 Port Royal Road, Springfield Virginia, 22161 for more information. Reports without Accession Numbers were not available from NTIS at the time of printing. For a current complete list of EERC reports (from EERC 67-1) and availablity information, please contact University of California, EERC, NISEE, 1301 South 46th Street, Richmond, California 94804.

UCB/EERC-80/01 "Earthquake Response of Concrete Gravity Dams Including Hydrodynamic and Foundation Interaction Effects," by Chopra, A.K., Chakrabarti, P. and Gupta, S., January 1980, (AD-A087297)A10.

UCB/EERC-80/02 "Rocking Response of Rigid Blocks to Earthquakes," by Yim, C.S., Chopra, A.K. and Penzien, J., January 1980, (PB80 166 002)A04.

UCB/EERC-80/03 "Optimum Inelastic Design of Seismic-Resistant Reinforced Concrete Frame Structures," by Zagajeski, S.W. and Bertero, V.V., January 1980, (PB80 164 635)A06.

UCB/EERC-80/04 "Effects of Amount and Arrangement of Wall-Panel Reinforcement on Hysteretic Behavior of Reinforced Concrete Walls," by Iliya, R. and Bertero, V.V., February 1980, (PB81 122 525)A09.

UCB/EERC-80/05 "Shaking Table Research on Concrete Dam Models," by Niwa, A. and Clough, R.W., September 1980, (PB81 122 368)A06.

UCB/EERC-80/06 "The Design of Steel Energy-Absorbing Restrainers and their Incorporation into Nuclear Power Plants for Enhanced Safety (Vol 1a): Piping with Energy Absorbing Restrainers: Parameter Study on Small Systems," by Powell, G.H., Oughourlian, C. and Simons, J., June 1980.

UCB/EERC-80/07 "Inelastic Torsional Response of Structures Subjected to Earthquake Ground Motions," by Yamazaki, Y., April 1980, (PB81 122 327)A08.

UCB/EERC-80/08 "Study of X-Braced Steel Frame Structures under Earthquake Simulation," by Ghanaat, Y., April 1980, (PB81 122 335)A11.

UCB/EERC-80/09 "Hybrid Modelling of Soil-Structure Interaction," by Gupta, S., Lin, T.W. and Penzien, J., May 1980, (PB81 122 319)A07.

UCB/EERC-80/10 "General Applicability of a Nonlinear Model of a One Story Steel Frame," by Sveinsson, B.I. and McNiven, H.D., May 1980, (PB81 124 877)A06.

UCB/EERC-80/11 "A Green-Function Method for Wave Interaction with a Submerged Body," by Kioka, W., April 1980, (PB81 122 269)A07.

UCB/EERC-80/12 "Hydrodynamic Pressure and Added Mass for Axisymmetric Bodies.," by Nilrat, F., May 1980, (PB81 122 343)A08.

UCB/EERC-80/13 "Treatment of Non-Linear Drag Forces Acting on Offshore Platforms," by Dao, B.V. and Penzien, J., May 1980, (PB81 153 413)A07.

UCB/EERC-80/14 "2D Plane/Axisymmetric Solid Element (Type 3-Elastic or Elastic-Perfectly Plastic)for the ANSR-II Program," by Mondkar, D.P. and Powell, G.H., July 1980, (PB81 122 350)A03.

UCB/EERC-80/15 "A Response Spectrum Method for Random Vibrations," by Der Kiureghian, A., June 1981, (PB81 122 301)A03.

UCB/EERC-80/16 "Cyclic Inelastic Buckling of Tubular Steel Braces," by Zayas, V.A., Popov, E.P. and Mahin, S.A., June 1981, (PB81 124 885)A10.

UCB/EERC-80/17 "Dynamic Response of Simple Arch Dams Including Hydrodynamic Interaction," by Porter, C.S. and Chopra, A.K., July 1981, (PB81 124 000)A13.

UCB/EERC-80/18 "Experimental Testing of a Friction Damped Aseismic Base Isolation System with Fail-Safe Characteristics," by Kelly, J.M., Beucke, K.E. and Skinner, M.S., July 1980, (PB81 148 595)A04.

UCB/EERC-80/19 "The Design of Steel Energy-Absorbing Restrainers and their Incorporation into Nuclear Power Plants for Enhanced Safety (Vol.1B): Stochastic Seismic Analyses of Nuclear Power Plant Structures and Piping Systems Subjected to Multiple Supported Excitations," by Lee, M.C. and Penzien, J., June 1980, (PB82 201 872)A08.

UCB/EERC-80/20 "The Design of Steel Energy-Absorbing Restrainers and their Incorporation into Nuclear Power Plants for Enhanced Safety (Vol 1C): Numerical Method for Dynamic Substructure Analysis," by Dickens, J.M. and Wilson, E.L., June 1980.

UCB/EERC-80/21 "The Design of Steel Energy-Absorbing Restrainers and their Incorporation into Nuclear Power Plants for Enhanced Safety (Vol 2): Development and Testing of Restraints for Nuclear Piping Systems," by Kelly, J.M. and Skinner, M.S., June 1980.

UCB/EERC-80/22 "3D Solid Element (Type 4-Elastic or Elastic-Perfectly-Plastic) for the ANSR-II Program," by Mondkar, D.P. and Powell, G.H., July 1980, (PB81 123 242)A03.

UCB/EERC-80/23 "Gap-Friction Element (Type 5) for the Ansr-II Program," by Mondkar, D.P. and Powell, G.H., July 1980, (PB81 122 285)A03.

UCB/EERC-80/24 "U-Bar Restraint Element (Type 11) for the ANSR-II Program," by Oughourlian, C. and Powell, G.H., July 1980, (PB81 122 293)A03.

UCB/EERC-80/25 "Testing of a Natural Rubber Base Isolation System by an Explosively Simulated Earthquake," by Kelly, J.M., August 1980, (PB81 201 360)A04.

UCB/EERC-80/26 "Input Identification from Structural Vibrational Response," by Hu, Y., August 1980, (PB81 152 308)A05.

UCB/EERC-80/27 "Cyclic Inelastic Behavior of Steel Offshore Structures," by Zayas, V.A., Mahin, S.A. and Popov, E.P., August 1980, (PB81 196 180)A15.

UCB/EERC-80/28 "Shaking Table Testing of a Reinforced Concrete Frame with Biaxial Response," by Oliva, M.G., October 1980, (PB81 154 304)A10.

UCB/EERC-80/29 "Dynamic Properties of a Twelve-Story Prefabricated Panel Building," by Bouwkamp, J.G., Kollegger, J.P. and Stephen, R.M., October 1980, (PB82 138 777)A07.

UCB/EERC-80/30 "Dynamic Properties of an Eight-Story Prefabricated Panel Building," by Bouwkamp, J.G., Kollegger, J.P. and Stephen, R.M., October 1980, (PB81 200 313)A05.

UCB/EERC-80/31 "Predictive Dynamic Response of Panel Type Structures under Earthquakes," by Kollegger, J.P. and Bouwkamp, J.G., October 1980, (PB81 152 316)A04.

UCB/EERC-80/32 "The Design of Steel Energy-Absorbing Restrainers and their Incorporation into Nuclear Power Plants for Enhanced Safety (Vol 3): Testing of Commercial Steels in Low-Cycle Torsional Fatique," by Spanner, P., Parker, E.R., Jongewaard, E. and Dory, M., 1980.

UCB/EERC-80/33 "The Design of Steel Energy-Absorbing Restrainers and their Incorporation into Nuclear Power Plants for Enhanced Safety (Vol 4): Shaking Table Tests of Piping Systems with Energy-Absorbing Restrainers," by Stiemer, S.F. and Godden, W.G., September 1980, (PB82 201 880)A05.

UCB/EERC-80/34 "The Design of Steel Energy-Absorbing Restrainers and their Incorporation into Nuclear Power Plants for Enhanced Safety (Vol 5): Summary Report," by Spencer, P., 1980.

UCB/EERC-80/35 "Experimental Testing of an Energy-Absorbing Base Isolation System," by Kelly, J.M., Skinner, M.S. and Beucke, K.E., October 1980, (PB81 154 072)A04.

UCB/EERC-80/36 "Simulating and Analyzing Artificial Non-Stationary Earth Ground Motions," by Nau, R.F., Oliver, R.M. and Pister, K.S., October 1980, (PB81 153 397)A04.

UCB/EERC-80/37 "Earthquake Engineering at Berkeley - 1980," by , September 1980, (PB81 205 674)A09.

UCB/EERC-80/38 "Inelastic Seismic Analysis of Large Panel Buildings," by Schricker, V. and Powell, G.H., September 1980, (PB81 154 338)A13.

UCB/EERC-80/39 "Dynamic Response of Embankment, Concrete-Gavity and Arch Dams Including Hydrodynamic Interation," by Hall, J.F. and Chopra, A.K., October 1980, (PB81 152 324)A11.

UCB/EERC-80/40 "Inelastic Buckling of Steel Struts under Cyclic Load Reversal.," by Black, R.G., Wenger, W.A. and Popov, E.P., October 1980, (PB81 154 312)A08.

UCB/EERC-80/41 "Influence of Site Characteristics on Buildings Damage during the October 3,1974 Lima Earthquake," by Repetto, P., Arango, I. and Seed, H.B., September 1980, (PB81 161 739)A05.

UCB/EERC-80/42 "Evaluation of a Shaking Table Test Program on Response Behavior of a Two Story Reinforced Concrete Frame," by Blondet, J.M., Clough, R.W. and Mahin, S.A., December 1980, (PB82 196 544)A11.

UCB/EERC-80/43 "Modelling of Soil-Structure Interaction by Finite and Infinite Elements," by Medina, F., December 1980, (PB81 229 270)A04.

UCB/EERC-81/01 "Control of Seismic Response of Piping Systems and Other Structures by Base Isolation," by Kelly, J.M., January 1981, (PB81 200 735)A05.

UCB/EERC-81/02 "OPTNSR- An Interactive Software System for Optimal Design of Statically and Dynamically Loaded Structures with Nonlinear Response," by Bhatti, M.A., Ciampi, V. and Pister, K.S., January 1981, (PB81 218 851)A09.

UCB/EERC-81/03 "Analysis of Local Variations in Free Field Seismic Ground Motions," by Chen, J.-C., Lysmer, J. and Seed, H.B., January 1981, (AD-A099508)A13.

UCB/EERC-81/04 "Inelastic Structural Modeling of Braced Offshore Platforms for Seismic Loading," by Zayas, V.A., Shing, P.-S.B., Mahin, S.A. and Popov, E.P., January 1981, (PB82 138 777)A07.

UCB/EERC-81/05 "Dynamic Response of Light Equipment in Structures," by Der Kiureghian, A., Sackman, J.L. and Nour-Omid, B., April 1981, (PB81 218 497)A04.

UCB/EERC-81/06 "Preliminary Experimental Investigation of a Broad Base Liquid Storage Tank," by Bouwkamp, J.G., Kollegger, J.P. and Stephen, R.M., May 1981, (PB82 140 385)A03.

UCB/EERC-81/07 "The Seismic Resistant Design of Reinforced Concrete Coupled Structural Walls," by Aktan, A.E. and Bertero, V.V., June 1981, (PB82 113 358)A11.

UCB/EERC-81/08 "Unassigned," by Unassigned, 1981.

UCB/EERC-81/09 "Experimental Behavior of a Spatial Piping System with Steel Energy Absorbers Subjected to a Simulated Differential Seismic Input," by Stiemer, S.F., Godden, W.G. and Kelly, J.M., July 1981, (PB82 201 898)A04.

UCB/EERC-81/10 "Evaluation of Seismic Design Provisions for Masonry in the United States," by Sveinsson, B.I., Mayes, R.L. and McNiven, H.D., August 1981, (PB82 166 075)A08.

UCB/EERC-81/11 "Two-Dimensional Hybrid Modelling of Soil-Structure Interaction," by Tzong, T.-J., Gupta, S. and Penzien, J., August 1981, (PB82 142 118)A04.

UCB/EERC-81/12 "Studies on Effects of Infills in Seismic Resistant R/C Construction," by Brokken, S. and Bertero, V.V., October 1981, (PB82 166 190)A09.

UCB/EERC-81/13 "Linear Models to Predict the Nonlinear Seismic Behavior of a One-Story Steel Frame," by Valdimarsson, H., Shah, A.H. and McNiven, H.D., September 1981, (PB82 138 793)A07.

UCB/EERC-81/14 "TLUSH: A Computer Program for the Three-Dimensional Dynamic Analysis of Earth Dams," by Kagawa, T., Mejia, L.H., Seed, H.B. and Lysmer, J., September 1981, (PB82 139 940)A06.

UCB/EERC-81/15 "Three Dimensional Dynamic Response Analysis of Earth Dams," by Mejia, L.H. and Seed, H.B., September 1981, (PB82 137 274)A12.

UCB/EERC-81/16 "Experimental Study of Lead and Elastomeric Dampers for Base Isolation Systems," by Kelly, J.M. and Hodder, S.B., October 1981, (PB82 166 182)A05.

UCB/EERC-81/17 "The Influence of Base Isolation on the Seismic Response of Light Secondary Equipment," by Kelly, J.M., April 1981, (PB82 255 266)A04.

UCB/EERC-81/18 "Studies on Evaluation of Shaking Table Response Analysis Procedures," by Blondet, J. M., November 1981, (PB82 197 278)A10.

UCB/EERC-81/19 "DELIGHT.STRUCT: A Computer-Aided Design Environment for Structural Engineering," by Balling, R.J., Pister, K.S. and Polak, E., December 1981, (PB82 218 496)A07.

UCB/EERC-81/20 "Optimal Design of Seismic-Resistant Planar Steel Frames," by Balling, R.J., Ciampi, V. and Pister, K.S., December 1981, (PB82 220 179)A07.

UCB/EERC-82/01 "Dynamic Behavior of Ground for Seismic Analysis of Lifeline Systems," by Sato, T. and Der Kiureghian, A., January 1982, (PB82 218 926)A05.

UCB/EERC-82/02 "Shaking Table Tests of a Tubular Steel Frame Model," by Ghanaat, Y. and Clough, R.W., January 1982, (PB82 220 161)A07.

UCB/EERC-82/03 "Behavior of a Piping System under Seismic Excitation: Experimental Investigations of a Spatial Piping System supported by Mechanical Shock Arrestors," by Schneider, S., Lee, H.-M. and Godden, W. G., May 1982, (PB83 172 544)A09.

UCB/EERC-82/04 "New Approaches for the Dynamic Analysis of Large Structural Systems," by Wilson, E.L., June 1982, (PB83 148 080)A05.

UCB/EERC-82/05 "Model Study of Effects of Damage on the Vibration Properties of Steel Offshore Platforms," by Shahrivar, F. and Bouwkamp, J.G., June 1982, (PB83 148 742)A10.

UCB/EERC-82/06 "States of the Art and Pratice in the Optimum Seismic Design and Analytical Response Prediction of R/C Frame Wall Structures," by Aktan, A.E. and Bertero, V.V., July 1982, (PB83 147 736)A05.

UCB/EERC-82/07 "Further Study of the Earthquake Response of a Broad Cylindrical Liquid-Storage Tank Model," by Manos, G.C. and Clough, R.W., July 1982, (PB83 147 744)A11.

UCB/EERC-82/08 "An Evaluation of the Design and Analytical Seismic Response of a Seven Story Reinforced Concrete Frame," by Charney, F.A. and Bertero, V.V., July 1982, (PB83 157 628)A09.

UCB/EERC-82/09 "Fluid-Structure Interactions: Added Mass Computations for Incompressible Fluid," by Kuo, J.S.-H., August 1982, (PB83 156 281)A07.

UCB/EERC-82/10 "Joint-Opening Nonlinear Mechanism: Interface Smeared Crack Model," by Kuo, J.S.-H., August 1982, (PB83 149 195)A05.

UCB/EERC-82/11 "Dynamic Response Analysis of Techi Dam," by Clough, R.W., Stephen, R.M. and Kuo, J.S.-H., August 1982, (PB83 147 496)A06.

UCB/EERC-82/12 "Prediction of the Seismic Response of R/C Frame-Coupled Wall Structures," by Aktan, A.E., Bertero, V.V. and Piazzo, M., August 1982, (PB83 149 203)A09.

UCB/EERC-82/13 "Preliminary Report on the Smart 1 Strong Motion Array in Taiwan," by Bolt, B.A., Loh, C.H., Penzien, J. and Tsai, Y.B., August 1982, (PB83 159 400)A10.

UCB/EERC-82/14 "Shaking-Table Studies of an Eccentrically X-Braced Steel Structure," by Yang, M.S., September 1982, (PB83 260 778)A12.

UCB/EERC-82/15 "The Performance of Stairways in Earthquakes," by Roha, C., Axley, J.W. and Bertero, V.V., September 1982, (PB83 157 693)A07.

UCB/EERC-82/16 "The Behavior of Submerged Multiple Bodies in Earthquakes," by Liao, W.-G., September 1982, (PB83 158 709)A07.

UCB/EERC-82/17 "Effects of Concrete Types and Loading Conditions on Local Bond-Slip Relationships," by Cowell, A.D., Popov, E.P. and Bertero, V.V., September 1982, (PB83 153 577)A04.

UCB/EERC-82/18 "Mechanical Behavior of Shear Wall Vertical Boundary Members: An Experimental Investigation," by Wagner, M.T. and Bertero, V.V., October 1982, (PB83 159 764)A05.

UCB/EERC-82/19 "Experimental Studies of Multi-support Seismic Loading on Piping Systems," by Kelly, J.M. and Cowell, A.D., November 1982.

UCB/EERC-82/20 "Generalized Plastic Hinge Concepts for 3D Beam-Column Elements," by Chen, P. F.-S. and Powell, G.H., November 1982, (PB83 247 981)A13.

UCB/EERC-82/21 "ANSR-II: General Computer Program for Nonlinear Structural Analysis," by Oughourlian, C.V. and Powell, G.H., November 1982, (PB83 251 330)A12.

UCB/EERC-82/22 "Solution Strategies for Statically Loaded Nonlinear Structures," by Simons, J.W. and Powell, G.H., November 1982, (PB83 197 970)A06.

UCB/EERC-82/23 "Analytical Model of Deformed Bar Anchorages under Generalized Excitations," by Ciampi, V., Eligehausen, R., Bertero, V.V. and Popov, E.P., November 1982, (PB83 169 532)A06.

UCB/EERC-82/24 "A Mathematical Model for the Response of Masonry Walls to Dynamic Excitations," by Sucuoglu, H., Mengi, Y. and McNiven, H.D., November 1982, (PB83 169 011)A07.

UCB/EERC-82/25 "Earthquake Response Considerations of Broad Liquid Storage Tanks," by Cambra, F.J., November 1982, (PB83 251 215)A09.

UCB/EERC-82/26 "Computational Models for Cyclic Plasticity, Rate Dependence and Creep," by Mosaddad, B. and Powell, G.H., November 1982, (PB83 245 829)A08.

UCB/EERC-82/27 "Inelastic Analysis of Piping and Tubular Structures," by Mahasuverachai, M. and Powell, G.H., November 1982, (PB83 249 987)A07.

UCB/EERC-83/01 "The Economic Feasibility of Seismic Rehabilitation of Buildings by Base Isolation," by Kelly, J.M., January 1983, (PB83 197 988)A05.

UCB/EERC-83/02 "Seismic Moment Connections for Moment-Resisting Steel Frames.," by Popov, E.P., January 1983, (PB83 195 412)A04.

UCB/EERC-83/03 "Design of Links and Beam-to-Column Connections for Eccentrically Braced Steel Frames," by Popov, E.P. and Malley, J.O., January 1983, (PB83 194 811)A04.

UCB/EERC-83/04 "Numerical Techniques for the Evaluation of Soil-Structure Interaction Effects in the Time Domain," by Bayo, E. and Wilson, E.L., February 1983, (PB83 245 605)A09.

UCB/EERC-83/05 "A Transducer for Measuring the Internal Forces in the Columns of a Frame-Wall Reinforced Concrete Structure," by Sause, R. and Bertero, V.V., May 1983, (PB84 119 494)A06.

UCB/EERC-83/06 "Dynamic Interactions Between Floating Ice and Offshore Structures," by Croteau, P., May 1983, (PB84 119 486)A16.

UCB/EERC-83/07 "Dynamic Analysis of Multiply Tuned and Arbitrarily Supported Secondary Systems," by Igusa, T. and Der Kiureghian, A., July 1983, (PB84 118 272)A11.

UCB/EERC-83/08 "A Laboratory Study of Submerged Multi-body Systems in Earthquakes," by Ansari, G.R., June 1983, (PB83 261 842)A17.

UCB/EERC-83/09 "Effects of Transient Foundation Uplift on Earthquake Response of Structures," by Yim, C.-S. and Chopra, A.K., June 1983, (PB83 261 396)A07.

UCB/EERC-83/10 "Optimal Design of Friction-Braced Frames under Seismic Loading," by Austin, M.A. and Pister, K.S., June 1983, (PB84 119 288)A06.

UCB/EERC-83/11 "Shaking Table Study of Single-Story Masonry Houses: Dynamic Performance under Three Component Seismic Input and Recommendations," by Manos, G.C., Clough, R.W. and Mayes, R.L., July 1983, (UCB/EERC-83/11)A08.

UCB/EERC-83/12 "Experimental Error Propagation in Pseudodynamic Testing," by Shiing, P.B. and Mahin, S.A., June 1983, (PB84 119 270)A09.

UCB/EERC-83/13 "Experimental and Analytical Predictions of the Mechanical Characteristics of a 1/5-scale Model of a 7-story R/C Frame-Wall Building Structure," by Aktan, A.E., Bertero, V.V., Chowdhury, A.A. and Nagashima, T., June 1983, (PB84 119 213)A07.

UCB/EERC-83/14 "Shaking Table Tests of Large-Panel Precast Concrete Building System Assemblages," by Oliva, M.G. and Clough, R.W., June 1983, (PB86 110 210/AS)A11.

UCB/EERC-83/15 "Seismic Behavior of Active Beam Links in Eccentrically Braced Frames," by Hjelmstad, K.D. and Popov, E.P., July 1983, (PB84 119 676)A09.

UCB/EERC-83/16 "System Identification of Structures with Joint Rotation," by Dimsdale, J.S., July 1983, (PB84 192 210)A06.

UCB/EERC-83/17 "Construction of Inelastic Response Spectra for Single-Degree-of-Freedom Systems," by Mahin, S. and Lin, J., June 1983, (PB84 208 834)A05.

UCB/EERC-83/18 "Interactive Computer Analysis Methods for Predicting the Inelastic Cyclic Behaviour of Structural Sections," by Kaba, S. and Mahin, S., July 1983, (PB84 192 012)A06.

UCB/EERC-83/19 "Effects of Bond Deterioration on Hysteretic Behavior of Reinforced Concrete Joints," by Filippou, F.C., Popov, E.P. and Bertero, V.V., August 1983, (PB84 192 020)A10.

UCB/EERC-83/20 "Analytical and Experimental Correlation of Large-Panel Precast Building System Performance," by Oliva, M.G., Clough, R.W., Velkov, M. and Gavrilovic, P., November 1983.

UCB/EERC-83/21 "Mechanical Characteristics of Materials Used in a 1/5 Scale Model of a 7-Story Reinforced Concrete Test Structure," by Bertero, V.V., Aktan, A.E., Harris, H.G. and Chowdhury, A.A., October 1983, (PB84 193 697)A05.

UCB/EERC-83/22 "Hybrid Modelling of Soil-Structure Interaction in Layered Media," by Tzong, T.-J. and Penzien, J., October 1983, (PB84 192 178)A08.

UCB/EERC-83/23 "Local Bond Stress-Slip Relationships of Deformed Bars under Generalized Excitations," by Eligehausen, R., Popov, E.P. and Bertero, V.V., October 1983, (PB84 192 848)A09.

UCB/EERC-83/24 "Design Considerations for Shear Links in Eccentrically Braced Frames," by Malley, J.O. and Popov, E.P., November 1983, (PB84 192 186)A07.

UCB/EERC-84/01 "Pseudodynamic Test Method for Seismic Performance Evaluation: Theory and Implementation," by Shing, P.-S.B. and Mahin, S.A., January 1984, (PB84 190 644)A08.

UCB/EERC-84/02 "Dynamic Response Behavior of Kiang Hong Dian Dam," by Clough, R.W., Chang, K.-T., Chen, H.-Q. and Stephen, R.M., April 1984, (PB84 209 402)A08.

UCB/EERC-84/03 "Refined Modelling of Reinforced Concrete Columns for Seismic Analysis," by Kaba, S.A. and Mahin, S.A., April 1984, (PB84 234 384)A06.

UCB/EERC-84/04 "A New Floor Response Spectrum Method for Seismic Analysis of Multiply Supported Secondary Systems," by Asfura, A. and Der Kiureghian, A., June 1984, (PB84 239 417)A06.

UCB/EERC-84/05 "Earthquake Simulation Tests and Associated Studies of a 1/5th-scale Model of a 7-Story R/C Frame-Wall Test Structure," by Bertero, V.V., Aktan, A.E., Charney, F.A. and Sause, R., June 1984, (PB84 239 409)A09.

UCB/EERC-84/06 "R/C Structural Walls: Seismic Design for Shear," by Aktan, A.E. and Bertero, V.V., 1984.

UCB/EERC-84/07 "Behavior of Interior and Exterior Flat-Plate Connections subjected to Inelastic Load Reversals," by Zee, H.L. and Moehle, J.P., August 1984, (PB86 117 629/AS)A07.

UCB/EERC-84/08 "Experimental Study of the Seismic Behavior of a Two-Story Flat-Plate Structure," by Moehle, J.P. and Diebold, J.W., August 1984, (PB86 122 553/AS)A12.

UCB/EERC-84/09 "Phenomenological Modeling of Steel Braces under Cyclic Loading," by Ikeda, K., Mahin, S.A. and Dermitzakis, S.N., May 1984, (PB86 132 198/AS)A08.

UCB/EERC-84/10 "Earthquake Analysis and Response of Concrete Gravity Dams," by Fenves, G. and Chopra, A.K., August 1984, (PB85 193 902/AS)A11.

UCB/EERC-84/11 "EAGD-84: A Computer Program for Earthquake Analysis of Concrete Gravity Dams," by Fenves, G. and Chopra, A.K., August 1984, (PB85 193 613/AS)A05.

UCB/EERC-84/12 "A Refined Physical Theory Model for Predicting the Seismic Behavior of Braced Steel Frames," by Ikeda, K. and Mahin, S.A., July 1984, (PB85 191 450/AS)A09.

UCB/EERC-84/13 "Earthquake Engineering Research at Berkeley - 1984," by , August 1984, (PB85 197 341/AS)A10.

UCB/EERC-84/14 "Moduli and Damping Factors for Dynamic Analyses of Cohesionless Soils," by Seed, H.B., Wong, R.T., Idriss, I.M. and Tokimatsu, K., September 1984, (PB85 191 468/AS)A04.

UCB/EERC-84/15 "The Influence of SPT Procedures in Soil Liquefaction Resistance Evaluations," by Seed, H.B., Tokimatsu, K., Harder, L.F. and Chung, R.M., October 1984, (PB85 191 732/AS)A04.

UCB/EERC-84/16 "Simplified Procedures for the Evaluation of Settlements in Sands Due to Earthquake Shaking," by Tokimatsu, K. and Seed, H.B., October 1984, (PB85 197 887/AS)A03.

UCB/EERC-84/17 "Evaluation of Energy Absorption Characteristics of Bridges under Seismic Conditions," by Imbsen, R.A. and Penzien, J., November 1984.

UCB/EERC-84/18 "Structure-Foundation Interactions under Dynamic Loads," by Liu, W.D. and Penzien, J., November 1984, (PB87 124 889/AS)A11.

UCB/EERC-84/19 "Seismic Modelling of Deep Foundations," by Chen, C.-H. and Penzien, J., November 1984, (PB87 124 798/AS)A07.

UCB/EERC-84/20 "Dynamic Response Behavior of Quan Shui Dam," by Clough, R.W., Chang, K.-T., Chen, H.-Q., Stephen, R.M., Ghanaat, Y. and Qi, J.-H., November 1984, (PB86 115177/AS)A07.

UCB/EERC-85/01 "Simplified Methods of Analysis for Earthquake Resistant Design of Buildings," by Cruz, E.F. and Chopra, A.K., February 1985, (PB86 112299/AS)A12.

UCB/EERC-85/02 "Estimation of Seismic Wave Coherency and Rupture Velocity using the SMART 1 Strong-Motion Array Recordings," by Abrahamson, N.A., March 1985, (PB86 214 343)A07.

UCB/EERC-85/03 "Dynamic Properties of a Thirty Story Condominium Tower Building," by Stephen, R.M., Wilson, E.L. and Stander, N., April 1985, (PB86 118965/AS)A06.

UCB/EERC-85/04 "Development of Substructuring Techniques for On-Line Computer Controlled Seismic Performance Testing," by Dermitzakis, S. and Mahin, S., February 1985, (PB86 132941/AS)A08.

UCB/EERC-85/05 "A Simple Model for Reinforcing Bar Anchorages under Cyclic Excitations," by Filippou, F.C., March 1985, (PB86 112 919/AS)A05.

UCB/EERC-85/06 "Racking Behavior of Wood-framed Gypsum Panels under Dynamic Load," by Oliva, M.G., June 1985.

UCB/EERC-85/07 "Earthquake Analysis and Response of Concrete Arch Dams," by Fok, K.-L. and Chopra, A.K., June 1985, (PB86 139672/AS)A10.

UCB/EERC-85/08 "Effect of Inelastic Behavior on the Analysis and Design of Earthquake Resistant Structures," by Lin, J.P. and Mahin, S.A., June 1985, (PB86 135340/AS)A08.

UCB/EERC-85/09 "Earthquake Simulator Testing of a Base-Isolated Bridge Deck," by Kelly, J.M., Buckle, I.G. and Tsai, H.-C., January 1986, (PB87 124 152/AS)A06.

UCB/EERC-85/10 "Simplified Analysis for Earthquake Resistant Design of Concrete Gravity Dams," by Fenves, G. and Chopra, A.K., June 1986, (PB87 124 160/AS)A08.

UCB/EERC-85/11 "Dynamic Interaction Effects in Arch Dams," by Clough, R.W., Chang, K.-T., Chen, H.-Q. and Ghanaat, Y., October 1985, (PB86 135027/AS)A05.

UCB/EERC-85/12 "Dynamic Response of Long Valley Dam in the Mammoth Lake Earthquake Series of May 25-27, 1980," by Lai, S. and Seed, H.B., November 1985, (PB86 142304/AS)A05.

UCB/EERC-85/13 "A Methodology for Computer-Aided Design of Earthquake-Resistant Steel Structures," by Austin, M.A., Pister, K.S. and Mahin, S.A., December 1985, (PB86 159480/AS)A10 .

UCB/EERC-85/14 "Response of Tension-Leg Platforms to Vertical Seismic Excitations," by Liou, G.-S., Penzien, J. and Yeung, R.W., December 1985, (PB87 124 871/AS)A08.

UCB/EERC-85/15 "Cyclic Loading Tests of Masonry Single Piers: Volume 4 - Additional Tests with Height to Width Ratio of 1," by Sveinsson, B., McNiven, H.D. and Sucuoglu, H., December 1985.

UCB/EERC-85/16 "An Experimental Program for Studying the Dynamic Response of a Steel Frame with a Variety of Infill Partitions," by Yanev, B. and McNiven, H.D., December 1985.

UCB/EERC-86/01 "A Study of Seismically Resistant Eccentrically Braced Steel Frame Systems," by Kasai, K. and Popov, E.P., January 1986, (PB87 124 178/AS)A14.

UCB/EERC-86/02 "Design Problems in Soil Liquefaction," by Seed, H.B., February 1986, (PB87 124 186/AS)A03.

UCB/EERC-86/03 "Implications of Recent Earthquakes and Research on Earthquake-Resistant Design and Construction of Buildings," by Bertero, V.V., March 1986, (PB87 124 194/AS)A05.

UCB/EERC-86/04 "The Use of Load Dependent Vectors for Dynamic and Earthquake Analyses," by Leger, P., Wilson, E.L. and Clough, R.W., March 1986, (PB87 124 202/AS)A12.

UCB/EERC-86/05 "Two Beam-To-Column Web Connections," by Tsai, K.-C. and Popov, E.P., April 1986, (PB87 124 301/AS)A04.

UCB/EERC-86/06 "Determination of Penetration Resistance for Coarse-Grained Soils using the Becker Hammer Drill," by Harder, L.F. and Seed, H.B., May 1986, (PB87 124 210/AS)A07.

UCB/EERC-86/07 "A Mathematical Model for Predicting the Nonlinear Response of Unreinforced Masonry Walls to In-Plane Earthquake Excitations," by Mengi, Y. and McNiven, H.D., May 1986, (PB87 124 780/AS)A06.

UCB/EERC-86/08 "The 19 September 1985 Mexico Earthquake: Building Behavior," by Bertero, V.V., July 1986.

UCB/EERC-86/09 "EACD-3D: A Computer Program for Three-Dimensional Earthquake Analysis of Concrete Dams," by Fok, K.-L., Hall, J.F. and Chopra, A.K., July 1986, (PB87 124 228/AS)A08.

UCB/EERC-86/10 "Earthquake Simulation Tests and Associated Studies of a 0.3-Scale Model of a Six-Story Concentrically Braced Steel Structure," by Uang, C.-M. and Bertero, V.V., December 1986, (PB87 163 564/AS)A17.

UCB/EERC-86/11 "Mechanical Characteristics of Base Isolation Bearings for a Bridge Deck Model Test," by Kelly, J.M., Buckle, I.G. and Koh, C.-G., 1987.

UCB/EERC-86/12 "Effects of Axial Load on Elastomeric Isolation Bearings," by Koh, C.-G. and Kelly, J.M., 1987.

UCB/EERC-87/01 "The FPS Earthquake Resisting System: Experimental Report," by Zayas, V.A., Low, S.S. and Mahin, S.A., June 1987.

UCB/EERC-87/02 "Earthquake Simulator Tests and Associated Studies of a 0.3-Scale Model of a Six-Story Eccentrically Braced Steel Structure," by Whittaker, A., Uang, C.-M. and Bertero, V.V., July 1987.

UCB/EERC-87/03 "A Displacement Control and Uplift Restraint Device for Base-Isolated Structures," by Kelly, J.M., Griffith, M.C. and Aiken, I.D., April 1987.

UCB/EERC-87/04 "Earthquake Simulator Testing of a Combined Sliding Bearing and Rubber Bearing Isolation System," by Kelly, J.M. and Chalhoub, M.S., 1987.

UCB/EERC-87/05 "Three-Dimensional Inelastic Analysis of Reinforced Concrete Frame-Wall Structures," by Moazzami, S. and Bertero, V.V., May 1987.

UCB/EERC-87/06 "Experiments on Eccentrically Braced Frames with Composite Floors," by Ricles, J. and Popov, E., June 1987.

UCB/EERC-87/07 "Dynamic Analysis of Seismically Resistant Eccentrically Braced Frames," by Ricles, J. and Popov, E., June 1987.

UCB/EERC-87/08 "Undrained Cyclic Triaxial Testing of Gravels-The Effect of Membrane Compliance," by Evans, M.D. and Seed, H.B., July 1987.

UCB/EERC-87/09 "Hybrid Solution Techniques for Generalized Pseudo-Dynamic Testing," by Thewalt, C. and Mahin, S.A., July 1987.

UCB/EERC-87/10 "Ultimate Behavior of Butt Welded Splices in Heavy Rolled Steel Sections," by Bruneau, M. Mahin, S.A. and Popov, E., September 1987.

UCB/EERC-87/11 "Residual Strength of Sand from Dam Failures in the Chilean Earthquake of March 3, 1985," by De Alba, P., Seed, H.B., Retamal, E. and Seed, R.B., September 1987.

UCB/EERC-87/12 "Inelastic Seismic Response of Structures with Mass or Stiffness Eccentricities in Plan," by Bruneau, M. and Mahin, S.A., September 1987.

UCB/EERC-87/13 "CSTRUCT: An Interactive Computer Environment for the Design and Analysis of Earthquake Resistant Steel Structures," by Austin, M.A., Mahin, S.A. and Pister, K.S., September 1987.

UCB/EERC-87/14 "Experimental Study of Reinforced Concrete Columns Subjected to Multi-Axial Loading," by Low, S.S. and Moehle, J.P., September 1987.

UCB/EERC-87/15 "Relationships between Soil Conditions and Earthquake Ground Motions in Mexico City in the Earthquake of Sept. 19, 1985," by Seed, H.B., Romo, M.P., Sun, J., Jaime, A. and Lysmer, J., October 1987.

UCB/EERC-87/16 "Experimental Study of Seismic Response of R. C. Setback Buildings," by Shahrooz, B.M. and Moehle, J.P., October 1987.

UCB/EERC-87/17 "The Effect of Slabs on the Flexural Behavior of Beams," by Pantazopoulou, S.J. and Moehle, J.P., October 1987.

UCB/EERC-87/18 "Design Procedure for R-FBI Bearings," by Mostaghel, N. and Kelly, J.M., November 1987.

UCB/EERC-87/19 "Analytical Models for Predicting the Lateral Response of R C Shear Walls: Evaluation of their Reliability," by Vulcano, A. and Bertero, V.V., November 1987.

UCB/EERC-87/20 "Earthquake Response of Torsionally-Coupled Buildings," by Hejal, R. and Chopra, A.K., December 1987.

UCB/EERC-87/21 "Dynamic Reservoir Interaction with Monticello Dam," by Clough, R.W., Ghanaat, Y. and Qiu, X-F., December 1987.

UCB/EERC-87/22 "Strength Evaluation of Coarse-Grained Soils," by Siddiqi, F.H., Seed, R.B., Chan, C.K., Seed, H.B. and Pyke, R.M., December 1987.

UCB/EERC-88/01 "Seismic Behavior of Concentrically Braced Steel Frames," by Khatib, I., Mahin, S.A. and Pister, K.S., January 1988.

UCB/EERC-88/02 "Experimental Evaluation of Seismic Isolation of Medium-Rise Structures Subject to Uplift," by Griffith, M.C., Kelly, J.M., Coveney, V.A. and Koh, C.G., January 1988.

UCB/EERC-88/03 "Cyclic Behavior of Steel Double Angle Connections," by Astaneh-Asl, A. and Nader, M.N., January 1988.

UCB/EERC-88/04 "Re-evaluation of the Slide in the Lower San Fernando Dam in the Earthquake of Feb. 9, 1971," by Seed, H.B., Seed, R.B., Harder, L.F. and Jong, H.-L., April 1988.

UCB/EERC-88/05 "Experimental Evaluation of Seismic Isolation of a Nine-Story Braced Steel Frame Subject to Uplift," by Griffith, M.C., Kelly, J.M. and Aiken, I.D., May 1988.